THE UNIVERSITY OF MANITOBA

MEASUREMENT OF WIDE AND NARROW MASS DIFFERENCES ON THE MANITOBA II MASS SPECTROMETER

by

Frank Charles Gray Southon

A THESIS

SUBMITTED TO THE FACULTY OF GRADUATE STUDIES

IN PARTIAL FULFILMENT OF THE REQUIREMENTS FOR THE DEGREE

OF DOCTOR OF PHILOSOPHY

DEPARTMENT OF PHYSICS

WINNIPEG, MANITOBA

October 1973

MEASUREMENT OF WIDE AND NARROW MASS DIFFERENCES ON THE MANITOBA II MASS SPECTROMETER

by

Frank Charles Gray Southon

A dissertation submitted to the Faculty of Graduate Studies of the University of Manitoba in partial fulfillment of the requirements of the degree of

DOCTOR OF PHILOSOPHY

Doctor of Philosophy (1973) University of Manitoba
Physics Winnipeg, Manitoba.

Title: Measurement of Wide and Narrow Mass Differences on the Manitoba II Mass Spectrometer.

Author: Frank Charles Gray Southon MSc., University of Auckland (N.Z.).

Supervisor: Professor R.C. Barber.

Pages: ix, 148.

Scope and Contents:

The primary objective of this work has been the measurement of mass doublets having a greater spacing than those previously measured by this group, i.e. doublets for which ($\Delta M/M > 1/17,000$). Instrumental modifications are described, and the present experimental limitations for precise measurements is discussed.

With the system developed, measurements were made to improve the knowledge of the $^{37}Cl - ^{35}Cl$ mass difference, and to correlate the ends of a long chain of mass differences

measured in this and previous work, viz. by linking lutetium and neodymium nuclides.

Some narrow mass differences are reported, and a new type of computer - assisted matching system is discussed.

Previous mass measurements carried out in this laboratory have been corrected for the systematic errors discovered in this work and a new adjustment carried out.

Our knowledge of systematic variations of the double neutron separation energy (S_{2n}) for $104 \leqslant N \leqslant 112$ has been extended and is discussed herein.

ACKNOWLEDGEMENTS

This research has been supported by the National Research Council, and the University of Manitoba has contributed to personal maintenance.

I want to thank my supervisor, Dr. R.C. Barber who has managed this group, and has guided and supported me throughout, and Dr. H.E. Duckworth who initiated this group and remains a guiding influence. Thanks are also due to Drs. J.O. Meredith, P. Williams and R.L. Bishop and Messrs. D. Burrell and P. Rookhuyzen as well as the others with whom I have worked and shared mutual stimulation.

I also thank my wife who helped support me for several years and has suffered through a seemingly eternal part-time thesis writing process.

CONTENTS

LIST OF FIGURES

LIST OF TABLES

CHAPTER 1

INTRODUCTION

Mass spectroscopy started early this century with Thomsons's analysis of positive rays by the parabola method (Th07). Since then, the field has steadily progressed with the achievment, in atomic mass determinations, of approximately an order of magnitude improvment in precision for each decade (fig. F1-1).

Thomson provided the first evidence of isotopic structure of matter with his work on neon. Although he used instruments with both photographic and electrical detection (Th13), the terms 'mass spectrometer' and 'mass spectrograph' are normally reserved* for the later deflection instruments such as those built by Dempster (De18) and Aston (As19). During the twenties, instruments which were capable

*According to Aston (As42 p38), the term 'mass spectrograph' applies only to those apparatus capable of producing a focussed spectrum of lines on a photographic plate, and not to the parabola method. The term 'mass spectrometer' applies to an instrument where the ions are focussed on a fixed slit, and are detected electrically.

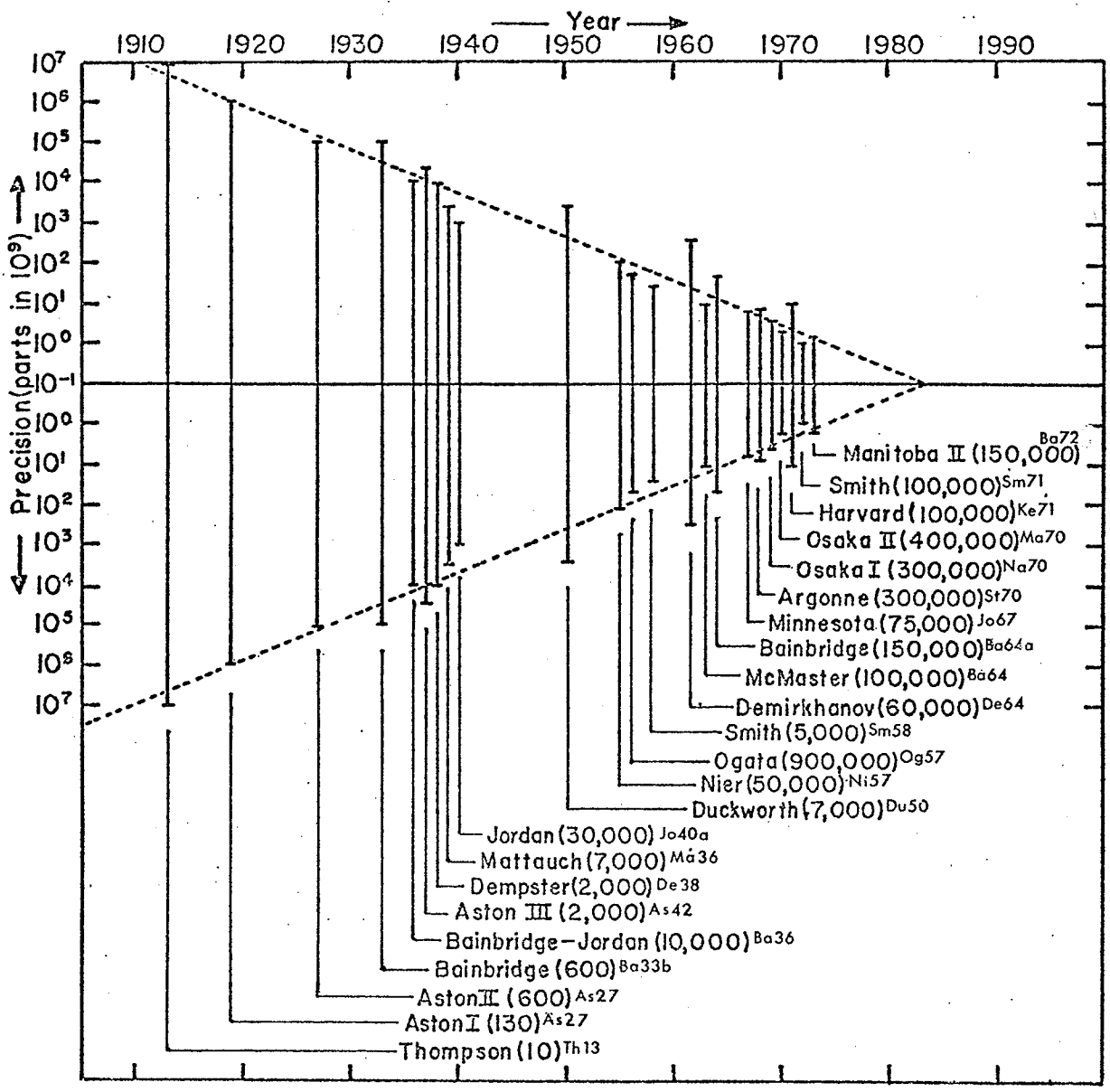

FOLLOWING WILLIAMS AND DUCKWORTH, Wi72

FIG F I-1 DEVELOPMENT OF PRECISION IN MASS SPECTROSCOPY

of resolving powers of several hundred were available and, with these, the three objectives of isotope identification, natural abundance measurement and mass measurement were pursued (As27, As33). Most of the prominent isotopes were identified, and the masses of many of these measured, from which an outline 'packing fraction' curve was formed.

A greater specialisation in mass measurement occurred in the thirties with the development of a second generation of mass spectrographs with improved ion optics (sect. 2.1) - instruments capable of achieving resolving powers up to 30,000 (Jo40). Mass spectroscopy was used to determine the masses of important nuclides (referred usually to organic molecules) and nuclear reaction data filled in the finer details (Du57).

In the fifties, the theory of ion optics was further improved (sect. 2.2), and a number of very large instruments were constructed, some of which used photographic detection (Og57, Ev57), while others used electrical detection (Du57, Co57, St60). Resolving powers in excess of 100,000 were obtained. The successive developments of peak matching (sect. 2.3), signal averaging (sect. 4.1), and computer-assisted matching (sect. 4.2) have contributed to the continued advance in the precision attained with these

instruments. Following a parallel but separate development, r. f. mass spectrometers have also made an important contribution to these studies (sect. 2.4). More detailed accounts of the historical development of mass spectroscopy have been written by a number of authors (e.g. As42, De58, Wi72).

Apart from the elucidation of chemical atomic weights provided early in this century, mass spectroscopy has contributed to our knowledge of the nature of nuclear structure. Mass spectroscopic data on the details of the systematic variation of nuclear mass as a function of N and Z have become competitive with reaction data, and much useful information has been revealed by the separation and pairing energies derived (Du69, Me72). Unfortunately, the theory has not been able to keep up with progress in mass measurements, so that the difference between mass laws and experimental values is currently of the order of 0.5 milli mass units (Se72), or about 100 times the measurement errors.

The measurement of atomic masses requires some convenient standard on which to base the values. Aston chose ^{16}O as a reference (As33, p165) when it was discovered that oxygen had more than one stable nuclide. However the

small but significant difference between the physical (^{16}O = 16 units) and chemical (O = 16 units) mass scales, the experimental necessity to rely on carbon as a substandard, and the difficulty in comparing the masses of carbon and oxygen (Va57), finally motivated a transfer from the ^{16}O standard to the ^{12}C standard (^{12}C = 12 units) in 1960.

Although mass spectroscopy is capable of comparing atomic masses with a precision as high as a part in one billion in some cases (Sm71), the masses cannot be expressed in absolute mass units to this precision. Unlike the absolute length and time standards which are now based on atomic scale phenomena, the basic mass standard remains the platinum-iridium 1Kgm. Hence the present uncertainty of 6.6 parts per million in Avogadro's number (Ta70) limits our knowledge of atomic masses in terms of the absolute mass standard.

CHAPTER 2

PRINCIPLES OF MASS SPECTROSCOPY

2.1 DOUBLE FOCUSSING

In high resolution mass spectroscopy the deflection of a beam of charged particles by a combination of electric and magnetic fields is used to separate particles having different mass to charge ratios (m/e). The beam of ions enters the instrument, is separated into its mass components by the electric and magnetic fields, and is focussed on a photographic plate or an exit slit. The radial electrostatic and uniform magnetic fields both possess the properties of direction focussing as well as characteristic dispersion properties - the electric field produces energy dispersion, and the magnetic field momentum dispersion.

The focussing properties of electrostatic and magnetic fields have been appreciated since the early days of mass spectroscopy. In particular, the direction focussing characteristic of the 180 degree magnetic field was used early (Cl07), and later constituted the basis of Dempster's

instrument (De18). Aston also was aware of the direction focussing properties of the electrostatic analyser and sector magnetic fields (AS19), although his instrument relied primarily on slit collimation for control of angular spread. However he used the counteracting energy and momentum dispersions of electric and magnetic fields to acheive velocity focussing in his first mass spectrograph.

The focussing theory for radial electrostatic analysers was further developed by Hughes and Rojansky (Hu29), Smythe (Sm34) and others, and that for magnetic analysers by Barber (Ba33), Stephens (St34) and others. Finally Herzog (He34) presented a general analysis of the focussing properties of cylindrical electrostatic analysers, and of uniform magnetic analysers and gave equations from which the focussing properties could be calculated.

Although the possibility of combining both direction and velocity focussing (double focussing) was considered by Dempster in 1922 (De22), it was not until the development of the general focussing theory by Herzog that double focussing was achieved. Shortly thereafter instruments possessing double focussing (at one point) were built by Dempster (De35) and Bainbridge (Ba36), while Mattauch (Ma36), on the basis of an analysis of the general double focussing

conditions, designed a mass spectrograph that acheived double focussing over the whole photographic plate.

The principle of the attainment of mass dispersion without velocity dispersion may be described as follows. We define the trajectory of an ion of mass m_0 whose velocity is v_0 to be the optic axis, and describe specific ions of mass m and velocity v in terms of the dimensionless variables (γ, β), viz.,

$$m = m_0(1 + \gamma)$$
$$v = v_0(1 + \beta) \quad . \qquad (2\text{-}1)$$

To first order, we can describe the lateral displacement of the ions from the optic axis at the detector by

$$b_e = k_e(\gamma + 2\beta) \quad . \qquad (2\text{-}2)$$

where b_e results from the energy dispersion of the electrostatic analyser. Similarly in a magnetic field the corresponding displacement due to momentum dispersion would be

$$b_p = k_p(\gamma + \beta) \quad . \qquad (2\text{-}3)$$

For a tandem arrangement of electric and magnetic fields we combine these two dispersions to get a resultant dispersion

$$b = b_e + b_p = (k_e + k_p)\gamma + (2k_e + k_p)\beta \quad . \quad (2\text{-}4)$$

If the instrument is designed so that

$$k_p = -2k_e \qquad (2\text{-}5)$$

then the velocity dispersion is zero (i.e. there is velocity focussing), but the mass dispersion is given by

$$b = (-k_e)\gamma = \tfrac{1}{2}k_p\gamma \,. \qquad (2\text{-}6)$$

2.2 SECOND AND HIGHER ORDER ANALYSIS

The focussing equations of Herzog (He34) were derived from a calculation which involved a first order approximation in the half angular spread of the beam at the object (α) and in the velocity spread, β. The lateral displacement of the beam, after passing through a tandem combination of electrostatic analyser and magnetic analyser, can be expressed more exactly by the equation

$$b = r_m(B_1\alpha + B_2\beta + B_{11}\alpha^2 + B_{12}\alpha\beta + B_{22}\beta^2 + \text{higher order terms in } \alpha,\beta + \text{terms in } \alpha_z) \qquad (2\text{-}7)$$

where:

b is the lateral position of an ion with respect to the optic axis at the exit slit.

α is the angular deviation of the ion from the mean path in the median plane,

α_z is the angular deviation perpendicular to the median plane,

and β is the proportional velocity deviation as defined in equin 2-1.

The B coefficients express the focussing properties of the instrument. Thus first order direction focussing is acheived if $B_1 = 0$, and velocity focussing if $B_2 = 0$. The coefficients B_{11}, B_{12}, B_{22} express the second order focussing properties.

Second order focussing was first considered by Aston (As22a), although only for velocity (i.e. $B_{22} = 0$). He attempted to obtain it in his second instrument (As27) and acheived it in his third (As42, p103). Much later Johnson and Nier (Jo53) described a second order angle analysis (setting $B_{11} = 0$) which became the basis of the high resolution instruments at the University of Minnesota (Ni51,Ni57). Other larger instruments having similar focussing characteristics were also constructed at Harvard (Co57) and Argonne (St60). A more general second order analysis was considered by Ewald and Hintenberger in 1953 (Ew53) and developed over the following six years. Assuming abrupt field boundaries, Hintenberger and Konig analysed median plane trajectories (Hi55, Hi57, Ko57, Ko58), and proposed a wide range of instrument geometries which produce double focussing to second order (Hi55, Hi59). Ewald and Liebl have included trajectories off the median plane in their analysis (Ew57, Li57, Li57a, Li59). Subsequent studies

have extended the work to include the effects of fringing fields (Wo65, Ma71a), and to perform second order three dimensional analysis (Wo65a). Some third order analysis has also been carried out (Ma71).

Hintenberger et al. were the first to attempt the construction of an instrument on the basis of a complete second order analysis (Hi59). However computational errors (Hi59, p31) resulted in an instrument which had second order angle focussing only ($B_1 = B_2 = B_{11} = 0$). Subsequently Barber et al. built the instrument used in the work reported here on the basis of one of the later designs of Hintenberger and Konig (sect. 3.1). This instrument is now called the Manitoba II Mass Spectrometer.

Analysis of non-uniform magnetic fields, particularly the 1/r fields between conical pole faces (Ta59, Ta60, Ru66) led to the construction by Matsuda et al. of a 'very large dispersion' mass spectrometer (Ma66a) with a resolving power up to 500,000. Magnetic fields of the 1/r form do not produce direction focussing and thus allow large angles of deflection and hence increased dispersion. Unfortunately the complete second order focussing, which was anticipated on the basis of design calculations, was not achieved experimentally (Ma70).

Burrell has recently carried out a ray tracing analysis of the Manitoba II instrument using the measured magnetic fringing field (Bu72). His results differ significantly from those predicted by theoretical analysis, and are closer to the experienced behaviour of the instrument. Other work also indicates that the theory of fringing fields has not been properly understood (Ma70a).

2.3 MEASUREMENT OF ATOMIC MASS DIFFERENCES

Bleakney (Bl36) (Appendix) has shown that, as a consequence of the Lorentz force equation, two ions of different mass will follow identical paths through a combination of electric and magnetic fields provided the following conditions are obeyed at all points:

$$\frac{e'E'}{K'} = \frac{e''E''}{K''} \qquad (2\text{-}8a)$$

$$\frac{e'B'}{P'} = \frac{e''B''}{P''} \qquad (2\text{-}8b)$$

where K',K" are the respective kinetic energies

P',P" are the respective Momenta

E',E" are the respective Electric Fields

B',B" are the respective Magnetic Fields

e',e" are the respective charges.

If a constant magnetic field, B, is maintained, then for identical trajectories

$$P'/e' = P''/e'' . \qquad (2\text{-}9)$$

Condition 2-8a, then, converts to

$$\frac{E'M'}{e'} = \frac{E''M''}{e''} \qquad (2\text{-}10)$$

or, where these electric fields result from potentials V', V" applied to electrodes, and are proportional to the potentials, then

$$\frac{V'M'}{e'} = \frac{V''M''}{e''} . \qquad (2\text{-}11)$$

These conditions thus apply to all of the electric fields encountered by the ion travelling along the given trajectory.

All the early instruments used this equation to measure some mass differences (De18, As20, As22, Co25, Ba33a). The improvement of mass spectrographs in the thirties, however, permitted the resolution of close doublets, and determination of atomic mass relied predominantly on the knowledge of instrumental mass dispersions derived from larger mass differences. The mass spectrometer was reintroduced by Nier (Ni51) who applied eqn. 2-11 to close doublets in the following form (assuming

identical charge):

$$\frac{M'' - M'}{M'} = \frac{V' - V''}{V''} \qquad (2\text{-}12)$$

more generally known as

$$\Delta M/M = \Delta V/V \ . \qquad (2\text{-}13)$$

Thus a small mass difference between two ions can be determined to a much greater precision than the mass of either of the ions is known.

Shortly after its construction, Nier's instrument was converted to peak matching (Gi54), a system which was originally used by Smith on his mass synchrometer (Ni57), and is now almost universally employed in mass measurement with deflection instruments. The most usual form of the technique uses a small linear (sawtooth) modulation field synchronised with the horizontal sweep of an oscilloscope to deflect the beam and sweep a small portion of the spectrum across the exit slit. The beam passing through the fine slit is detected by an electron multiplier and a fast amplifier whose voltage output controls the vertical position of the oscilliscope spot. A portion of the spectrum is thus displayed on the screen, with ions of different masses grouped in successive 'peaks.'

If, after a sweep which displays a spectrum with peak

M' on the screen, all the voltages generating electrostatic fields are switched in accordance with eqn. 2-12, then on the subsequent sweep the peak of mass M" will appear on the screen at the same position. Conversely, peak coincidence can be used as a test that eqn. 2-12 is satisfied.

In an ideal double focussing instrument, the only potential influencing the peak position is the electrostatic analyser potential V_e, so we can rewrite eqn. 2-13 as

$$\Delta M = M \, \Delta V_e / V_e \, . \qquad (2\text{-}14)$$

Hence a method of determining mass differences in terms of electric potentials is derived. The experiment thus involves two major features: the determination of peak coincidence (see Chapter 4) and the measurement of electric fields encountered by the ion beam.

In a real instrument, however, imperfections may need to be taken into account. A crucial factor is the effect of any departure from eqn. 2-12 for any particular potential, and the interactions between the different discrepancies. If we express, to first order, the change in position (dP_1) of the final peak position produced by the change in a particular voltage dV_1 in terms of a constant k_1

$$dP_1 = k_1 dV_1 \qquad (2\text{-}15)$$

then any error dV_1 in the voltage difference $V_1' - V_1''$ will

produce an error in the peak position dP_1. If the determination of peak position, or 'matching', is done within an error of dP_c, then the condition for the error dV_1 in the switching of voltage V_1 is

$$dV_1 << dP_c/k_1 \quad . \qquad (2\text{-}16)$$

If eqn. 2-16 is not satisfied, then the final peak coincidence must be achieved by compensating errors in another voltage V_2 given by

$$dV_2 = -dV_1 \, k_1/k_2 \quad . \qquad (2\text{-}17)$$

V_2 will, most probably, be the electrostatic analyser potential V_e, and thus errors in the mass measurement as calculated from equation (2-14) will result. Corrective calculation can sometimes be carried out (sect. 5.5).

A few points should be noted here:

1. The acceleration potential V_a must be adjusted to ensure that condition 2-12 is obeyed as closely as possible so that the ions do traverse the same paths.

2. The mass spectrometer must be focussed and tested to ensure that velocity focussing conditions exist (i.e. the corresponding constant in equn. 2-15, k_a, is small).

3. There must not be any electric field in the path of the ions that is not switched according to eqn. 2-12

within the limits of eqn. 2-16.

4. All electric fields influencing the ion beam, especially the electrostatic analyser field, must be proportional to the voltages applied (see Ch 5).

5. As the width of the doublet measured increases, the requirements on voltage switching generally become more stringent (see sect. 4.3).

6. Magnetic fields must remain constant, except for the magnetic sweep which must be identical for both ions.

7. Equation 2-14 may be put into two forms:

$$\Delta M/M' = \Delta V_e/V_e" \qquad (2\text{-}18)$$

or

$$\Delta M/M" = \Delta V_e/V_e' \qquad (2\text{-}19)$$

If M' is the lighter mass, then V_e' will be the higher voltage. Equation 2-18 then expresses a situation where ΔV_e is added on to the denominator ($V_e"$) and eqn. 2-19 where ΔV_e is subtracted from the denominator (V_e'). These present two possible forms of measurement, called "add" form and "subtract" form. The same V_e is actually used for both forms, producing slightly different ΔV_e's for the same mass difference measurement:

$$\Delta M = M'\Delta V_{add}/V_e \qquad (2\text{-}20)$$

$$\Delta M = M"\Delta V_{sub}/V_e \qquad (2\text{-}21)$$

Section 4.2 describes the use of the two forms and section 5.4 the use of the formula.

8. It has been considered likely by several investigators (Ee66, Ke70, Ke71), that particular problems are involved in the comparison of ions consisting of different atomic fragments arising from the difference in the ions' initial velocities in the source. This factor has been taken into consideration in sections 5.4, 6.1 and 6.2.

2.4 RADIO FREQUENCY MASS SPECTROSCOPY

Significant contributions have been made at an early stage to atomic mass determination by a variety of radio frequency experiments, notably the omegatron (So51), the microwave spectrometer (Ge57), and the mass synchrometers. The first two types, however, have not generally remained competitive in precision, in contrast with the last series of instruments, designed by Smith and based on the cyclotron frequency of ions in a circular orbit in a magnetic field (Sm51, Sm56, Sm67, Sm71). His most recent 'R.F. mass spectrometer' (Sm67, Sm71) has achieved a resolving power of 100,000. The primary advantage of this system is the precision with which frequencies can be compared, viz., a few parts in 10^{10}. A large number of fundamental

measurements have been made with the R. F. spectrometer (Sm71, Sm72) (sect. 4.3). It is not, however, completely devoid of the problems associated with voltage measuring instruments (sect. 5.1).

A somewhat different instrument by Luxon and Rich (Lu72) involves measuring the cyclotron frequency of particles trapped within a magnetic well. Preliminary results have been reported, and possible improvements in the technique have been proposed, but the results are not yet competitive in precision.

CHAPTER 3

THE MANITOBA SECOND ORDER DOUBLE FOCUSSING INSTRUMENT

3.1 INSTRUMENT GEOMETRY

The geometry of the instrument used here (fig. F3-1) is one of a number of geometries calculated by Hintenberger and König (Hi57, Hi59) which produce complete second order-double focussing. This particular one was chosen since it possessed all of the following desirable features:

1. An intermediate direction focus which allows independent control by an intermediate slit of the energy range which can be transmitted by the instrument (see also sect. 5.1).

2. A compact design in which the path length is short for the dispersion produced. The relatively small overall dimensions reduce the vacuum requirements, and permit easier protection from vibration.

3. Straight magnetic analyser boundaries, which are easier to construct and to adjust for fringing field effects.

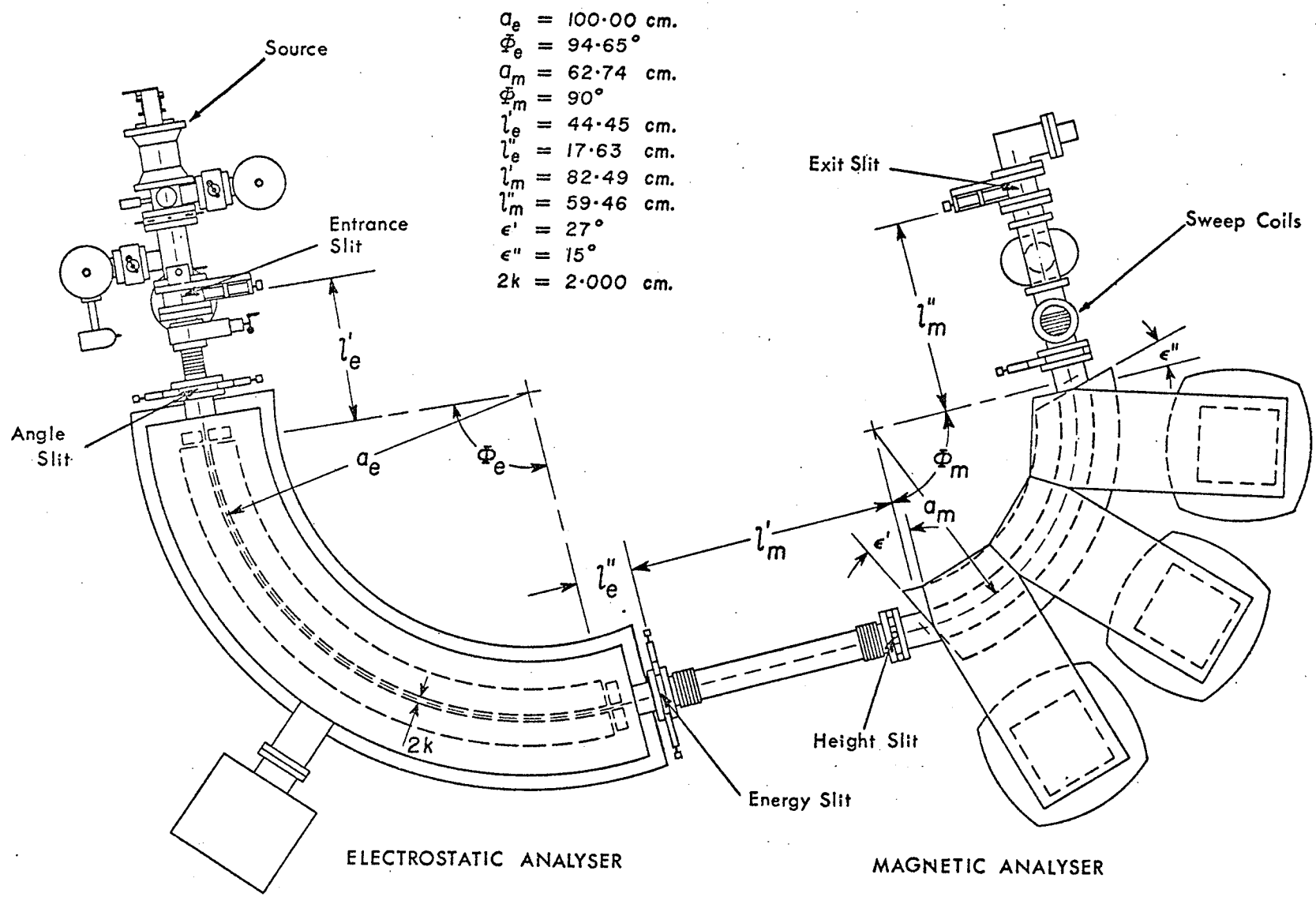

FIG F3–1 GEOMETRY OF THE MANITOBA II MASS SPECTROMETER

4. An overall magnification of 0.5, which permits less stringent requirements on the entrance slit quality than on that for the exit slit. The entrance slit quality gradually deteriorates as a result of sputtering under ion bombardment. This effect is negligible for the exit slit.

A convenient size was obtained by setting the electrostatic analyser radius at 1 metre, and thereby determining the other parameters as given in fig. F3-1. The path length between principle and exit slits is 4.95 metres, and the dispersion is .53ΔM/M metres. Ion groups differing in mass by 1/100,000 will be 5.3 microns apart at the exit slit.

3.2 INSTRUMENT CONSTRUCTION

The geometry of the instrument used in this work is shown in figure F3-1, and a photograph is presented as figure F3-2. The details of the electrostatic and magnetic analysers, slits, vacuum system and mounting have been described elsewhere (Ba67, Ba71, Bi69, Me71). We note here that significant features of the instrument are:

(a) low background pressure and a relatively oil-free main chamber,

(b) a high degree of uniformity in the magnetic

FIGURE F3-2

PHOTOGRAPH OF THE

MANITOBA II MASS SPECTROMETER

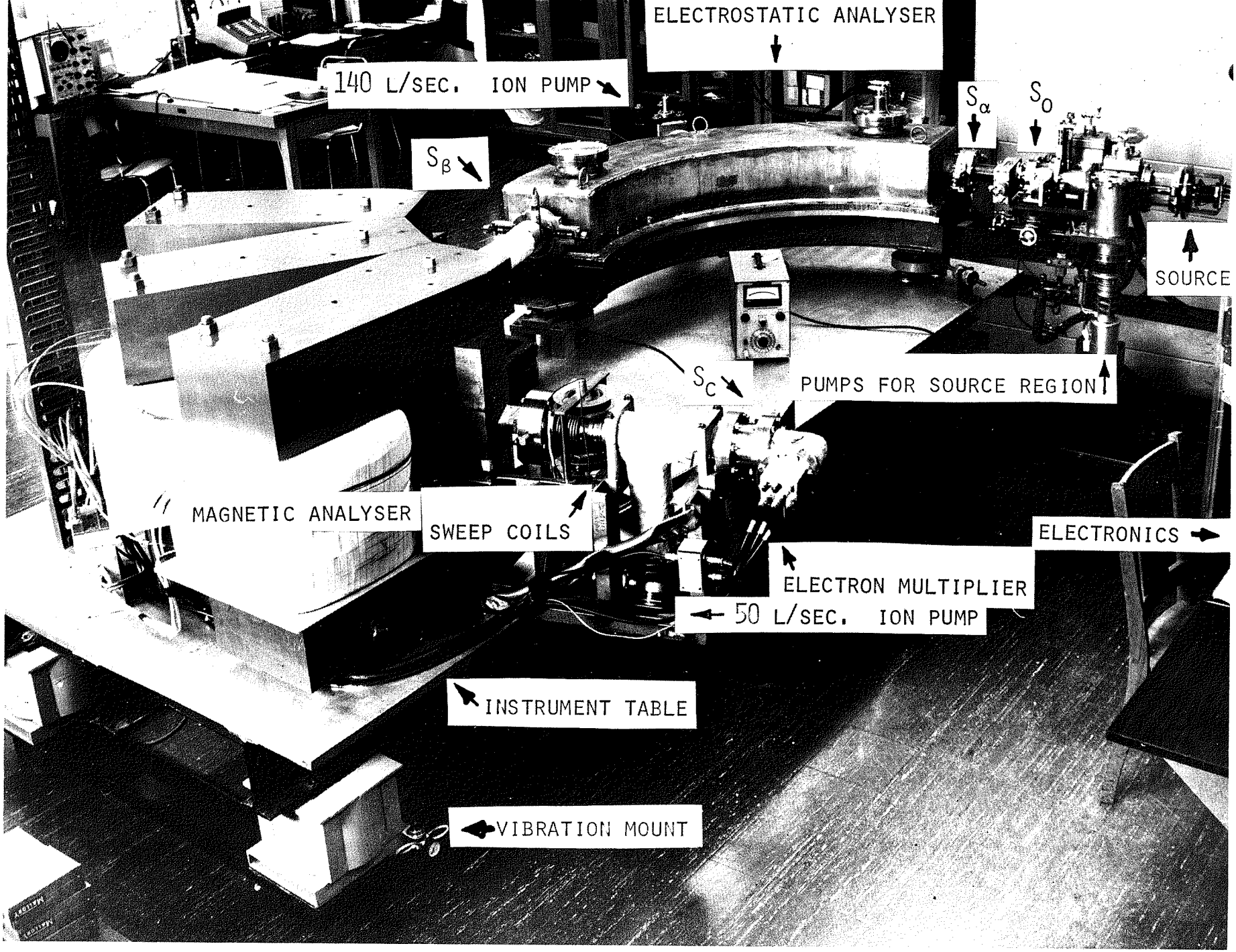
ELECTROSTATIC ANALYSER
140 L/SEC. ION PUMP
S_α
S_o
S_β
SOURCE
S_c
PUMPS FOR SOURCE REGION
MAGNETIC ANALYSER
SWEEP COILS
ELECTRONICS
ELECTRON MULTIPLIER
50 L/SEC. ION PUMP
INSTRUMENT TABLE
VIBRATION MOUNT

field,

(c) isolation of the instrument from building vibrations,

(d) high uniformity in the z-direction (at a given r) for radial electrostatic field, and small tolerances in the gap, and

(e) second order focussing (sect. 2.2).

3.3 ION SOURCES

The source is an ion bombardment type with a basic design similar to that given by Finkelstein as described by von Ardenne (Vo62). It has been described previously (Bi69, Me71, Ba71) and is shown in a slightly modified form in fig. F3-3. Different ovens were used to provide suitable gas pressures of the different samples. For the rare earth chlorides a strongly heated tantalum oven was required as described by Meredith (Me71). For hafnium chloride it was necessary to warm the oven only slightly, and introduce carbon tetrachloride through a leak valve. The reaction between CCl_4 vapour and Hf vapour in the plasma compensated for the loss of chlorine through dissociation of the hafnium chloride when initially heated.

Figure F3-4 shows the end view of the source and

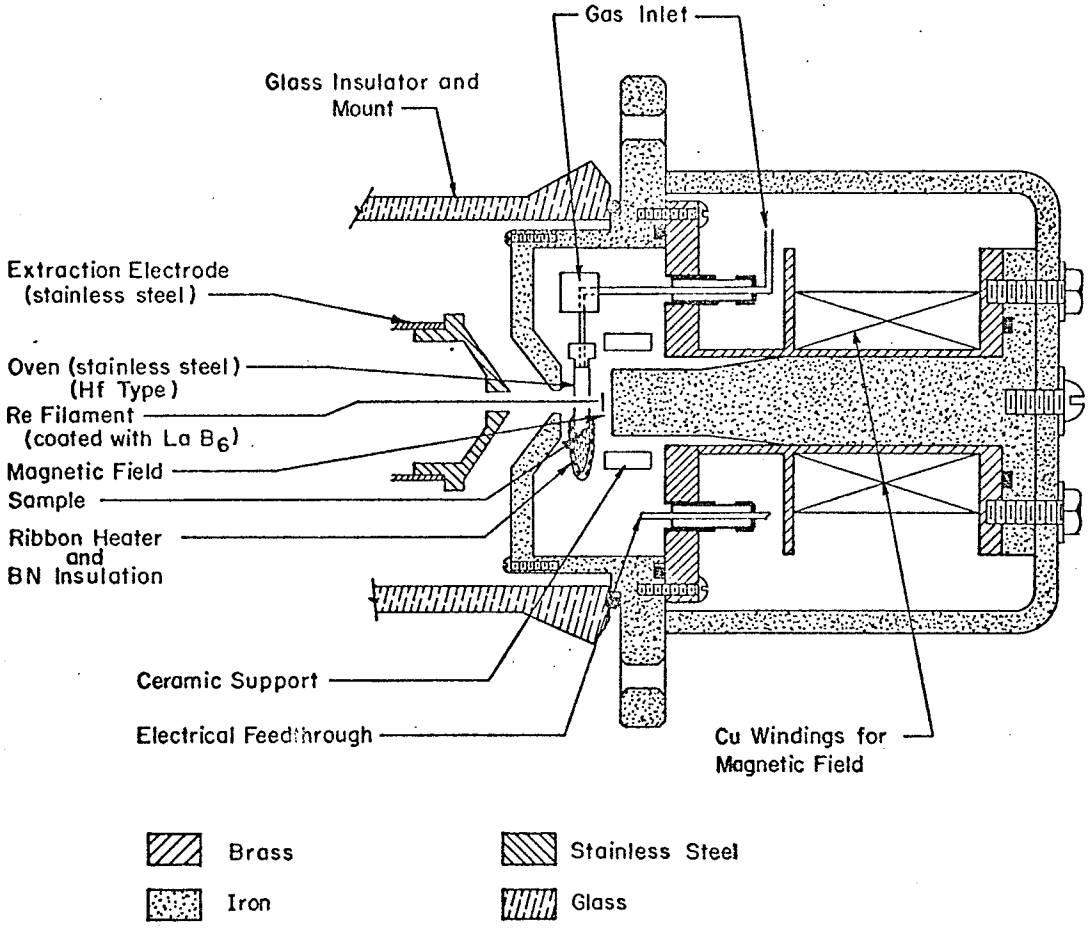

FIG. F3 - 3 SOURCE ASSEMBLY (SIDE VIEW)

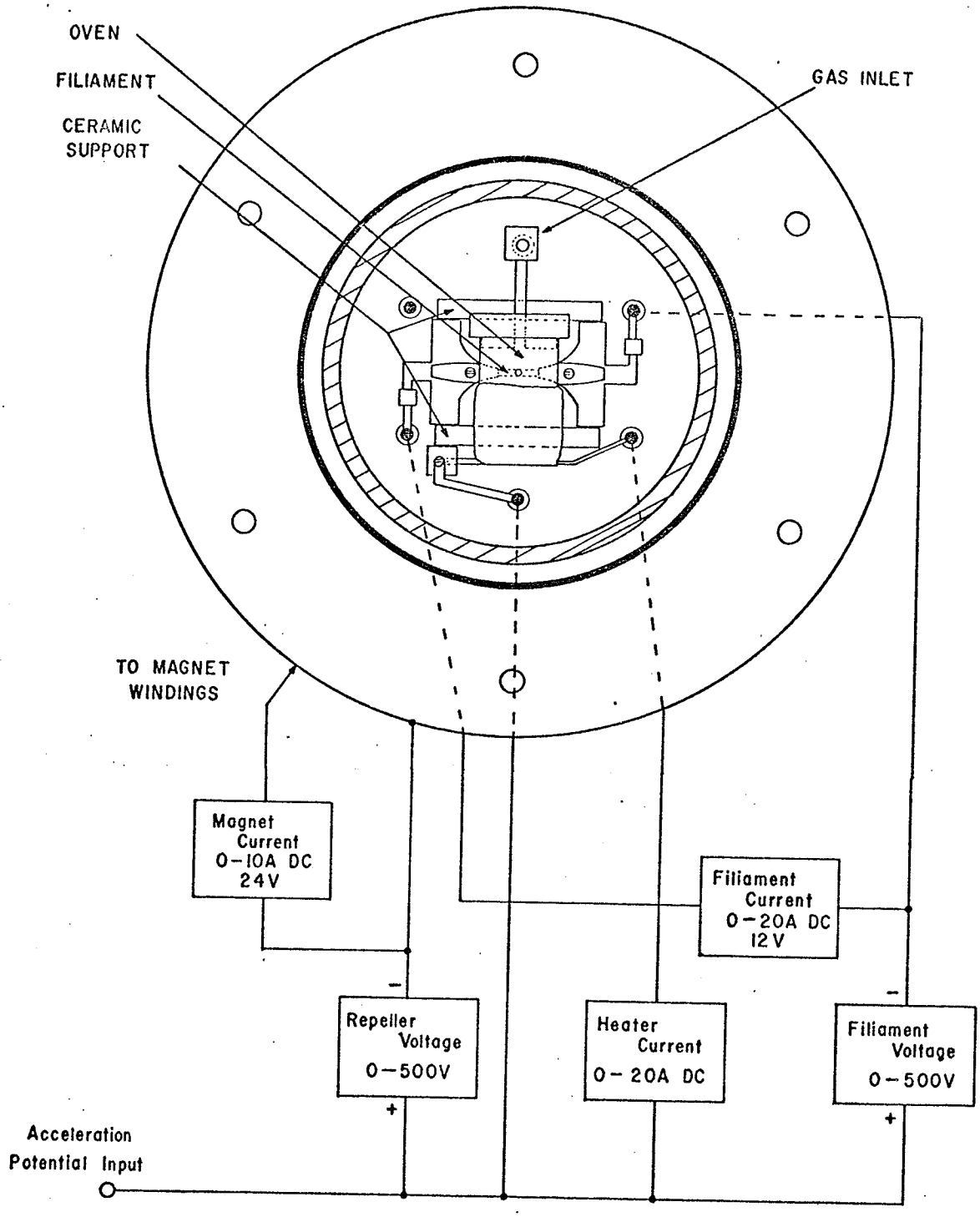

FIG. F3-4 FRONT VIEW OF SOURCE WITH POWER SUPPLIES

indicates the power supplies used. Note that the high voltage is connected directly to the oven to give optimum definition to the ion potential, while the body of the source is used as an electron repeller behind the filiament.

The source is normally operated with a filiament voltage between -100V and -300V with respect to the oven, with the repeller voltage somewhat higher. The rhenium filiament is .052 x 1.3 mm in cross section and is heated by a current of 7-10A d.c. Under certain conditions a plasma could be generated in the oven, but this was not the most common mode of operation.

The energy spread of the ions produced by this type of source can be less than one volt, although the range observed in this work was up to 20 volts and occasionally higher.

3.4 FOCUSSING AND STEERING

In previous work an electrostatic quadrupole lens was used both to focus the ion beam from the source to a line image at the principle slit and to centre it on the slit by offsetting the potentials on opposite electrodes (Wh66, Bi69). The voltages applied (V_q) were not switched since the appropriate switching voltage (up to 20mV in 700V) was

sufficiently small that the error introduced in this way was negligible. (Under normal focussing conditions the quadrupoles have very little influence on the peak position (i.e. the corresponding constant in eqn. 2-15, k_q, is small). For the wide doublets studied in this work, the required changes in the voltages were much larger (0.2V for measured doublets and up to 14V for calibration doublets) and could no longer be ignored (sect. 5.1). As it was difficult to achieve reliable voltage switching with the complex circuit which controlled the quadrupole potentials, the lens was redesigned with separate steering and focussing electrodes (fig. F3-5, F3-6).

The supply circuit (fig. F3-7) used an emitter follower system to remove the dependence of the voltage step (ΔV_q) on the network resistance. A six digit voltmeter (Hewlett Packard 3406A) was used to calibrate the circuit within the limits previously tolerated (20mV). The calibration has been stable for about two years, and was found to be unaffected by transistor replacements or temperature change. Checks were made on the influence of temperature changes on the transistors, on the linearity of the resistor network, and on the variation of the ratio $\Delta V_q/V_q$ with V_q. Time constants for the voltage changes were

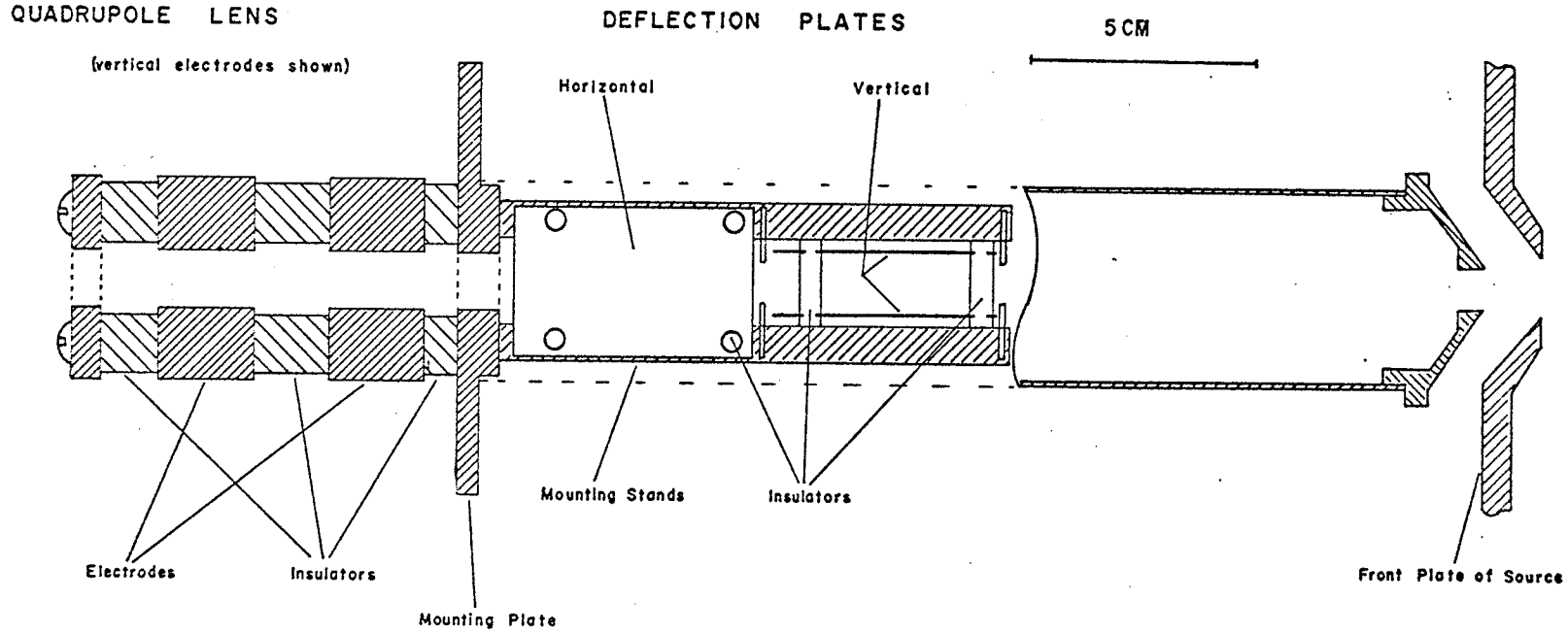

FIG. F3-5 FOCUSSING AND STEERING ELETRODES

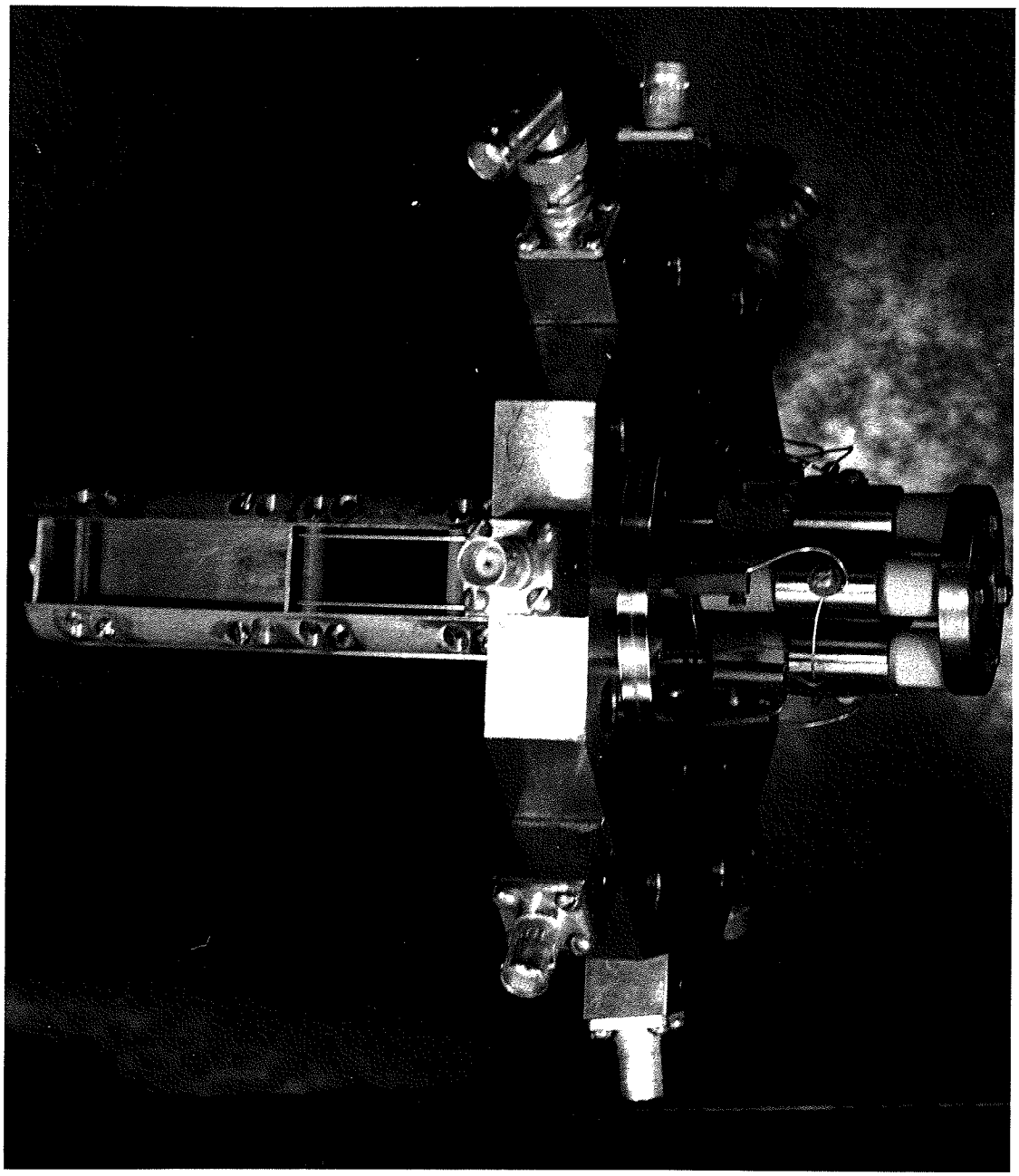

FIG. F3-6 FOCUSSING AND STEERING ELECTRODES

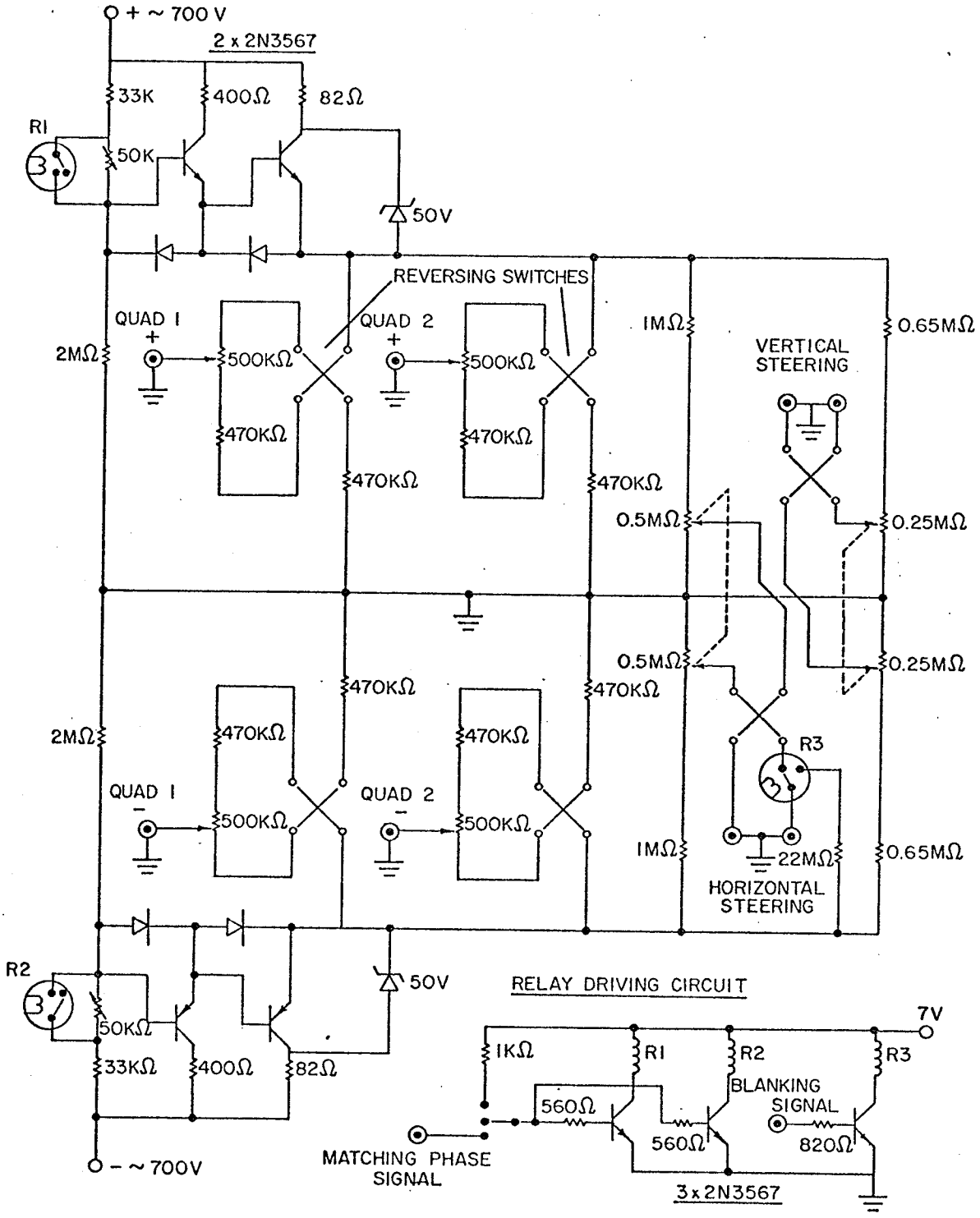

FIG. F3-7 QUADRUPOLE AND STEERING SUPPLY SYSTEM

below 50 microseconds.

3.5 ELECTROSTATIC ANALYSER SUPPLY SYSTEM

The system that applies and measures the voltage to the plates of the electrostatic analyser was designed and built by Bishop and Barber and is described in detail (Bi69, Ba71). Fig. F3-8 shows the circuit after some recent modifications.

The analyser voltage (V_e) is applied to the plates by a set of 97.2V mercury batteries and the small stepping voltage (ΔV_e) from a separate source (sect 4.4) is applied to R_0, such that it is added to or subtracted from V_e. Measurements are made by a potentiometer system consisting of a 2.5 megohm chain of precision resistors (R_1-R_9) and a 7 decade 100 kilohm Kelvin - Varley divider (VDR). The potentiometer is driven by a 100V power supply using as a reference a separate 97.2V mercury battery. The potential of each mercury battery in the V_e supply can be measured by comparing it against the potential between points a and b (fig. 3-8) and ΔV_e can be measured by balancing it against the potential between points a and d.

The resistor chain components can be accurately compared with the VDR total resistance by means of a

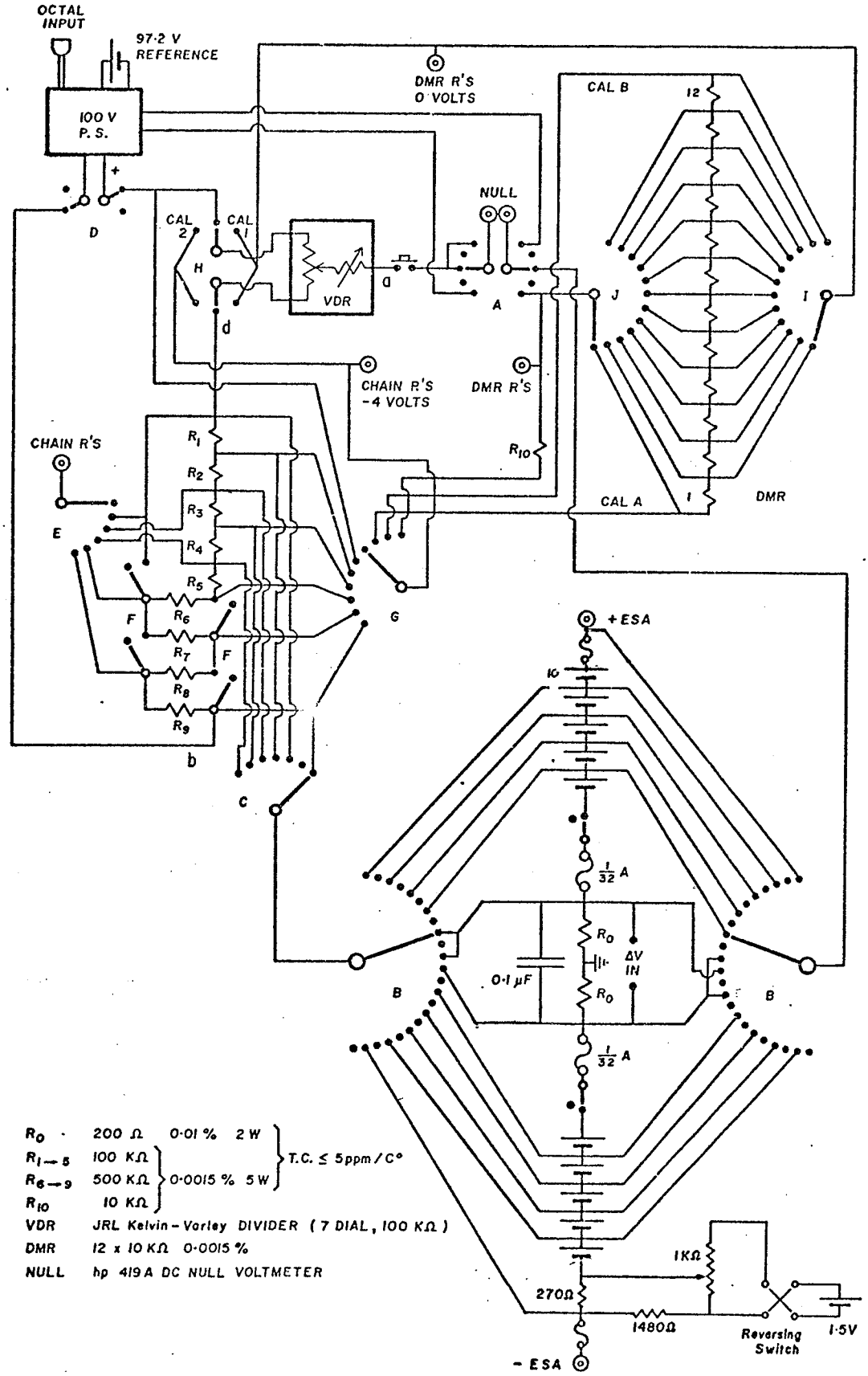

R_0	200 Ω	0·01 % 2 W	T.C. ≤ 5ppm/C°
R_{1-5}	100 KΩ	0·0015 % 5 W	
R_{6-9}	500 KΩ		
R_{10}	10 KΩ		
VDR	JRL Kelvin-Varley DIVIDER (7 DIAL, 100 KΩ)		
DMR	12 x 10 KΩ 0·0015 %		
NULL	hp 419A DC NULL VOLTMETER		

FIG. F3-8 ELECTROSTATIC ANALYSER SUPPLY SYSTEM

wheatstone bridge. The following independent calibration methods are available:

(a) a comparison of each of R_1 through R_5 with the VDR, followed by a comparison of each of R_6 through R_9 with the sum of R_1 through R_5, and

(b) a comparison of the parallel combination of R_6 through R_9 in parallel with the series combination of R_1 through R_5 with the VDR.

These two calibration techniques are regularly in close agreement (less than 1ppm).

The remaining feature in the calibration of the potentiometer is the establishment of the linearity of the VDR. This is done by the comparison of many ratios with a subsidiary chain of resistors (DMR)(see Bi69).

On the basis of the chain to VDR resistance ratio calibration and the linearity check on the VDR, the desired-voltage ratio ($\Delta V_e/V_e$) can be established with a precision of $0.5 \times 10^{-6}\ \Delta V_e$ and $0.5 \times 10^{-9}\ V_e$.

The divider has been calibrated a number of times, and the results are shown in table T3-1. The correction factors relating the individual sections of the chain show similar variations. Thus changes significant to the measurement of ($\Delta V_e/V_e$) occur primarily in the VDR. Moreover there is no

TABLE T3-1

POTENTIOMETER CALIBRATION FACTOR

DATE	CALIBRATION FACTOR (ppm)
Oct 1968	10.0 ± .3
Dec 1968	10.4 ± .3
July 1970	12.4 ± .2
June 1971	6.1 ± .1

evidence of switch resistance contributing to the error.

The most crucial mass measurements were undertaken during the first six months of 1971. The calibration correction over this period was obtained by a linear interpolation between the last two figures of table T3-1, and a 3ppm error on the correction was estimated. This made a significant contribution to the final error (see sect. 6.1).

Tests were made on the way in which the measurement of ΔV_e (0-12V) was affected by moving the point at which the potentiometer was grounded. Variations up to 30 μV were detected with associated time constants of about 2 minutes. These variations were found to be associated with leakage in the power supply for the potentiometer. A redesigned power supply with a specially constructed isolation transformer (fig. F3-9) overcame this problem. The isolation resistance of the potentiometer circuit was thus improved to over 10^{12} ohms, and the 60 cycle interference was reduced to 100μV.

Although ten batteries may be used to supply V_e as indicated in fig F3-8, only eight actually were used (as in previous work (Bi70)), so that the electrostatic analyser voltage was 778V. In addition, each of the single Eveready

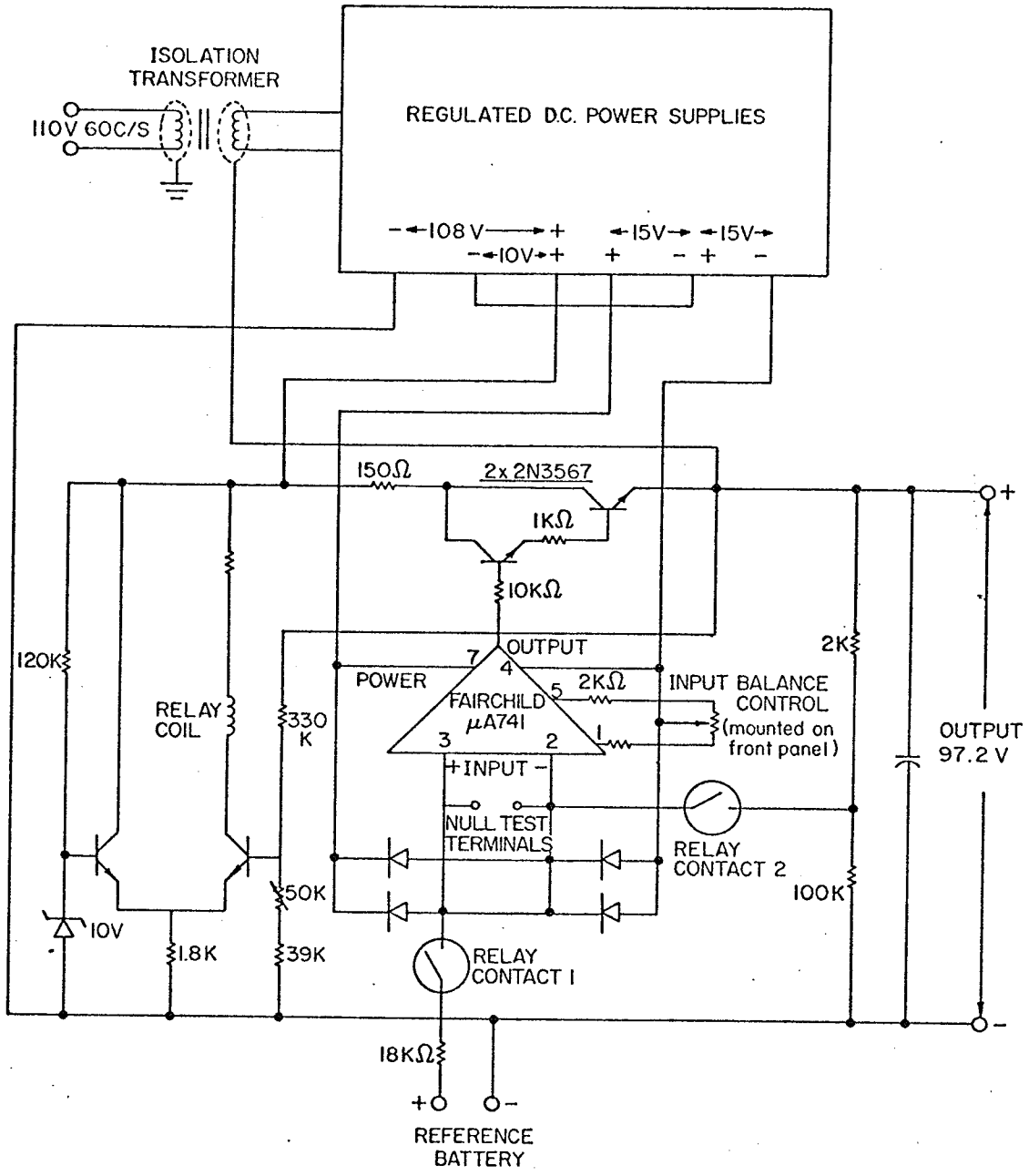

FIG. F3-9 POTENTIOMETER POWER SUPPLY

E-302462 97.2V batteries was replaced by twelve Mallory TR-136R 8.1V batteries in order to take advantage of cheaper replacement and faster supply. Stability in V_e during a day's operation was better than 50 μV and day to day changes were seldom above 1mV.

Other modifications made to the potentiometer system are the following:

(a) Switch C was changed to allow access to the end of resistor R_4, so that the measurable range for ΔV_e was extend to 19.5V and ratios of $\Delta V_e/V_e$ measurable were extended to 1/40.

(b) The positions of the switches and fuses in the battery chain were moved to avoid introduction of thermal effects in the measurement of ΔV_e. Spurious voltages up to 20μV had been measured.

(c) A small voltage supply was added to one of the batteries (see fig. F3-8) to permit the adjustment of the voltage of the positive analyser plate and thus to apply V_e to the analyser symmetrically about ground.

3.6 BASIC ELECTRONICS

Magnet Supply

The power supply for the magnetic analyser provides up

to 60 amps at 40 volts. High stability is required to prevent movement of the peaks during measurement, and the resulting artificial broadening of the peak as it is accumulated in the signal averager.

A small fractional change in the magnetic field strength ($\Delta B/B$) will produce a shift in the peak position equivalent to that produced by a change of mass $\Delta M/M$. These are related (appendix, eqn. A-12) by the equation:

$$\Delta M/M = 2\Delta B/B \quad . \qquad (3\text{-}1)$$

Therefore the fractional variations in the magnetic field must be half those pemissable in the equivalent fractional mass shift, which is a small fraction of the resolution required. Stability approaching $1/(6\times10^{6})$ in several minutes was achieved using two parallel control systems (fig. F3-10):

(a) A D.C. control for long term stability. The difference potential between a reference voltage and the voltage developed by a .122 ohm shunt is amplified by over 10^{6}, and controls a transistor pass bank.

(b) An A.C. control for short term stability. The voltage generated by current fluctuations over the inductance of the magnet windings is integrated with a time constant of 0.15 seconds, amplified by approx. 10^{3} and

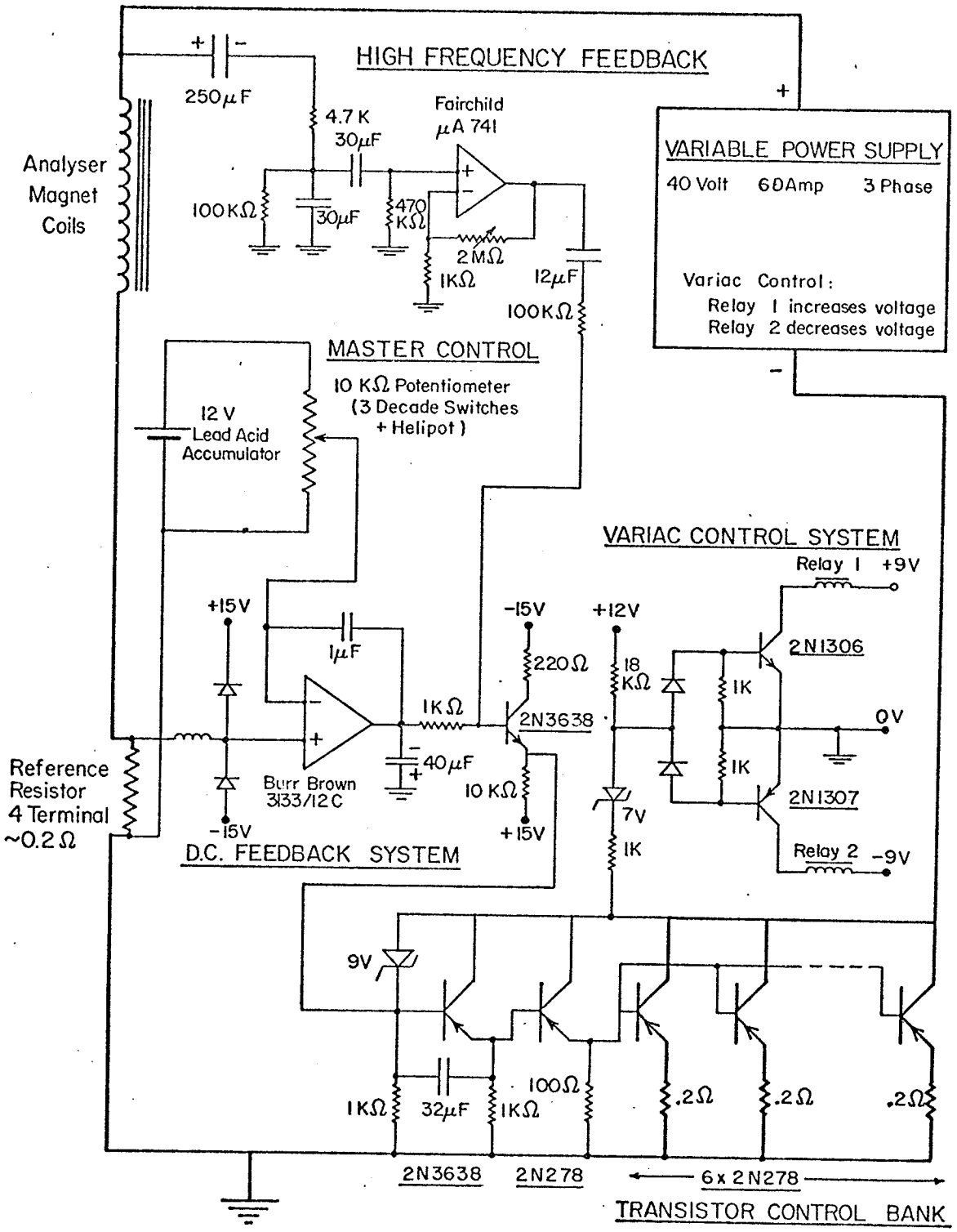

FIG. F3-10 ANALYSER MAGNET SUPPLY SYSTEM

combined with the D.C. control of the transistor pass bank.

Magnetic Sweep.

The magnetic sweep for the spectrum display (sect 2.2) is provided by Helmholtz coils mounted immediately after the magnetic analyser (fig. F3-1) and the power supply is shown in figure F3-11. The requirements for the sweep signal are:

1. synchronisation with the oscilloscope and with the signal averager,

2. linearity of the ramp, and

3. reproducibility on successive sweeps.

The sawtooth control signal is derived from the horizontal sweep output of the oscilloscope which is synchronised with the signal averager as described in sect. 4.4.

Sufficient linearity of the ramp and reproducibility on successive sweeps was attained by:

(a) use of a current defining amplifier for current in the Helmholtz coils,

(b) careful regulation of the sawtooth amplifier power supply, and

(c) reduction of the influence of variation in dead times between successive sweeps by selecting relatively long dead times (fig. F4-6).

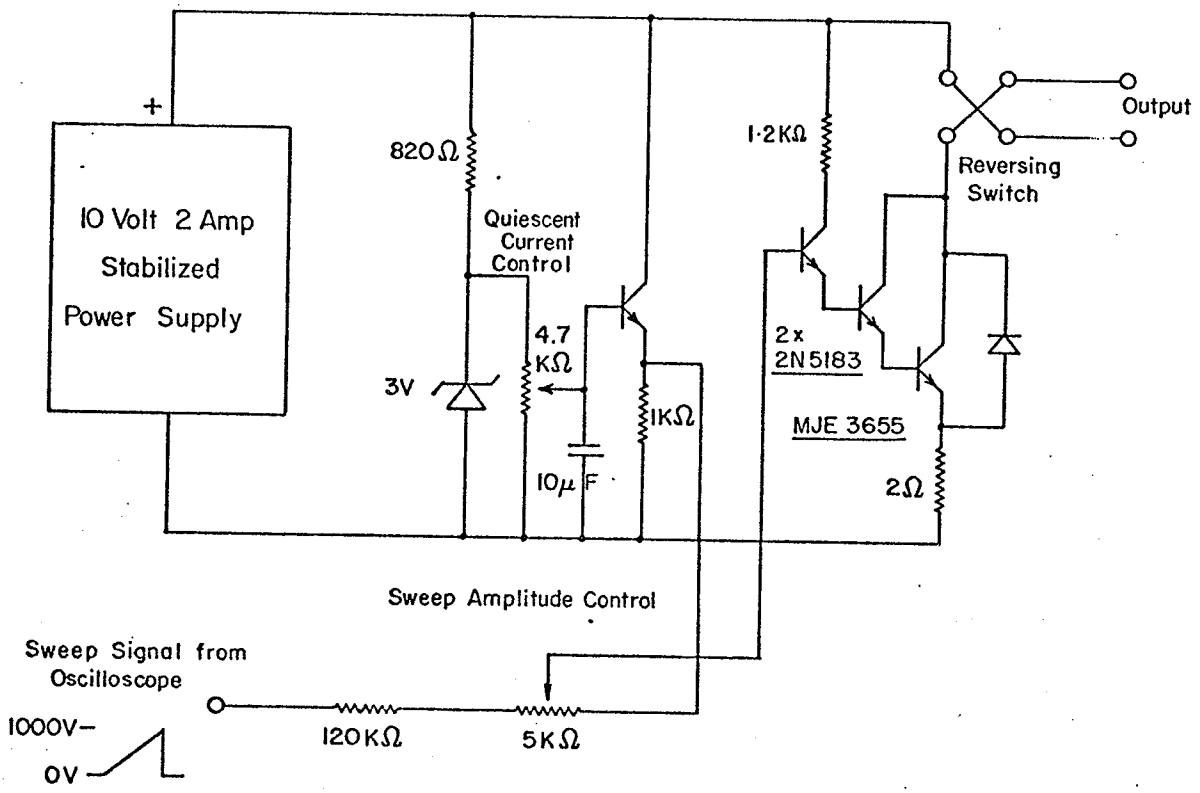

FIG. F3–11 MAGNETIC SWEEP SUPPLY CIRCUIT

High Voltage Supply and Control.

The source potential (V_a) is supplied by a Universal Voltronics Model BRE 20-2, 30 kilovolt, 2 milliamp, variable voltage supply, having a short term stability of better than 0.5 volts. The various power supplies for the source, and the circuit used to add ΔV_a to the source voltage, are contained in an insulated cabinet with a common connection at the source potential V_a (usually 20KV).

The ΔV_a system had to be improved to provide the required stability and control for the measurement of the wide mass doublet. ΔV_a was derived from a Kepco ABC-425, 425volt programmable power supply (fig. F3-12), which was controlled by a pair of ten turn potentiometers. The stability of ΔV_a was 2mV, and the resolution in adjustment was 10mV. Two alternate controls were provided, and certain fixed voltages could be selected and added to ΔV_a to allow for a check on the velocity focussing at any time (sect. 4.3). The system was protected against high voltage breakdown in the source by a spark gap and neon bulbs. The voltage was switched by a non-shorting reed relay driven by a neon-photocell coupling link which transmitted the signal into the insulated cabinet. Phasing details are given in section 4.4. The switched wave form had a slight oscillation

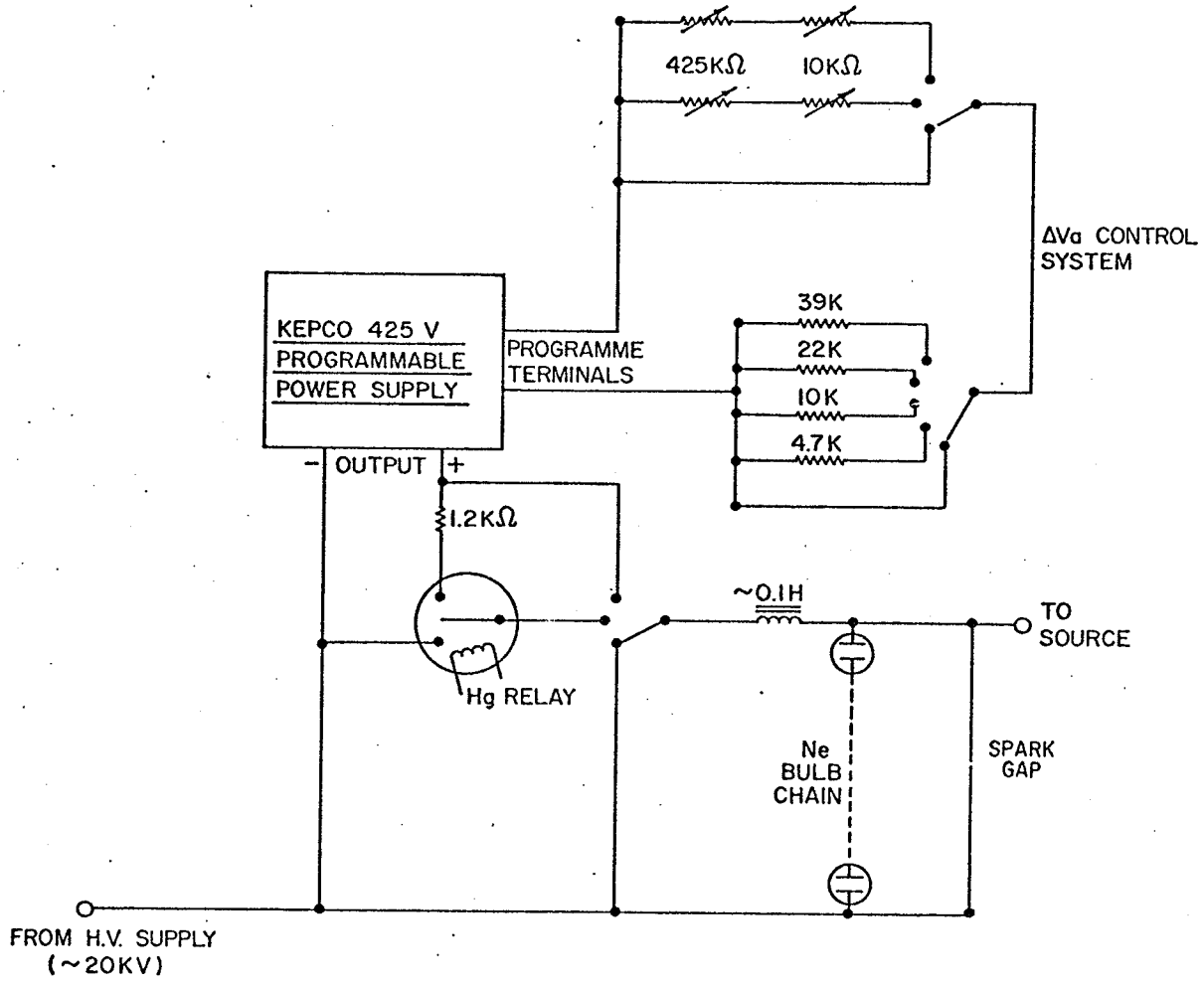

FIG. F3-12 ACCELERATION POTENTIAL SWITCHING SYSTEM

with a decay constant of approx. 0.1 milliseconds.

A block diagram of the power supplies for the high voltage system is given in fig. F3-4.

CHAPTER 4

PEAK MATCHING

4.0 INTRODUCTION

Section 2.3 describes how comparison of ion masses can be obtained by determining the coincidence of ion peaks on an oscilloscope display. This chapter describes the determination of peak coincidence conditions. Two methods were used: visual matching as a quick, medium precision method for wide calibration doublets ($\sigma/M \sim 10^{-7}$), and the computer - assisted method for high precision measurements.

4.1 VISUAL MATCHING

Although Smith originated the visual matching technique, the first published description of it was given by the Minnesota group in the early fifties (Gi54). The matching was done by displacing alternate traces on an oscilloscope screen, and lining up the peaks, one above the other. Improvements have since been made in the determination of the matched condition by splitting one of

the peak forms (Sm56, Mo64), or differentiating the wave forms (Og67). A related, but much more precise system using a lock-in amplifier was developed by Bainbridge and Dewdney (Ba67a).

The "visual null" matching system used here employs a digital signal averager on line to determine the difference between the peak forms. This technique, which was first used by Benson and Johnson in 1965 (Be65, Be66), and soon after by Macdougall (Ma66) and others (St67, Ba67) is of comparable precision to that of the method using the lock-in amplifier.

The electron multiplier output signal which appears on the oscilloscope display (sect. 2.2) is also sent to the signal averager. The oscilloscope and the signal averager sweeps are synchronised. The signal averager memory is switched alternately from the add mode to the subtract mode, so that one peak is added into the memory, while the other is subtracted. The memory contents, which are continuously displayed, show the difference between the peak forms as the results of a large number of scans are accumulated. The amplitudes and relative positions of the two peaks are adjusted so that the difference wave form is a completely symmetric noise pattern, indicating that the peaks are in

coincidence. A more detailed description of this technique is given by Bishop (Bi69). Section 5.5 describes the use of these measurements in this work, and section 4.4 the electrical circuits used.

4.2 COMPUTER - ASSISTED MATCHING

The matched condition may be determined by finding the degree of mismatch for several different nearly - matched conditions which bracket the matched configuration. Aston (As22) and Costa (Co25) used this method, referred to as the "method of bracketing", in which two close determinations were taken simultaneously on a photographic plate. Several recent investigators also have taken a number of determinations in sequence using different techniques (St67, Ke70, Ma70). Kayser (Ka72) has incorporated the basic method with a system of "peak unfolding", i.e. the separation of unresolved peaks.

The system used here for the earlier measurements, which comprise the majority of the chlorine measurements (sect. 6.1), has been described by Meredith (Me71, Me73). Three different closely-matched conditions are obtained in effect simultaneously. A cycle of four different sweeps is made about ten times per second, each sweep having a

different potential added to the electrostatic analyser potential as shown in fig. F4-1. When the original circuit was used voltage stability problems were experienced with the larger ΔV_e values required in the wider mass difference measurements. These problems were eliminated by altering the sequence of potentials as shown in figures F4-1, F4-2. The modified system was used for the remainder of the measurements. The value of δV is typically around 200 μV, and the shift about 1/50 of a peak width.

The signal averager cycles in phase with the linear ramp of the sawtooth described above. The memory of the signal averager is divided into four "quadrants" in which are stored the four separate spectra corresponding to the four different analyser potentials. When sufficient information is stored in the signal averager, it is recorded on magnetic tape, and, together with the appropriate voltage readings (taken manually at the time of the measurement), is analysed off line by an IBM 360/65 computer to determine the matched conditions.

The circuit that provides the appropriate voltages to the electrostatic analyser is described in section 4.3, the computer analysis in section 4.4, and the error analysis in section 5.6.

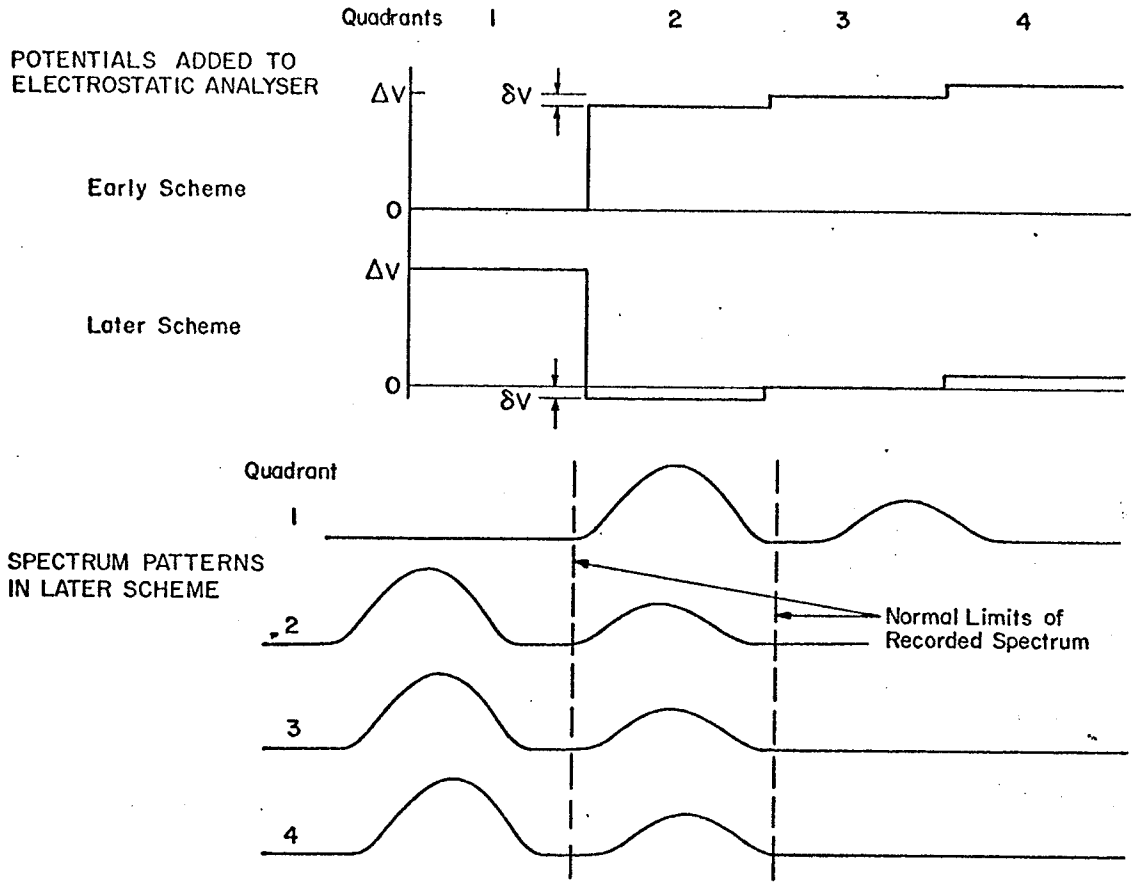

FIG. F4-1 .BASIC SWEEP SEQUENCES FOR COMPUTER-ASSISTED MATCHING

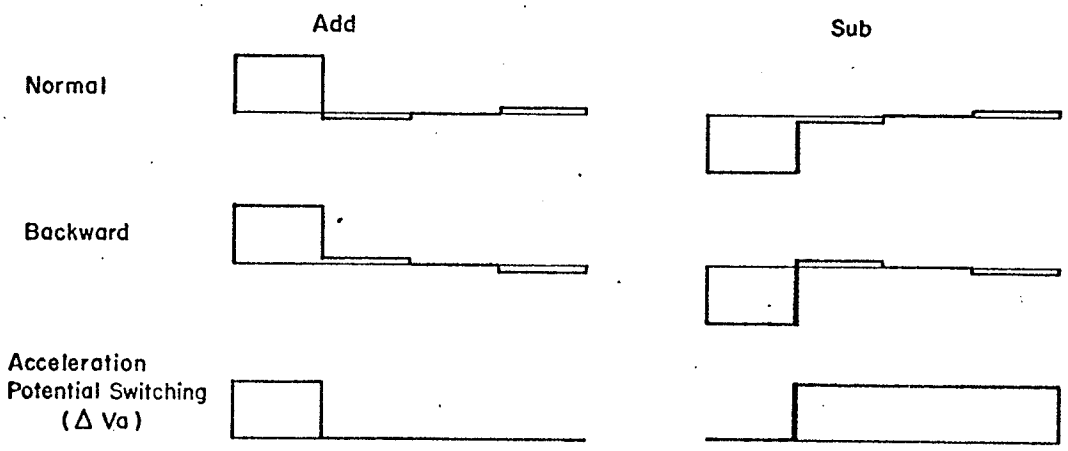

FIG. F4-2 PERMUTATIONS OF SWEEP SEQUENCES

In a manner which is similar to previous visual or computer matching done by this group, the matches are taken in sets of eight, called a "run", where each match consists of a different permutation of the sign of all unsymmetric switchable functions. In this case they are the following:

1. Polarity of ΔV_e (add/sub). This changes the roles of the two peaks (see sect. 2.3).

2. Polarity of δV (normal/backwards)

3. Direction of the current in the magnetic sweep coils (foreward/reverse). This changes the direction of the sweep of the beam across the exit slit.

Figure 4-2 shows the sequences of voltages added to the electrostatic analyser (ΔV_e) and the acceleration voltage (ΔV_a).

The results of these matches are combined in order to compensate for systematic errors that may derive from these factors.

The procedure for a complete run is as follows:

1. The δV voltages are applied across the battery chain resistors R_0 (fig. F3-8) and measured with the potentiometer. The actual voltages applied in quadrants two and four for both the normal and the backwards modes are measured to allow for differences in thermal effects and

resistance values. A measurement is also taken in quadrant three (no potential applied) to check for any zero error in the potentiometer.

2. Eight matches are made, one for each permutation described above. For each match the signals are accumulated for up to about three minutes, or until the averager memory is full, and then the memory is recorded on magnetic tape. A measurement is made of ΔV_e, the signal averager memory zeroed and the next match taken.

3. δV measurements are repeated as in 1. above. If there are any changes in the δV readings before and after the run (usually less than 1 microvolt), an average is calculated, and applied to the whole run.

There are several possible error sources which are cancelled out by the sequence of matching configurations used and these have been considered in detail by Meredith (Me71). Comparisons were made between the average result for each matching configuration and the final overall average value determined for the mass doublet. Although there were some quite marked differences within results for a given doublet, the pattern was not consistent with that for results of other doublets. For example, a significant add/sub difference occurring in the chlorine measurements

was reversed for the Nd - Lu measurements.

4.3 MATCHING CONTROL SYSTEMS

Analyser Stepping for Visual Matching.

This system (fig. F4-3) is a modified version of the system described by Bishop (Bi69). The chopper is installed within the temperature controlled box of the electrostatic analyser supply system and ΔV_e is applied directly to the battery chain resistors, while the d.c. supply is mounted outside. The system is controlled by the same Guildline 9742A, 4pole, low thermal E.M.F. chopper, driven by a synchronous motor through an O-ring and pulley drive. This drive arrangement results in a reasonably stable chopper frequency that is not a harmonic of the mains frequency. A sense circuit has been introduced to provide for the new large ΔV_e supply system (see later this section), leaving two poles in parallel to switch the ΔV_e signal. Precautions have been taken to reduce resistance due to spark wear by setting one of the two contacts to open first and close last, thus protecting it from sparking. As before, dummy resistors have been provided to present the same load to the supply in both on and off positions. Bistable mercury switches replaced toggle switches for on/off and reversing

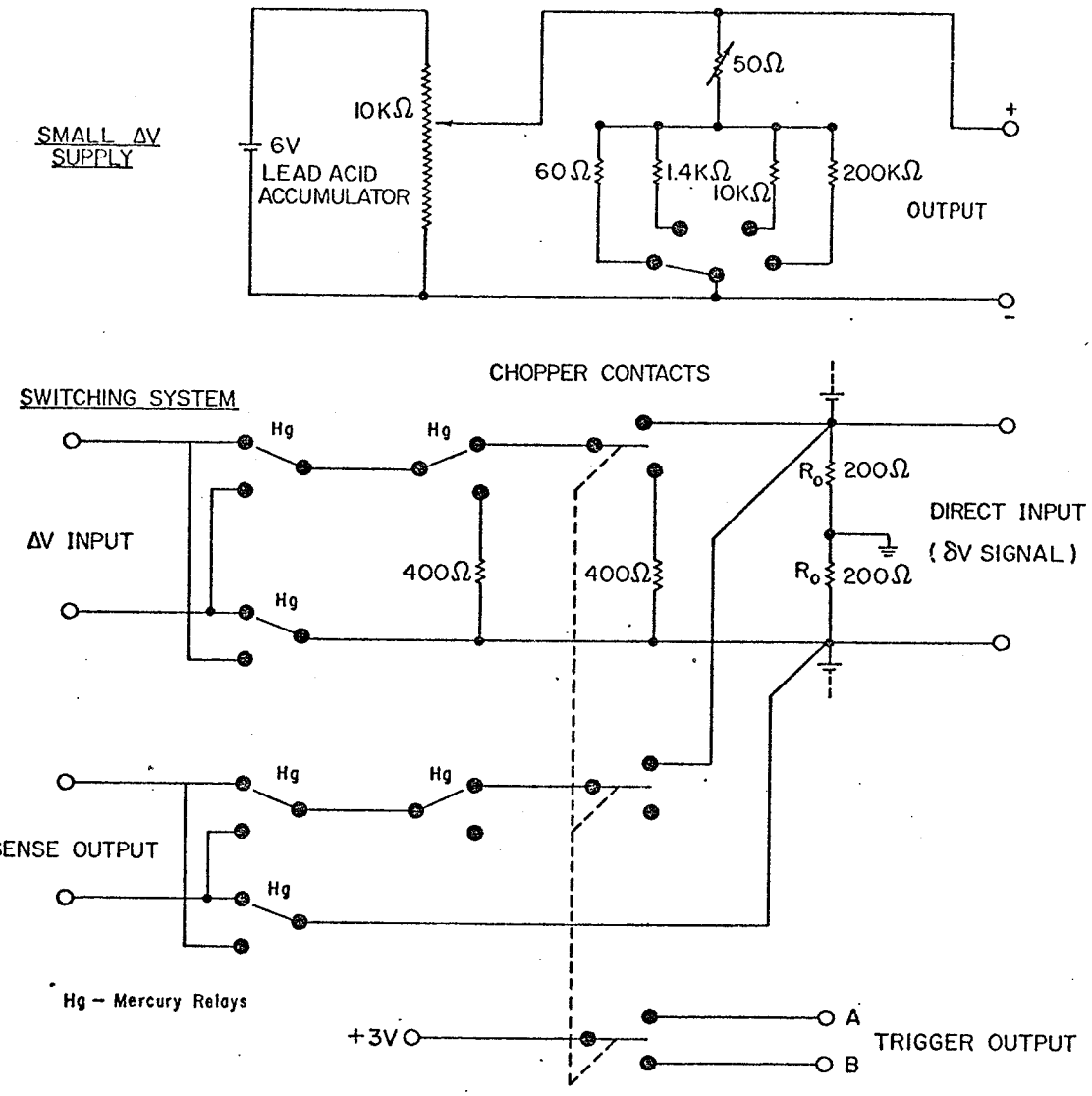

FIG. F4-3 VISUAL MATCHING CONTROL SYSTEM

functions. The mercury contacts give a consistent resistance, and are operated by very short pulses ($\sim$ 5ms) which produce a negligible heating effect.

Analyser Stepping for Computer - Assisted Matching.

Two circuits have been used in these measurements as described in section 4.2. The first was described by Meredith (Me71) while the second is shown in fig. F4-4. The system sits outside, but close to, the temperature controlled box of the electrostatic analyser supply system.

ΔV_e and δV (sect. 4.2) are generated and applied independently to the load resistors R_o (fig. F4-3). An external decade potentiometer driven by a lead acid accumulator proved to be adequate as a ΔV_e supply for the voltage range used (<0.3V). The output terminals of the chopper are connected to the ΔV_e terminals of the potentiometer box (fig. F4-3). The chopper for the "visual null" method must be left in the "on" position. The signal then can be switched and reversed by using the "visual null" matching controls.

The δV supply is a low impedance chain whose output is supplied to the battery chain through the direct terminals shown in fig. F4-3. The range of δV is 10 - 500 μV, and the

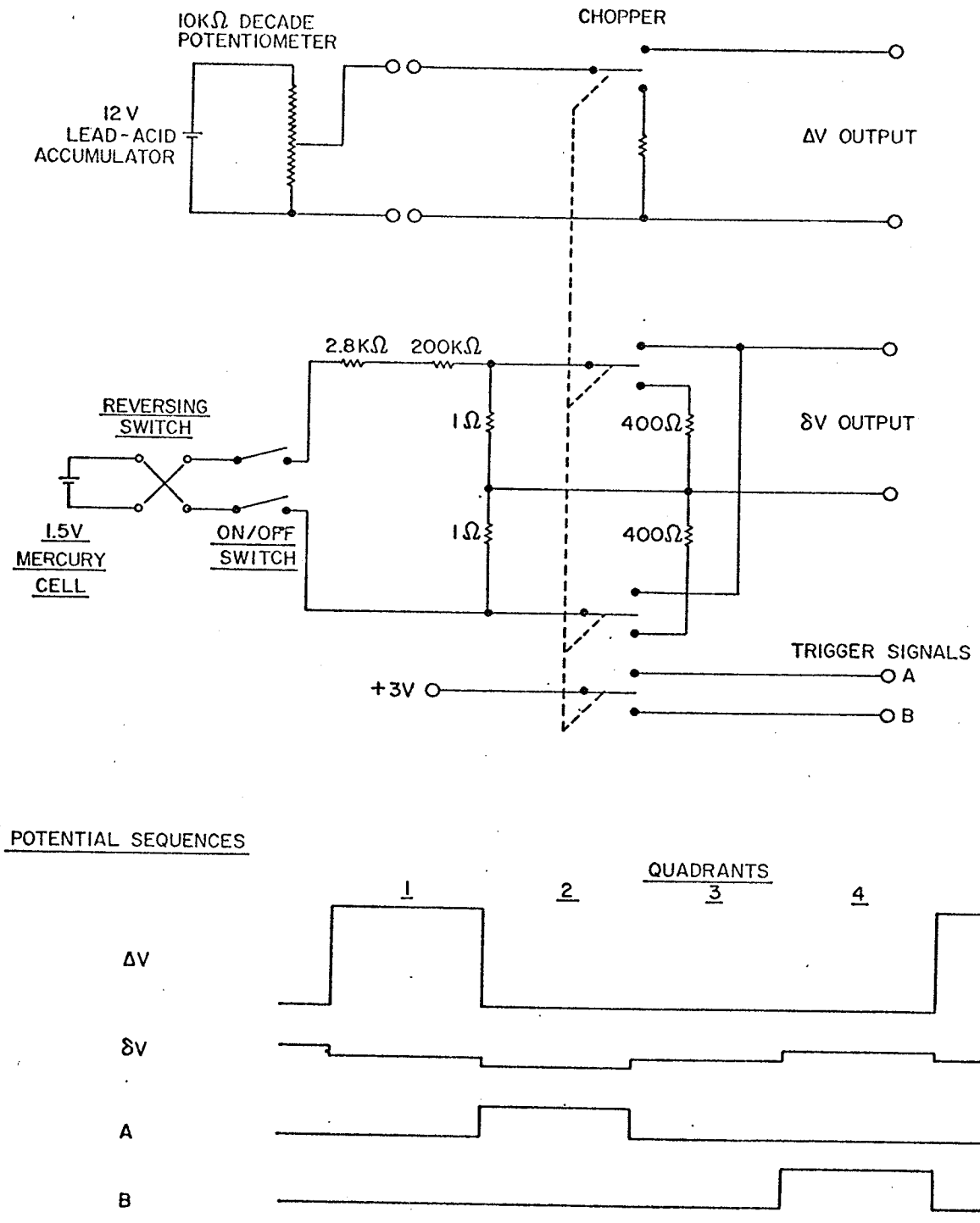

FIG. F4 - 4 COMPUTER - ASSISTED MATCHING CONTROL SYSTEM

normal operating region is 200 μV. Although some variation of thermal effects due to temperature change may be detected, the supply is sufficiently stable for reliable results during normal running (<1 μV variation).

Trigger System.

A block diagram of the trigger control circuit is shown in fig. F4-5, and the wave forms are shown in fig. F4-6. The following points should be noted:

1. The chopper triggers the signal averager. In computer matching, external circuitry stops the signal averager between quadrants.

2. The oscilloscope is triggered by the fourth binary on the signal averager address register, i.e. the eighth channel of each quadrant. This ensures that the oscilloscope, which provides the signal to drive the beam sweep, is always in phase with the signal averager memory. The trigger signal has a 50 nanosecond rise time to reduce errors in triggering.

3. The subsidiary control signals (acceleration and quadrupole potential switching) are switched immediately after the oscilloscope sweep finishes to provide maximum delay time for the voltages to stabilise. The switching is

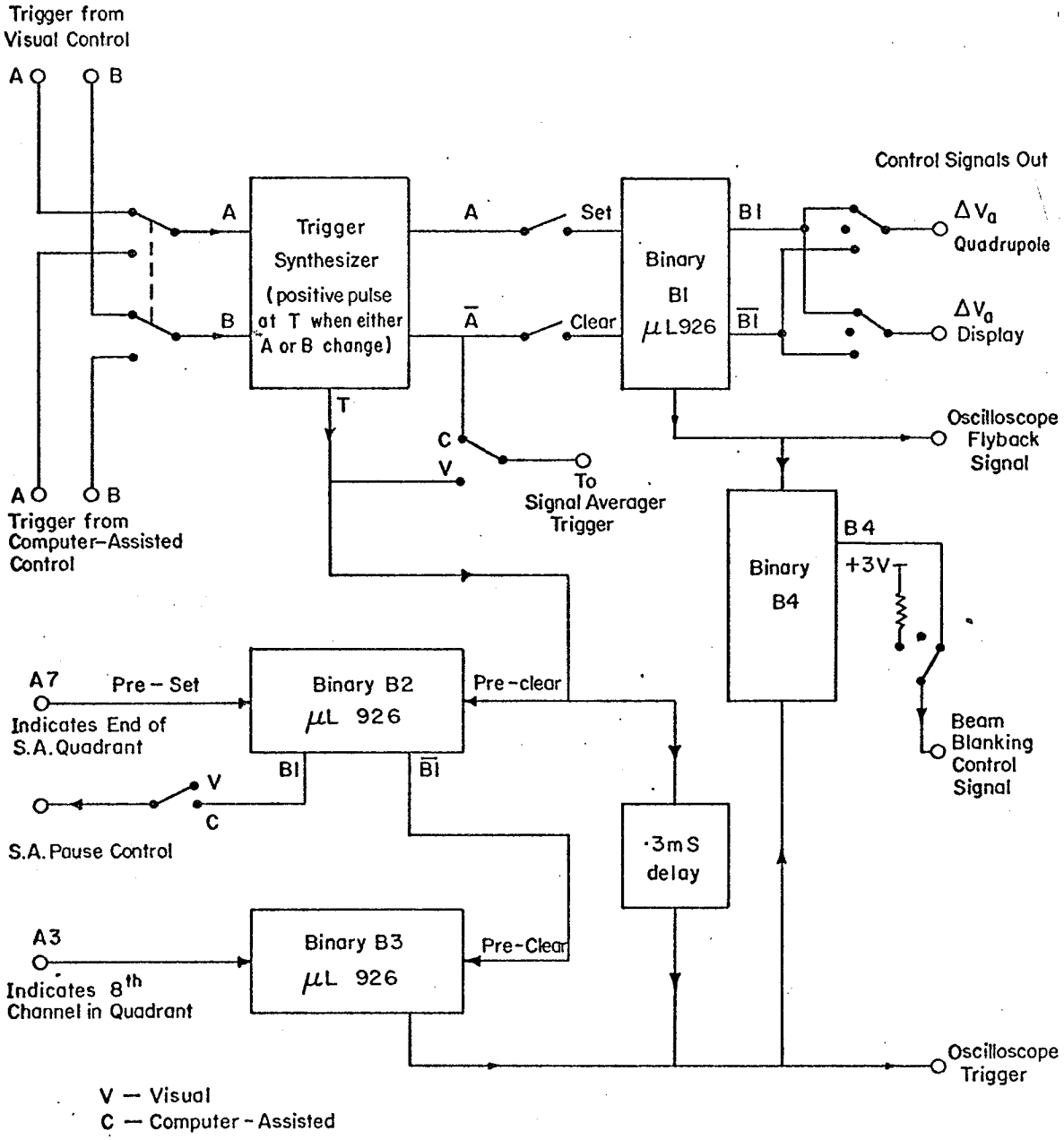

FIG. F4-5 TRIGGER CONTROL SYSTEM

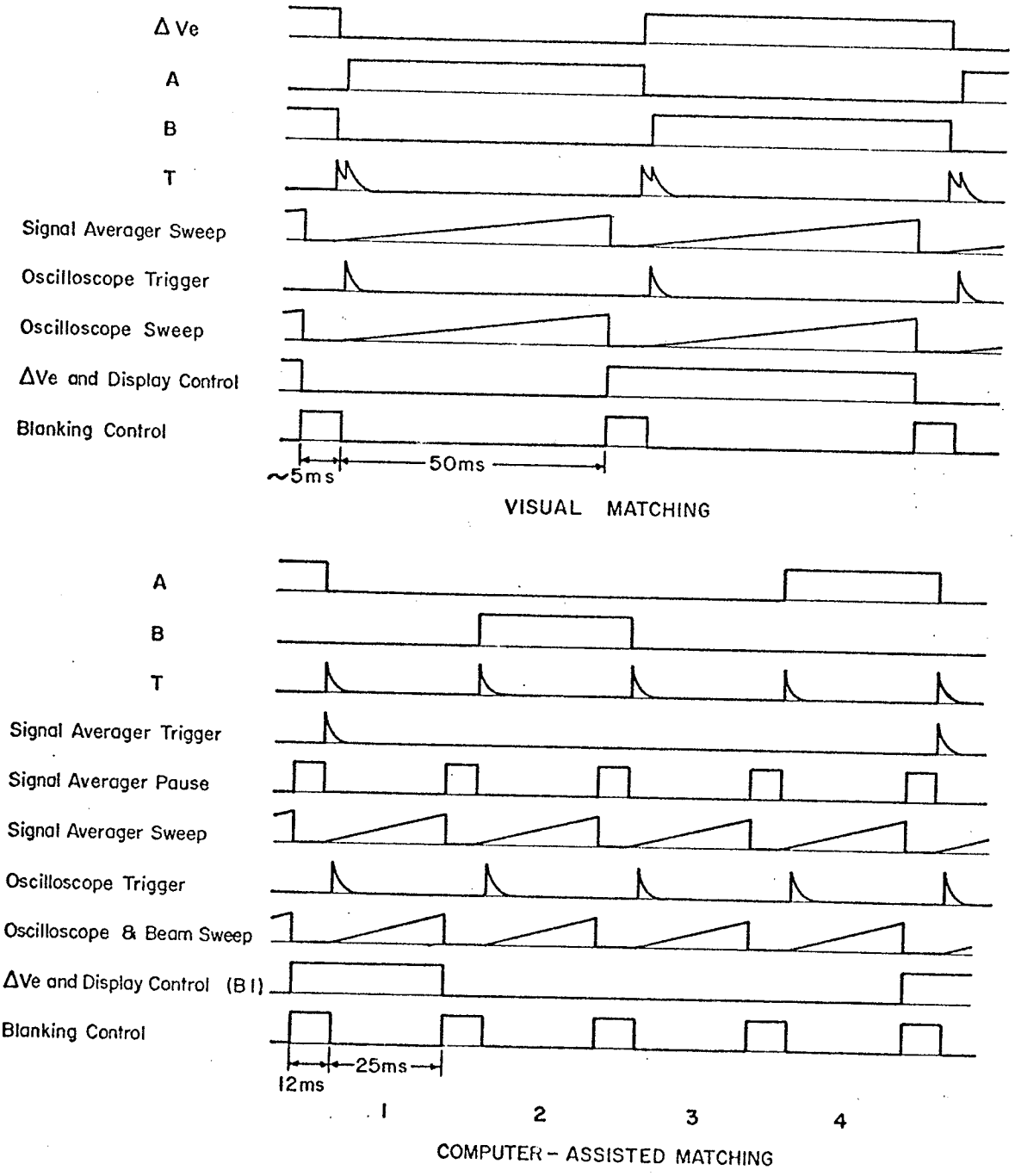

FIG. F4-6 CONTROL SYSTEM WAVE FORMS

triggered by the oscilloscope sweep flyback, and the switched state is determined by the A signal state at that time (fig. F4-5).

4. The beam-blanking control (sect. 5.5) can be activated during the oscilloscope dead time.

Figure F4-7 shows the overall control system for the instrument.

Large ΔV_e Supply

This was developed initially to supply a highly stabilized voltage of up to 10 volts into a load of 400 ohms as required for precise wide doublet measurements (sect. 5.1). The supply was subsequently modified and retained for use in supplying the large ΔV_e (up to 16V) required for the calibration doublets (fig. F4-8).

A reference voltage is obtained from a decade box driven by an 18V lead acid battery. The last decade of the potentiometer was replaced by a helipot mounted for convenience near the operator to provide fine control. The power supply follows this reference voltage by comparing it with the "sense" signal derived from the 400 ohm load-resistor. In this way, the voltage across the load is accurately referred to the reference voltage, and is

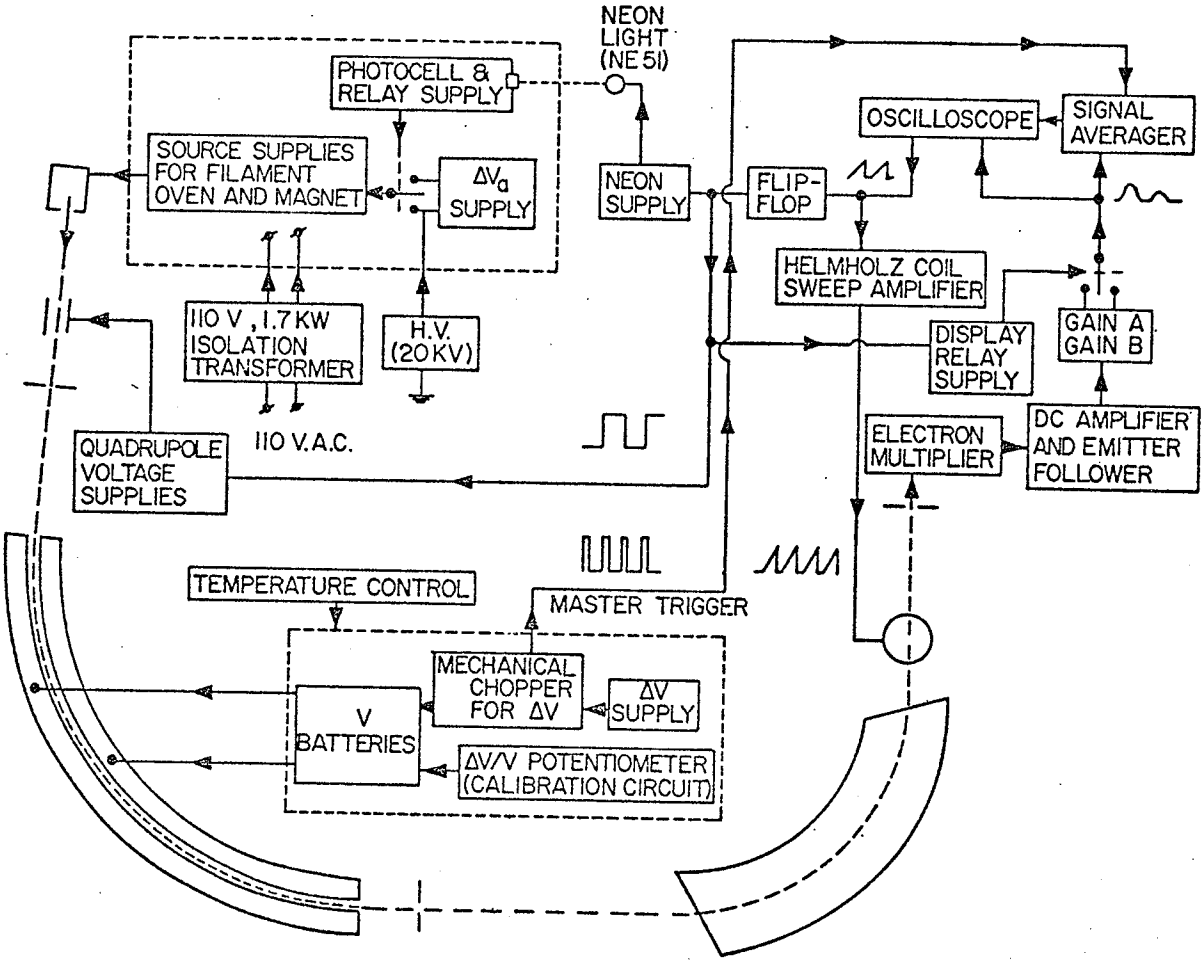

FIG F4-7 OVERALL CONTROL SYSTEM

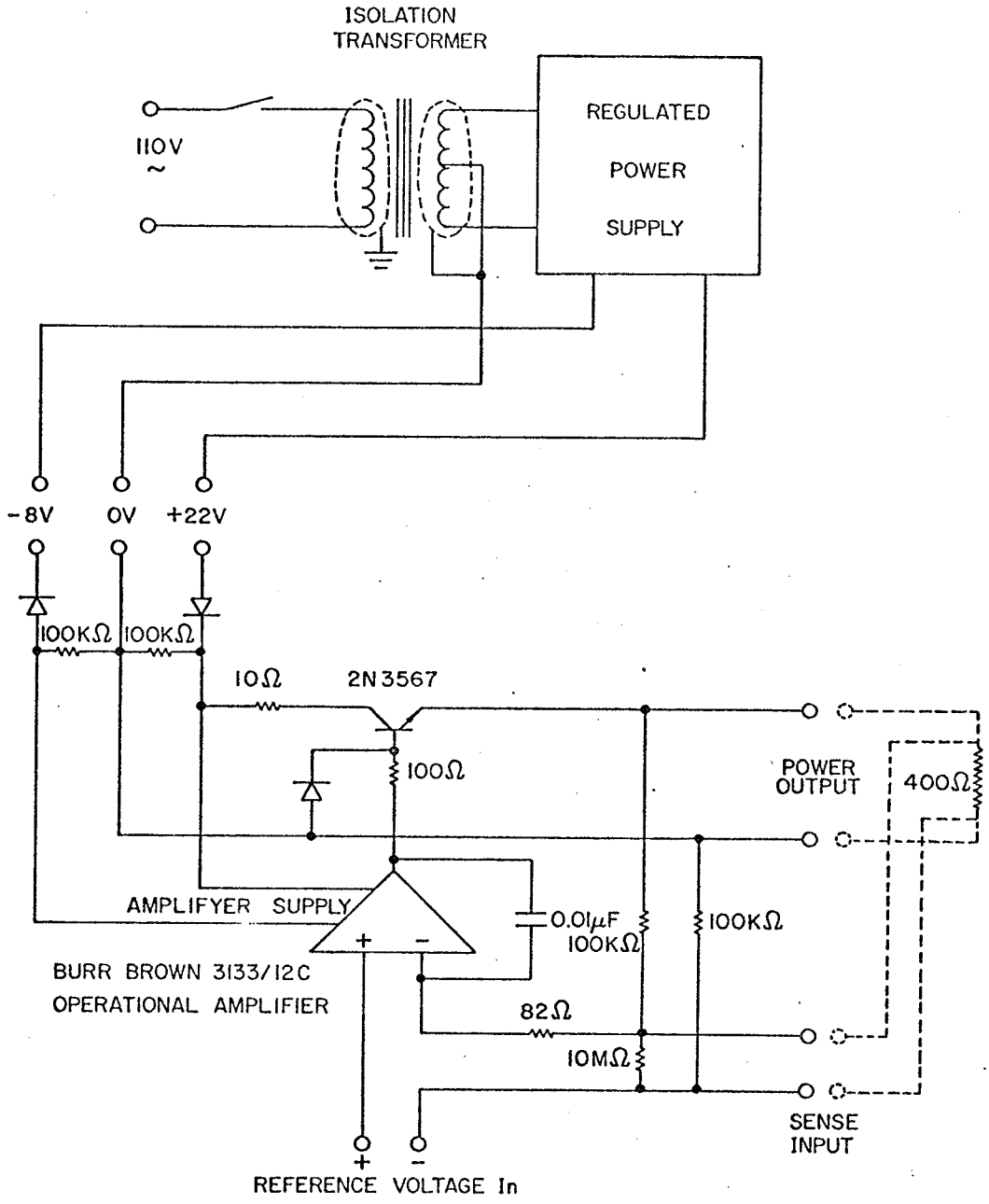

FIG. F4-8 LARGE ΔVe SUPPLY

independent of any changes in resistance in the supply cables or switches. The sense signal is chopped so as to be compatable with the supplied voltage (fig. F4-3).

4.4 COMPUTER ANALYSIS

Apart from the spectrum subtraction used for visual matching (sect. 4.1), several variations of digital analysis have been used to improve peak matching (Stevens (St67), Kaiser (Ka72), and Meredith (Me71, Me73)). In the computer matching analysis used extensively by this group, Meredith calculates peak displacements from the peak centroids using an IBM 360/65 computer off line. An alternate system of comparing peak positions was used here which was inspired by Stevens' system and is similar, in principle, to the "visual null" matching system (sect. 4.1). It is based on the subtraction of two peaks, one being modified by appropriate displacements and height ratio.

The data collection system in which four peaks are accumulated in the four quadrants of the signal averager memory is described in section 4.2. Figure F4-9 illustrates the method of peak comparison. Shown are the two peaks $V_1(x)$ and $V_2(x)$, each stored as a sequence of 256 numbers. Peak limits, X_1, X_2, in each quadrant are defined identically for

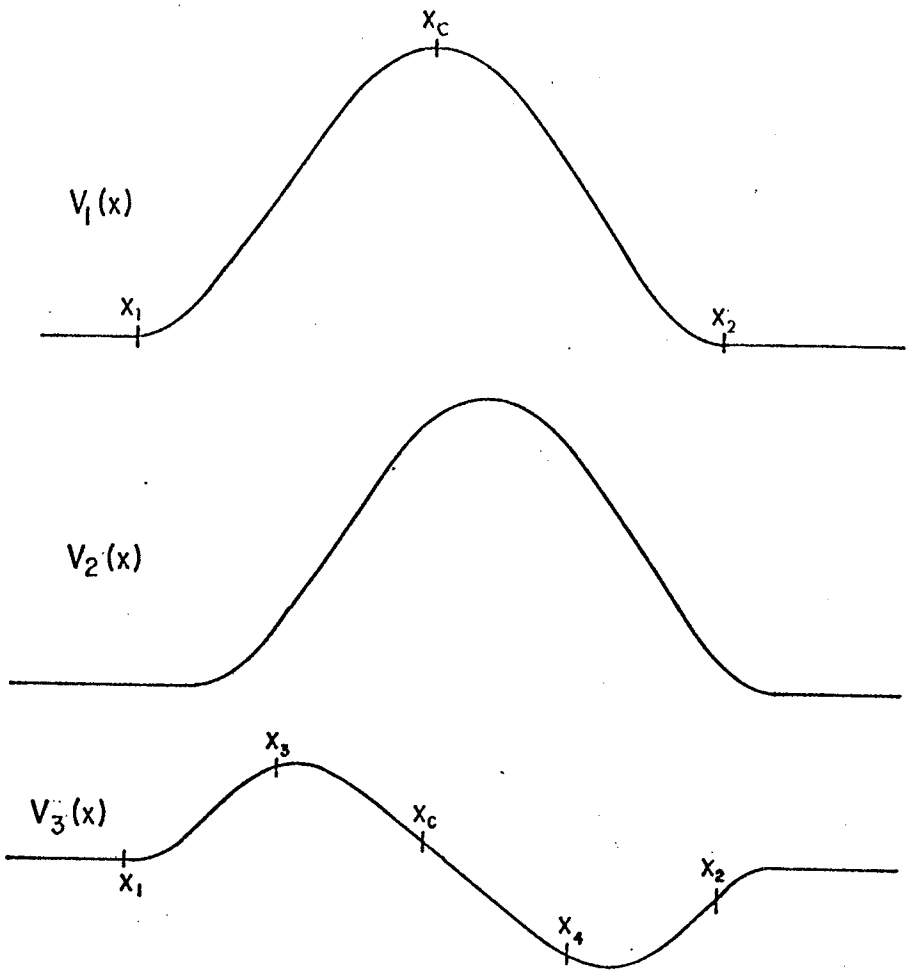

$$V_3'(x) = V_1(x) - F \times V_2(x - D) \qquad (4-1)$$

$$V_3(x) = V_3'(x) - \overline{V_3'} \qquad (4-2)$$

$\overline{V_3'}$ = average of $V_3'(x)$

$$T_1 = \sum_{X_1}^{X_3} V_3(x) - \sum_{X_3}^{X_4} V_3(x) + \sum_{X_4}^{X_2} V_3(x) \qquad (4-3)$$

$$T_2 = \sum_{X_1}^{X_c} V_3(x) - \sum_{X_c}^{X_2} V_3(x) \qquad (4-4)$$

$$\left(X_q = \tfrac{1}{4}(X_2 - X_1), \quad X_3 = X_c - X_q, \quad X_4 = X_c + X_q \right) \qquad (4-5)$$

FIG. F4-9 COMPUTER MATCHING SCHEME

all quadrants in a particular match. These can be specified either for each match individually, or generally for all matches in a run. An approximate baseline is obtained by averaging three points about X_1 and three points about X_2 for both peaks, and peak centroids and areas are calculated with respect to these baselines. From this calculation three things are derived: the centroid of the first peak X_c which provides a centre for the subsequent analysis; the separation between the two centroids which gives an approximate displacement D; and the ratio of the areas which gives an approximate height ratio F. The peak V_2 is shifted the distance D, multiplied by the factor F and subtracted from V_1. A linear interpolation is taken between adjacent points of V_2 to permit fractional displacements. The resulting waveform (V_3') is then centred vertically around zero (eqn. 4-2), and F and D are adjusted to obtain a "null" difference signal i.e. $V_3(x)$ averages to a straight line. Firstly, F is adjusted to make $T_1 = 0$ (eqn. 4-3) and then D is adjusted to make $T_2 = 0$ (eqn. 4-4). If the second adjustment requires more than a 0.3 channel shift in D, then F and D are readjusted. The final value of D represents the relative peak position.

By this method, the position of the peak in the first

quadrant is compared with the position of the peaks in the other three quadrants. The results are then combined with corresponding voltage readings made at the time of the measurements. A linear relationship is assumed between the analyser voltage and the peak position over the very small span used, (Me69), and the appropriate matching potential is determined by an unweighted straight line fit:

$$V_f = \bar{V} - \frac{\sum_i (V_i - \bar{V})(D_i - \bar{D})}{\sum_i (D_i - \bar{D})^2} \bar{D} \qquad (4\text{-}6)$$

where $\bar{V}$, $\bar{D}$, are the average of the V_i and D_i respectively. These results are analysed as described in section 5.6.

The advantage of this system is that it does not rely critically on establishing an accurate baseline. The peak could be adjusted to occupy the entire spectrum, so that more efficient use of the avaliable ions is made. When this is done, it is no longer necessary to define the peak position for each match. In addition, the region of analysis can be constricted to reduce the effects of poor resolution. A fairly extensive investigation was carried out on the influence of the width of the analysis region on the result of a set of runs. On some doublets there was a significant effect, and it was found necessary to set the limits of the

region roughly equivalent to the 15% cut-off used by Meredith (Me71).

Comparison between this matching technique and that used by Meredith on the same data show that although the distribution of results within a match is very similar, the analysis used here leads to results for different runs which are more consistent with each other (table T6-5).

CHAPTER 5

WIDE DOUBLET MEASUREMENTS AND ERRORS

5.1 WIDE DOUBLETS

In section 2.3 we discussed the relationships that must hold between all voltages in a mass spectrometer in order that two groups of ions will travel the same path, viz.,

$$\Delta M/M = \Delta V/V \quad . \qquad (5\text{-}1)$$

The determination of a mass difference from this equation requires that

(a) the instrument be adjusted to the matched condition, and

(b) the ratio of $\Delta V/V$ so established be measured to sufficient precision.

In the measurement of narrow mass differences, one may define the "precision" of the instrument to be

$$\varepsilon_1 = \sigma/M \qquad (5\text{-}2)$$

where σ is the "absolute" error in the measurement. ε_1 has a lower limit principally determined by the resolution of the

instrument and the intensity of the ion current (Me73), as long as effects from other factors such as voltage measurement sensitivity, and thermal potentials are sufficiently small. For narrow doublets of the type studied to date, these other factors have indeed been small, and values of ε_1 have been in the region of 2×10^{-9}.

When doublets of greater width are studied, problems are encountered in producing stable voltages and in measuring them, as well as with proportional errors as discussed in this chapter. The effect of these factors tends to set a lower limit to the ratio

$$\varepsilon_2 = \sigma/\Delta M \quad . \qquad (5\text{-}3)$$

Typical values of ε_2 have been in the region of 10^{-6} (table T5-1).

The measurement of doublets having a large relative mass difference ($\Delta M/M$) played a prominent part in early mass spectroscopic work (As27). However, in the thirties and fourties, as a result of the problems in evaluating the instrumental dispersion from a photographic plate (i.e. placing a limit on ε_2), the emphasis shifted to narrow mass doublets. The increased accuracy of electrical measurement available for use with the mass spectrometers of the fifties and sixties subsequently allowed the width of mass

measurements to be increased while high precision was maintained.

These latter measurements achieved varying degrees of success. Table T5-1 shows the significant measurements since 1957. Generally the best measurement in any paper is cited, and both ε_1 and ε_2, as well as any applied correction, are given.

It was initially hoped that measurements with the Manitoba II instrument could be made for doublets where ($\Delta V/V$) was approaching the limit that the potentiometer (sect. 3.5) was then capable of measuring ($\Delta M/M \sim 1/70$), and that the precision previously obtained ($\varepsilon_1 \sim 2.5 \times 10^{-9}$) could be preserved. The problems which will be discussed in section 5.3 below severely limited the range of measurements for which this precision was possible. For these and other reasons (ch 6), measurements were made for $\Delta M/M \sim 1/3{,}000$ ($\varepsilon_2 \sim 6$ppm), calibrated against a known wide doublet (sect. 5.5). The calibration for the measurement of the chlorine mass difference (sect. 6.1) required that the limit of the doublet width measurable be extended to $\Delta M \sim M/50$. The requirement on the calibration measurement precision was $\varepsilon_1 < 10^{-7}$ or $\varepsilon_2 < 6$ppm.

There were four main areas of concern in measuring

TABLE T5-1

PRECISION OF WIDE MASS MEASUREMENTS

YEAR	LAB.	REF.	MEASUREMENTS	1/DBLT. WIDTH. (M/ΔM)	CORR. APPL. (ppm)	σ/ΔM (ppm)	σ/M $\times 10^{-8}$
1957	Min.	Qu57	C_2H_4 - CO	777		22	1.8
			H calibration (2±10ppm)			10	
1958	Pri.	Sm58	$^{11}B_5H_9$ - SO_2	410		12	3
			(considerable inconsistency in results)				
1959	Min.	Be59	H calibration (3±3ppm)	104		3	3
1966	Min.	Be66	^{138}Ba - ^{136}Ba	69		1.5	2
1967	Arg.	St67	C_9H_{20} - $C_{10}H_8$	1400	±0-50	4	.27
1968	Min.	Hu68	$^{57}Fe\ ^{37}Cl$ - $^{56}Fe\ ^{37}Cl$	93		1.4	1.5
1970	Arg.	St70	$C_{10}H_{18}$ - $C_2H_3\ ^{37}Cl_3$	630	40±1	4	0.7
1970	Har.	Ke70	$^{12}C_8\ ^{13}C\ H_7N$ - ^{130}Te	2200	20±2	4	0.5
1970	Osa.	Na70	C_2H_4 - CO	780	36±5	7	0.9
1971	Har.	Ke71	^{238}U - ^{235}U	80	30±2	3.2	4
1971	Pri.	Sm71	C_9H_{20} - $C_{10}H_2$	1500		1.0	0.06
			C_6H_{14} - $CH_2\ ^{35}Cl\ ^{37}Cl$	560		0.6	0.1
1972	Min.	Ka72	$\frac{1}{2}\ ^{235}U$ - C_9H_9	180	20±3	2.2	0.6
			(some inconsistencies)				
Present			C $^{35}ClD_2$ - C $^{37}ClH_2$	3300	30-160	6	0.17

Arg. - Argonne National Laboratory.
Har. - Harvard University.
Min. - University of Minnesota
Osa. - University of Osaka.
Pri. - Princeton University.

these wide doublets.

1. Electrostatic analyser voltages (V_e)

The stability requirement in V_e was increased to 1mV (in 800V), a figure which was easily achieved by the Mallory TR 136-R mercury batteries (sect. 3.5). The ΔV_e supplies had to provide up to 0.3V with a stability of about 1μV for doublets studied in this work, and up to 16V with a stability of 80 μV for the calibration doublets. These supplies are described in section 4.3. Because calibration mass measurements were used (sect. 5.5) the measurement of V_e was no longer critical, but high precision was required in the comparison of the large voltage step, ΔV_c, for the calibration doublet to the smaller voltage steps, ΔV_d, for the doublet under study (sect. 5.6).

2. Acceleration voltages (V_a)

The effect of errors in the amount that the acceleration voltage was switched (ΔV_a) was somewhat unpredictable since the corresponding factor in eqn. 2-15, k_a, depended on the extent to which velocity focussing was actually achieved at the time the measurement was taken. ΔV_a could easily be measured to 0.01V with a differential voltmeter but the method of determining the appropriate ΔV_a depended on the type of measurement being made. When

narrower doublets (other than the calibration doublets) in which the ions are chemically identical were matched, ΔV_a could be calculated from an approximate V_a value. In other situations, however, two problems presented themselves.

a. It was difficult to measure V_a sufficiently precisely for the wide calibration doublets.

b. Usually the difference in initial ion energies of chemically dissimilar ion fragments was not known (sect. 2.).

When calibration doublets, or doublets involving dissimilar ions were being compared, ΔV_a was adjusted by the following procedure: the instrument was set up for a visual match between the two ions to be measured, with an approximately correct ΔV_a. The electrostatic analyser switching potential (ΔV_e) was adjusted for a match, and the height ratio controls were set for equal heights. V_a was then decreased until only the high energy ions passed through the energy slit and ΔV_a was adjusted until the peaks disappeared simultaneously as V_a was further decreased. V_a was then increased for maximum peak height, and the ratio controls reset for balance. This routine may be repeated several times to get consistent results. The low energy side of the spectrum was seldom used in the adjustment of ΔV_a

because there was often a significant tail on this side of the energy distribution.

The velocity focussing was set particularly closely. A ΔV_a of 5 or 10 volts was applied and a peak matched to itself. Similarly, at any stage during matching, a voltage could be added to ΔV_a to check the error in the velocity focussing. Finally, the energy slits were set so as to restrict the energy spread of the ion passing through the slit to a few volts.

Since the direction and magnitude of any error in the result arising from a particular error in setting ΔV_a varied from day to day with the exact state of velocity focussing, these errors would be rather random over the period of a mass measurement. Therefore the accumulated effect in a set of runs would not change the mean value but rather increase the size of the statistical error.

3. Focussing and steering voltages (V_q)

The effect of these voltages, as with the acceleration voltages, changed very much with focussing conditions. In previous measurements (Bi69) they were not switched, since it was determined that the small voltage required (less than .04V) would not influence the measurements. In this work, 0.02V was taken as the smallest required tolerance for

precision switching, and potentiometers were set from previous calibrations (sect. 3.4). The instrument was adjusted so that any variation of the steering and focussing controls produced no perceptible change in the peak position.

4. Surface charge effects

The presence of charges residing on surfaces may give rise to electric fields which deflect the beam but which, in general, are not switched according to eqn. 5-1. These are considered further in section 5.4.

5.2 HISTORY OF INSTRUMENT ERRORS

Aston (As27) detected consistent deviations from the predicted behaviour in his first instrument, and an error of several parts in a thousand in matching by coincidence in his second instrument. The latter error was reduced to 5×10^{-4} by plating the electrostatic analyser with gold, but a correction had to be applied to most of his measurements. This error was due to the large ionic and neutral flux that struck the electrostatic analyser plates, depositing insulating layers and building up charges. Later instruments have been designed so as to avoid the possibility of ion beams striking the electrostatic analyser

(Ba36). The existence of this type of error in mass spectrographs has not generally been of major concern because small mass differences are measured simultaneously with a direct measurement of the dispersion. This charging process has, however, caused some difficulty with line shape (De35). Recently the problem has reappeared in experiments involving wide doublet measurements with the current generation of mass spectrometers (table T5-1).

The Minnesota measurements, which have been exceptionally free from errors, have been calibrated against the direct determination of the hydrogen mass between hydrocarbon fragments ($C_n H_{m+1} - C_n H_m$). A small correction factor of -3±2 ppm was applied in 1963 (Ri64). Subsequently an error of up to +60 ppm was measured (Be65), but this was reduced to -0.5±1.0 ppm by cleaning and baking the electrostatic analyser plates. More recently (Hu70), there has been evidence of errors up to 10ppm on single mass unit measurements, in spite of concurrent correct values for the hydrogen mass measurements. It was thought that the source of the discrepancy might possibly lie in differential ion energies (see sect. 2.3). Recently the source diffusion (oil) pump was replaced by an ion pump. Thereafter the correction required has reduced slowly to zero (Jo73).

The Harvard instrument has also suffered an error of -103±8 ppm (De65). Kerr (priv. comm.) later experienced errors that increased linearly with the time of beam passage through the electrostatic analyser. The error was reduced and stabilized to 20-30ppm with an error of 2ppm after the electrostatic analyser plates were coated with aquadag (colloidal graphite) (Ke70, Ke71).

Stephens and Moreland at Argonne, after coating the electrostatic analyser with aquadag, measured an error of ±0-50ppm which was stable over a day within several ppm, and tended to assume several distinct values (St67, St70).

Nakabushi et. al. (Na70) reported a systematic error of +36±5ppm while Matsuda et. al. experienced inconsistencies, but no apparent systematic error (Ma70).

Smith's mass synchrometer suffered from unresolved inconsistencies (Sm58), and a number of compensations had to be applied to his R. F. mass spectrometer (Sm71). He cancelled out errors by applying small unswitched voltages to his acceleration potential, electrostatic analyser potentials, and to the inner jaw of the phase defining slit. The basis for most of these adjustments has not been described. Errors were assigned for the adjustment of the potential applied to the phase defining slit, and have made

major contributions to the final error associated with some of his measurements.

For the doublets measured previously by this group both at McMaster (e.g. Ma70b, Mc70, Wh70) and Manitoba (Me71, Ba72) the width has been sufficiently small so that proportional errors hereto have not been considered significant. However it is possible that a consistent difference between Manitoba and McMaster results (Ba72) could be attributable to a systematic error of -790ppm in the McMaster instrument or to errors in both instruments which lead to a differential error of this amount. Recent measurements with this instrument (now the Manitoba I instrument) by Williams and Barnard, however, indicate a positive error. A negative error has been shown to be significant in recent mass differences measured with the Manitoba II instrument (see sect. 6.4). However the combined magnitude of these corrections as they currently exist is much smaller than the amount required for concordance.

5.3 LOCATION OF THE ERROR SOURCE

A systematic error of about -200ppm was first encountered on the Manitoba II mass spectrometer when mass

differences of one and two mass units were measured among rare earth chlorides. Initial tests involved determining the dependence of the error on different factors, including:

1. All source variables.

2. Acceleration potential (V_a) and switching potential (ΔV_a).

3. Quadrupole potentials (V_q) and switching potentials (ΔV_q).

4. Removal of grounding connections on test electrodes along the beam path.

5. Restriction of the beam angle, energy spread, and height distributions into different narrow regions by means of the appropriate slits.

6. Switching of the "repeller" potential on the source.

Although some of these factors appeared to have a small and often somewhat unpredictable influence on the error, none had any strong influence on it.

The magnetic analyser was then investigated, since there was the possibility that the error arose from surface potentials caused by ion bombardment of the side of the analyser beam tube. The following tests were undertaken.

1. The N_2 - CO doublet was measured. Here the

distribution of rejected ions around the magnet beam would be radically different to that for the rare earth chlorides.

2. Mass differences were measured with a pure mercury source. In this case impurity ion currents would be much reduced.

3. The magnet tube was degassed.

4. A Wien filter was installed between the source and the quadrupole lens to remove spurious ions. The filter, which consisted of a permanent magnet assembly acting across the horizontal steering plates, had a mass resolving power ($M/\Delta M$) of ~ 2.

5. A stainless steel liner was installed inside the vacuum chamber of the magnet along both walls to cover insulating deposits that might have been accumulated, and thus present a fresh surface to the ion beam.

Here again, there were no consistent changes in the error when the different tests were attempted.

The next region to be studied was the electrostatic analyser. The cover was removed and the electrode surfaces were cleaned in turn with acetone, alcohol, and distilled water. After the cover was replaced and the system pumped down, argon was released into the system to a pressure of about 400 microns. A radio frequency discharge was then set

up between the plates with a tesla coil as the system was pumped down again. This process was used as an alternative to degassing, which was impractical due to the size and weight of the analyser plates and cover. Unfortunately, the tesla coil could be applied to the electrodes only near one end of the analyser, and it was not possible to determine the extent of the discharge produced. The effect of this cleaning, however, was to reduce drastically the error to close to 0ppm, although the error rose slowly to approximately -40ppm over several weeks. Repeated application of the r.f. discharge would temporarily reduce or eliminate the error again, with diminished effectiveness. At times the error could be greatly increased by changing the acceleration potential sufficiently to sweep the beam over the analyser plates.

5.4 NATURE OF THE ERROR

The evidence described in section 5.3 points to surface potentials in the electrostatic analyser region as the primary cause for the error, although possible contributions of smaller magnitude from other causes cannot yet be eliminated. The typical error of -100ppm could be caused by a reduction of the potential difference, V_e,

between the plates by 0.08V (in 800V), or a surface potential of -0.04V on the positive plates and +0.04V on the negative plate. A surface potential distribution over a smaller area would require higher potentials.

Potentials developed on metal surfaces in a vacuum have been studied by Petit-Clerc and Carette. Potentials up to 0.5V were obtained after the surfaces had been bombarded with electron beam intensities of 2×10^{-9} amp / mm^2 at energies of 8-43eV and a residual potential of a few tenths of a volt was found to persist for an indefinite period (Pe68). Petit-Clerc concludes that charges are trapped in polymer films formed from organic contaminants (Pe70). The pump oil used in Petit-Clerc's first experiment, DC704, is similar to the DC705 silicone oil that has been used in the Manitoba instrument for several years. The oil diffusion pumps act only on the source arm and are protected continuously by water baffles, and by liquid nitrogen traps when the instrument is in operation; that is, when the gate valve between the analyser and the source arm is open. It is impossible, however, to preclude the transfer of some oil into the electrostatic analyser section. Experience with the Manitoba I instrument suggests that the silicone oil residing on the surface of the analyser plates and subject

to ion bombardment may produce glass-like layers, possibly having a higher resistivity than the layers produced by the carbon oil.

The current to the electrostatic analyser plates has a measured value of 10^{-11} amps when an estimated total ion current of 10^{-9} amps passes through the electrostatic analyser. It is roughly proportional to the ion current, and completely dependent on it. Figure F5-1 shows how the current measured at the analyser plate varies as the acceleration potential is changed. Similar currents have been measured in the Manitoba I instrument. Although these current densities are well below those used by Petit-Clerc, it is possible, and in agreement with experience, that the potential could build up over a period of time.

The following possible mechanisms for the accumulation of this surface charge have been considered.

1. Bombardment of the electrostatic analyser plates by the primary ion beam.

This would require some ions having a kinetic energy 200eV different from those travelling along the optic axis. Such ions have not been observed in normal operation, and their production, by the source used, is unlikely. Inelastic scattering of the beam from the principal slit is a

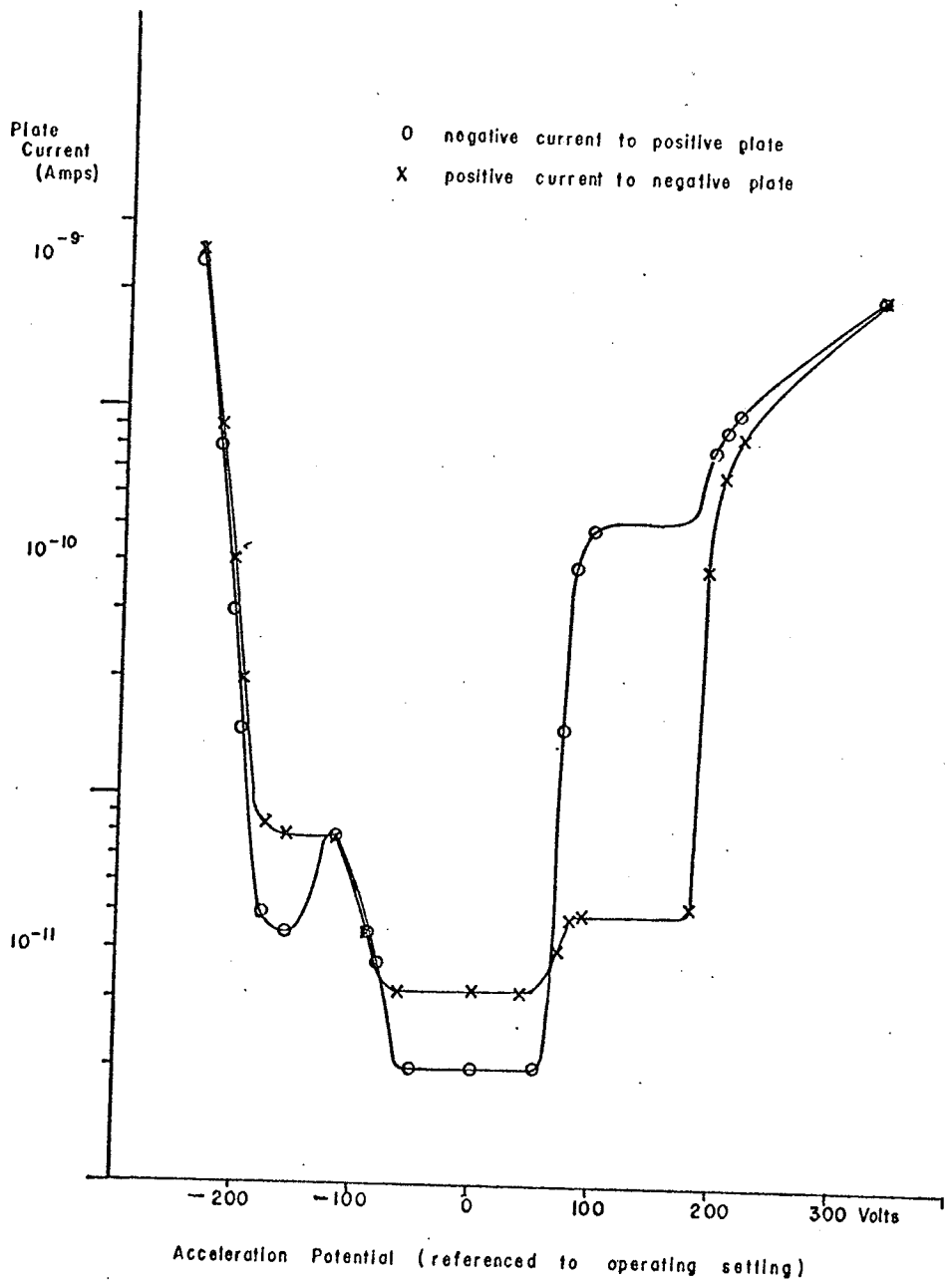

FIG F5−1 VARIATION OF PLATE CURRENT WITH ACCELERATION POTENTIAL

possible, though unlikely, cause of energy spread. In either case, if the primary beam were to hit the analyser plates, the area affected would be predominantly near the exit end of the plates and the surface potential required to produce the whole error would be correspondingly higher than 0.08V and possibly close to 1V. However, in initial adjustment procedures a transient plate bombardment may occur.

2. Bombardment of the exit fringe blocks by the primary beam.

This requires an ion potential 70V different from those travelling the optic axis, which may result from a misadjustment of V_a. As suggested by fig. F5-1, bombardment of the fringe blocks can produce current to the analyser plates, and the resulting surface potentials can be built up on both the fringe blocks and the analyser plates. The fringe blocks have adjacent surfaces 3cm wide, placed 7mm apart and parallel to the beam; thus can be struck by ions over their entire width. The potentials produced in this event would, for the same area, influence the beam more than corresponding ones on the electrostatic analyser on account of the reduced distance between the charged surfaces.

3. Bombardment of the analyser plates by

secondary ions produced between the analyser plates.

Two mechanisms have been considered.

(a) Charge exchange between the ion beam and the residual gas. Reaction cross sections as high as 10^{-15} cm^2 have been measured for a variety of ions and gases (Ha52). At a pressure of 10^{-7} mm Hg, about 0.2% of the beam would suffer such interaction. The resulting particles may then release electrons from the negative plate upon striking it. This process could account for much of the current arriving at the analyser plates.

(b) Ionic dissociation. There is a certain probability that in gas - beam collision processes the ion fragments will be dissociated. The effects of this would be similar to the effects of charge exchange processes. As in the case of charge exchange, this dissociation would be highly dependent on the type of ions produced by the source.

The influence of a surface charge on the ion beam and the measurement relationships must also be considered. If an ion, accelerated by a potential of V_a volts, passes perpendicularly through a stray electric field of E volts/metre for a distance of ℓ metres, then it suffers a deflection θ and a sideways displacement d given by

$$\theta = E\ell/2V_a \qquad (5\text{-}4)$$

and

$$d = E\ell^2/4V_a \quad . \qquad (5\text{-}5)$$

In the case of two ions of mass M', M" accelerated through potentials V_a', $V_a"$ respectively, by using eqn. 2-11, we find that

$$\theta'/\theta" = M'/M" \qquad (5\text{-}6)$$

and

$$\delta\theta/\theta" = \Delta M/M" \qquad (5\text{-}7)$$

in all cases, and similarly

$$\delta d/d" = \Delta M/M" \qquad (5\text{-}8)$$

where $\delta\theta$, δd are the differences in the deflections and the displacements received by the ions.

If the shift in final peak position is directly proportional to θ and d, then the relationship 2-15 will hold exactly, and the error in the measurement, given by eqn. 2-16, will be proportional to the mass difference measured. This proportionality will hold as long as there are no significant second order image aberrations. Such aberrations would arise in the case of very non-uniform fields in the beam path, such as those due to charge on the slit edges. Checks can be made on these non-uniform fields, either by testing the dependence of the error on changing ΔV_a (i.e. putting the two ion beams around different paths) or by testing the effect on the error of changing slit

positions. These tests were found to have negligible influence on the error (sect. 5.3).

5.5 CORRECTION FOR THE ERROR

Since it seemed unlikely that the error experienced could be satisfactorily eliminated, the possibility of using a wide doublet to calibrate the error for the measurement of a narrower doublet was considered. The nature of the error as determined in the work already described suggested that the necessary correction would be proportional to the doublet width. Tests were made on the linearity of the correction by measuring it for one and two mass unit differences for a number of different ions. The results of such measurements (table T5-2) indicate that the assumption of linearity is valid. With the confirmatory evidence noted in section 5.4 and below, it is now presumed that the discrepancies in the results before January 1971 arose from unintended bombardment of the electrostatic analyser plates by the ion beam.

On the basis of this understanding of the source of the systematic error and its behaviour, the measurement of doublets with $\Delta M/M \sim 1/3{,}000$ was undertaken. The doublets measured and the calibration doublets used are described in Chapter 6.

TABLE T5-2

LINEARITY TESTS

DATE	ION	PROP. ERROR FOR 2 MASS UNIT DIFF. / PROP. ERROR FOR 1 MASS UNIT DIFF.
1 Nov 1970	$CdCl_2$	.58 ± 0.5
9 Nov 1970	Cd Cl	.97 ± .15
10 Nov 1970	Cd Cl	.96 ± .05
22 Dec 1970	$CdCl_2$	.54 ± .03
26 Dec 1970	$CdCl_2$	.55 ± .06
20 Jan 1971	Cd Cl	.97 ± .10
6 Mar 1971	Cd Cl	.95 ± .10
9 Mar 1971	Cd Cl	1.00 ± .08
10 Mar 1971	Cd Cl	.94 ± .10
12 Mar 1971	Cd Cl	1.2 ± .3 1.02 ± .05

Calibration measurements usually consisted of four visual matches taken both before and after a group of runs. They were carried out at the same magnetic field setting as the measured doublets so that errors due to changing focussing properties would be avoided. This limited the measurements to either "add" or "subtract" types, depending on the relationship between the peaks. Usually the calibration doublet was lighter than the measured doublet, and "add" measurements were made. An error for the calibration is derived from the spread of the determinations made, and is included in the final error (sect. 5.6).

A further check was made on the validity of the error correction by plotting the final run results against the correction made on them, as shown in fig. F5-2. Finally, an independ nt confirmation is provided by the unusually good agreement between the chlorine measurement and Smith's results (see Chapter 6.1).

The following additional precautions were taken to minimise the error.

1. Blanking system: During the measurement of large mass differences for calibration, the acceleration potential was switched by amounts up to 400V. Any lack of synchronisation between ΔV_a and ΔV_e switching would cause

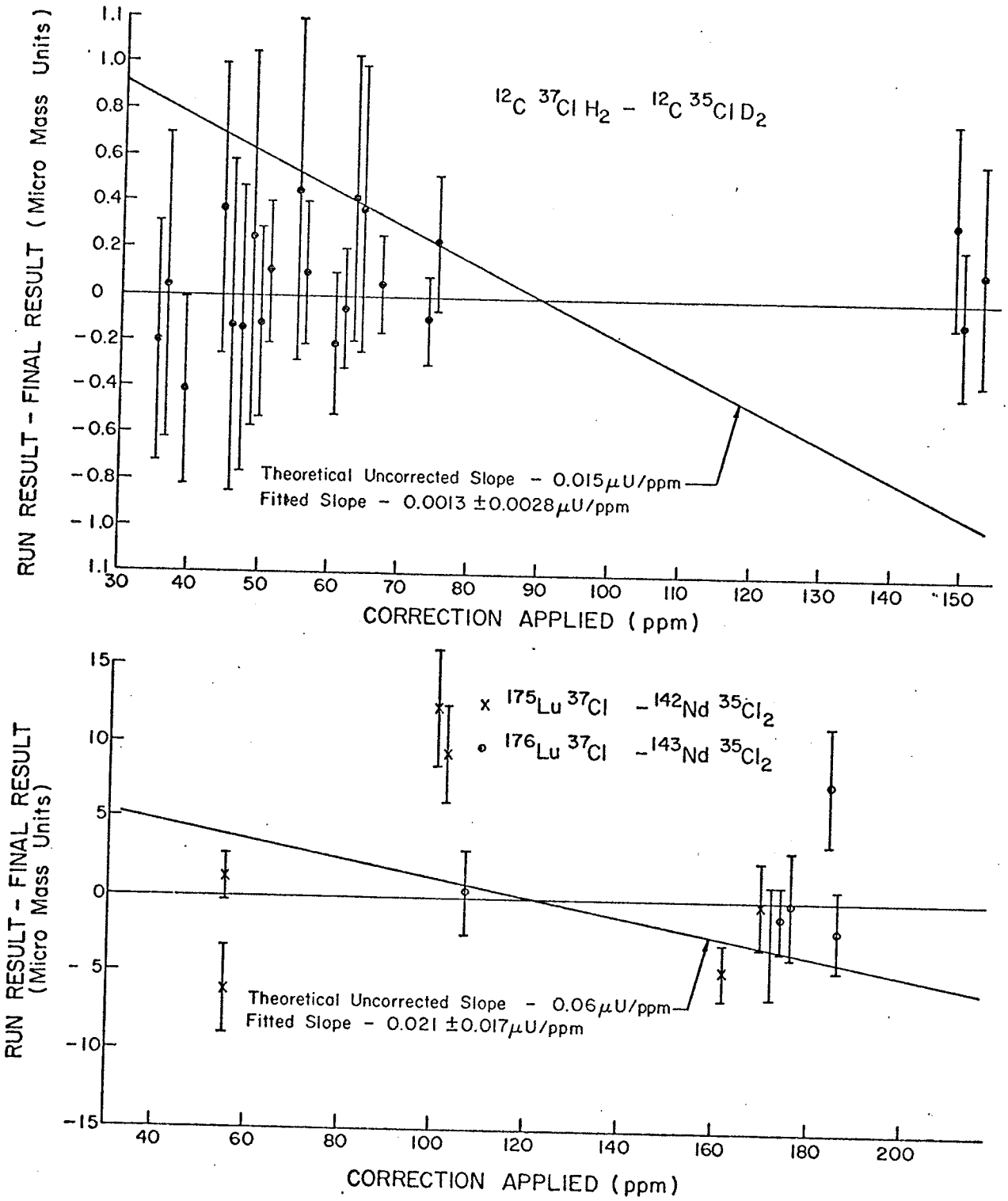

FIG. F5-2 DEPENDANCE OF RUN RESULT ON CORRECTION APPLIED FOR WIDE MASS MEASUREMENTS

the ion beam to hit the electrostatic analyser for short intervals. To prevent this, a blanking system was used to shut off the ion beam between oscilloscope sweeps (see sect. 3.4).

2. Change of the type of diffusion pump oil: As discussed in section 5.4, the use of silicone oil could lead to the formation of particularly undesirable glass-like layers on the surfaces of the analyser plates. For this reason, the DC705 oil in the diffusion pump was replaced by the carbon - based Convalex 10.

5.6 TREATMENT OF RESULTS AND ERRORS.

The result of the computer analysis of each match is a voltage (ΔV_e) appropriate for the optimum matched condition (sect. 4.4). From each of these voltages is calculated a mass difference, using eqn. 2-20 or 2-21 for the add and subtract modes respectively.

The masses calculated for each match are adjusted by the proportional correction determined from the measurement of the calibration doublet (sect 5.5). The simple average of the results of the eight matches in each run is taken and the standard deviation of the mean is calculated. An error in the correction is estimated from the spread of the

calibration measurements, and is then combined with the standard deviation of the mean to give the error quoted for that run.

The standard method of combining such partial run results to derive a final result with an error has been defined by Birge (Bi30). A weighted average of the results of the various runs is calculated along with an internal error and an external error:

$$m_s = \frac{\sum_r \left(1/\sigma_r^2 \right) m_r}{\sum_r \left(1/\sigma_r^2 \right)} \qquad (5\text{-}9)$$

$$\sigma_s\,(\text{ext}) = \frac{\sqrt{\sum_r [(1/\sigma_r)(m_r - m_s)]^2}}{(n-1)\sum_r 1/\sigma_r^2} \qquad (5\text{-}10)$$

$$\sigma_s\,(\text{int}) = \sqrt{1/[\textstyle\sum_r (1/\sigma_r^2)]} \qquad (5\text{-}11)$$

where m_r, σ_r are the results and errors of a run,

m_s, σ_s are the mean and errors of a series of runs, and n is the the number of runs involved in a measurement. The external error indicates the spread amoung the run results, while the internal error is a combination of run errors. Usually the expected value for $\sigma(\text{ext})/\ \sigma(\text{int})$ is ~ 1, and the final error quoted is taken to be the larger of the two errors calculated.

Because of the possible elimination of systematic errors by means of the combination of match types within a run (sect. 4.2), two arguments arise which conflict with the above analysis.

1. A systematic error which is eliminated should not inflate the final error. Thus errors characteristic of a given matching configuration would tend to cancel over a run, and the external error would express the true statistical variation between runs.

2. The size of the systematic error eliminated in any particular run (and reflected in the run error) should not influence the weight placed upon that run result. For this reason an unweighted average of the run results should be taken (as was the practice for visual matching measurements previously carried out by this group (Bi69)).

Due to the lack of precise knowledge of the errors that were eliminated, a full analysis was not possible. The Birge formulation was used with the following modifications.

1. Both errors are presented here to indicated any possible significance of the first argument.

2. The importance of the second argument was tested by comparing the simple and weighted averages of the run results. In cases where they differed by more than the

final quoted error, the errors on the most precise runs were raised until agreement was reached between the two averages. This process effectively increased the final error to take account of the statistical abnormalities among the measurements.

Other factors considered in arriving at a final result are:

1. The potentiometer chain calibration (sect 3.5) by which the relationship between ΔV_e and V_e is established. Since this applies to both the measurement error calibration and the measured doublet, the chain error can be neglected in both.

2. The lower chain calibration, which relates the resistance of the VDR and the lower chain members $R_1 - R_4$. This calibration was critical in the very wide calibration measurements (sect 6.1) and was estimated at 8.5±2 ppm over the period of the chlorine measurements (sect. 3.5). The error on the correction was combined with the total measurement error, since the corrected error was likely to be correlated over the whole measurement.

3. The VDR calibration, which tests the internal consistency of the VDR (sect. 3.5). The most critical factor in this calibration is the error in the resistors of the

most significant decade. This was fully calibrated by Bishop some time ago (Bi69), but a check was made near the setting used for the wide doublet measurement. The correction was +1.6±1 divisions in the seventh dial at 26.5 °C or 0.6±0.4μV ($\varepsilon_1 = (0.8\pm0.5)\times10^{-9}$). The corresponding correction according to Bishop is +3.2±0.8 divisions in the seventh dial.

4. Loss of the electron in the ion mass. The mass used in the calculations is that of the neutral atom, derived from atomic mass tables, but the particles used are positive ions. Corrections for the electron mass apply to both the calibration and the measured doublets, and are thus partially cancelled out. In the case of calibrations and measurements carried out at the same magnet setting, the remaining correction can be shown to be the factor

$$(1 + M_e \Delta M_c / M''(M_c - M_e)) \qquad (5\text{-}12)$$

where: M_e is the mass of an electron,

M_c is the mass of the calibration ion,

M'' is the mass of the measured ion,

and $\Delta M_c = M_c - M''$

The magnetic field is set on the reference ion M'. For the worst case, the chlorine measurement, the correction is 0.2ppm, which is negligible.

5. Relativistic corrections. The real mass of the

ion in flight is given by adding its energy to its rest mass.

$$\text{flight mass} = M_r + eV_a/c^2 \qquad (5\text{-}13)$$

where: V_a is the acceleration potential,

e is the electronic charge

M_r is the rest mass,

and c is the speed of light.

This correction also is cancelled out only partially by the calibration, the approximate residual factor for the type of calibration used is

$$(1 - 2eV_a \Delta M_c / c^2 M_c M'') \qquad (5\text{-}14)$$

and differs from 1 by 0.02ppm for the chlorine measurement.

5.7 PRECISION

The best "precision" ($\varepsilon_1 = \sigma/M$, sect. 5.1) acheived with this instrument previous to this work is 2.5×10^{-9} on the $^{169}Tm\ ^{35}Cl_2$ - $^{165}Ho\ ^{37}Cl_2$ doublet measured with 18 runs of visual matches in 1969. Meredith (Me71) has approached the same precision using computer - assisted matching, but with considerably fewer runs.

The best result reported here ($C\ ^{35}Cl\ D_2$ - $C\ ^{37}Cl\ H_2$) (sect. 6.1) has a precision of 1.7×10^{-9} on the final result with 20 computer - assisted runs taken. This error is

determined primarily by the distribution of results within the runs (internal error) and certain errors due to the width of the doublet measured.

Recent tests on the instrument reveal a mechanical oscillation of about 7 Hertz which sets up a beat frequency with the matching sequence (Me73). The beat frequency is sufficiently low that the precise time of starting and stopping data collection can influence the match results. This effect is larger for more intense doublets because of the shorter collection time.

CHAPTER 6

RESULTS AND DISCUSSION

6.1 THE ^{37}Cl - ^{35}Cl MASS DIFFERENCE

Since 1962 this group has used narrow mass doublets of the types

$$^{A}X\ ^{35}Cl - ^{A-2}Y\ ^{37}Cl = \Delta_1 \qquad (6\text{-}1)$$

and

$$^{A}X\ ^{35}Cl_2 - ^{A-4}Y\ ^{37}Cl_2 = \Delta_2 \qquad (6\text{-}2)$$

in order to obtain precise values for the mass differences of the types

$$^{A}X - ^{A-2}Y = \Delta_1 + (^{37}Cl - ^{35}Cl) \qquad (6\text{-}3)$$

and

$$^{A}X - ^{A-4}Y = \Delta_2 + 2(^{37}Cl - ^{35}Cl) \qquad (6\text{-}4)$$

where X, Y, may or may not be the same element and Δ_1, Δ_2 are the experimentally determined mass differences. In the special case where X, Y, are the same element, then the further relationships exist:

$$^{A}X - ^{A-2}Y = 2n - S_{2n} \qquad (6\text{-}5)$$

and

$$^{A}X - ^{A-4}Y = 4n - S_{4n} \qquad (6\text{-}6)$$

where n is the neutron mass and S_{2n}, S_{4n}, are the separation energies for the last two or four neutrons respectively.

The accumulation of an extensive body of this kind of

data, initially at McMaster University and later at the University of Manitoba, prompted several research groups to undertake the redetermination of the ^{37}Cl - ^{35}Cl mass difference to improve its precision and reliability as an important secondary mass standard. Table T6-1 summarises the results of these experiments, thus giving the available mass spectroscopic data on this difference at the time that the present work was initiated.

The continued interest in "chloride" doublets in the rare earth region (determined by this group first at McMaster University and later at the University of Manitoba, e.g. fig. F6-1), coupled with the progressive improvement in precision for these doublets, led us to attempt to obtain a much improved value for the ^{37}Cl - ^{35}Cl mass difference.

In the previous determinations the ^{37}Cl - ^{35}Cl mass difference has been compared against twice the hydrogen mass (Be66), the deuterium mass (Ka72) and twice the (D - H) mass difference (De65). An alternate approach, viz., the separate determination of the ^{37}Cl and ^{35}Cl masses against hydrocarbons, was used by the Argonne group (St70).

The approach adopted in the current work is the direct determination of the $C\,^{35}Cl\,D_2$ - $C\,^{37}Cl\,H_2$ doublet, deriving the ^{37}Cl - ^{35}Cl difference in terms of the 2(D - H) mass

TABLE T6-1

1970 STATUS OF MASS SPECTROSCOPIC MEASUREMENTS RELATED TO THE C ^{35}Cl D_2 - C ^{37}Cl H_2 DOUBLET.

(Units: micro - mass units)

$2 - (^{37}Cl - ^{35}Cl)$

2,951·11 ± 59	De 65
2,950·30 ± 60	Be 66
2,949·41 ± 42	St 70
2,950·06 ± 50	Weighted Mean

$H_2 - D$

1,548·081 ± 82	Sm 58
1,548·220 ± 50	Jo 67
1,548·070 ± 80	St 67
1,548·080 ± 80	Na 69a
1,548·143 ± 41	Weighted Mean

H - 1

7,824·958 ± 87	Sm 58
7,825·220 ± 30	Be 66
7,825·010 ± 28	St 67
7,825·055 ± 40	St 70
7,825·005 ± 49	Ka 70
7,825 081 ± 48	Weighted Mean

TABLE T6-1

(Continued)

(D-H) - 1
Calculated from [(H-1) - (H_2-D)]
6,276·938 ± 63

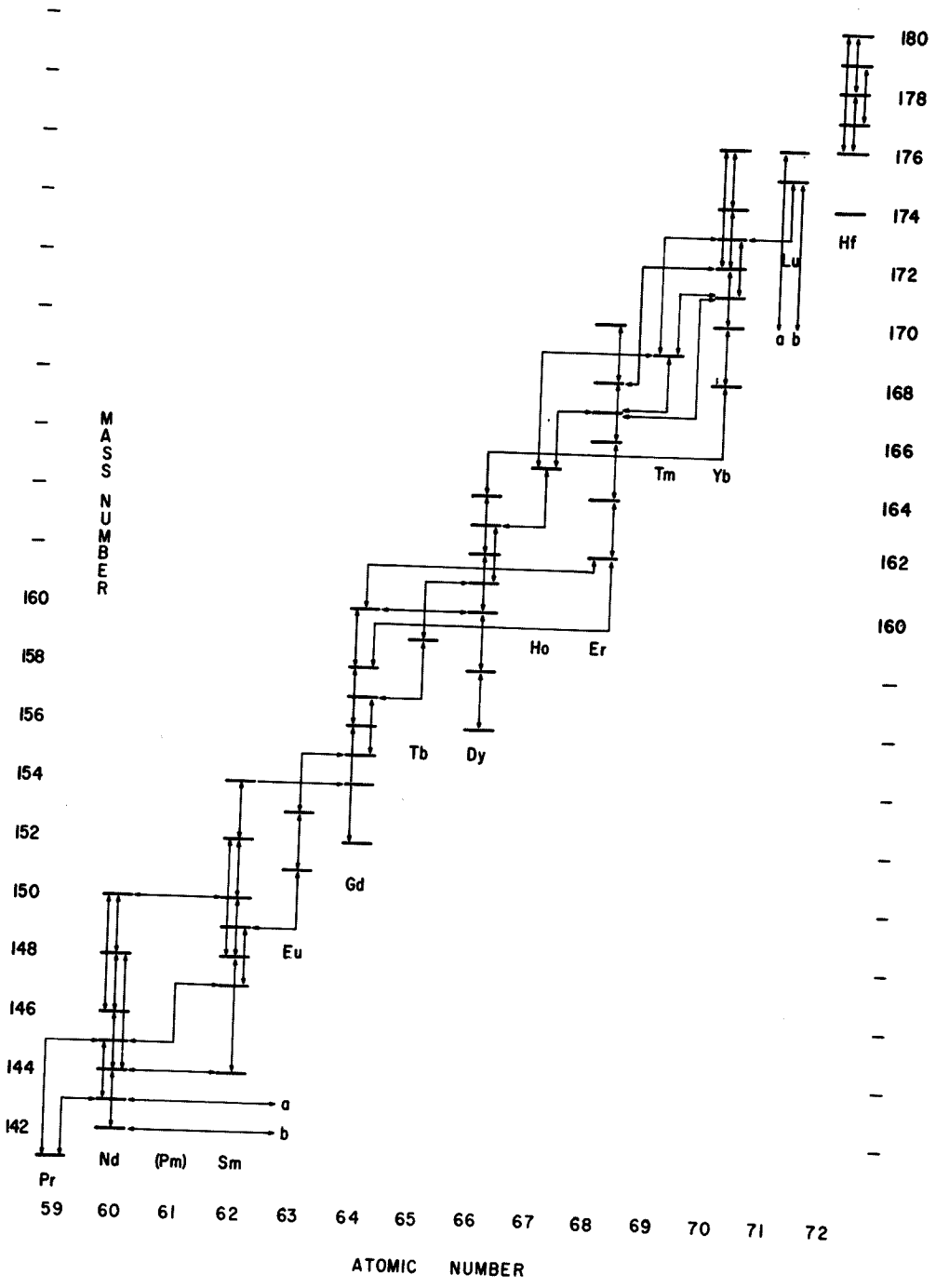

FIG 6-1 McMASTER AND MANITOBA MASS MEASUREMENTS

difference. The desirable features of this mass doublet were as follows:

1. The ions were chemically identical, and thus had similar source characteristics. This avoided problems previously attributed to the use of ions having different chemical structure (sect. 2.3).

2. The doublets had a suitable width (1/3,300), and suitable calibration doublets were available.

3. The D - H mass was known from direct measurements to an accuracy at that time of 0.063 μu (table T6-1).

The source used the vapour from a mixture of 75% normal methylene chloride and 25% fully deuterated methylene chloride.

Twenty runs using computer - assisted matching were taken on six different days spaced over a period of two months. The first seventeen used the voltage stepping method developed by Meredith and the remainder used the revised method (sect. 4.2). The calibration doublets used were the $C\,^{37}Cl\,H_2$ - $C\,^{37}Cl\,H$ and the $C\,^{35}Cl\,D_2$ - $C\,^{37}Cl\,H$ doublets.

In order to check for interference by contaminants the total spectrum was recorded at each mass number between masses 53 and 48, and the computer printout inspected. All

peaks detected were identified as fragments of the methylene chloride sample except for one peak at mass 51 with a mass excess of 10mu; 18 mu heavier than the ions measured. No explanation for this was discovered, but the possibility of any related peaks interfering with the measurement could be discounted. There was some concern that the mass of $^{31}P\,^{16}O$ differed by only 0.18mu from the mass of $C\,^{35}Cl$, and therefore would be unresolved in any of the spectra. Although phosphoric acid did exist in trace amounts in the LaB_6 mixture covering the filiament, it was considered very unlikely to have any significant effect due to the improbability of generating the $D_2{}^{31}P\,^{16}O$ ion. As an additional check, however, the last three runs were taken without any LaB_6 on the filament. No significant changes were detected.

The values, with corrections, are given in table T6-2. Errors on the systematic corrections are combined to give the final result. As stated in section 5.6, the larger of the internal and external errors was taken, in this case the internal error. However, according to argument 1 in section 5.6, the size of the external error suggests that a smaller final error might be justified. Also given in table T6-2 is the simple unweighted average and its standard deviation.

Figure F6-2 compares this measurement with the results

TABLE T6-2

C Cl D - C Cl H RESULTS

Date	Proportional Error	Result(μU)	Error(μU)
April 12	48	15504.11	0.81
"	53	15504.28	0.74
April 14	35	15503.88	0.66
"	35	15503.64	0.51
"	47	15503.69	0.62
"	47	15503.71	0.72
"	47	15504.21	0.63
April 17	38	15503.42	0.41
"	48	15503.93	0.31
"	60	15503.62	0.31
"	60	15503.77	0.26
April 29	74	15503.89	0.21
"	72	15503.73	0.19
"	72	15504.07	0.29
April 30	61	15504.25	0.63
"	61	15504.21	0.62
"	47	15503.71	0.41
June 10	147	15504.16	0.44
"	151	15503.95	0.48
"	147	15503.74	0.32
Weighted Average		15503.833	0.082 (Internal Error) 0.043
(Unweighted Average)		3.898	0.055
Corrections:			
Error in chain calibration		-.070	.030
Correction due to VDR calibration		+.040	.025
RESULT		15503.803	.091

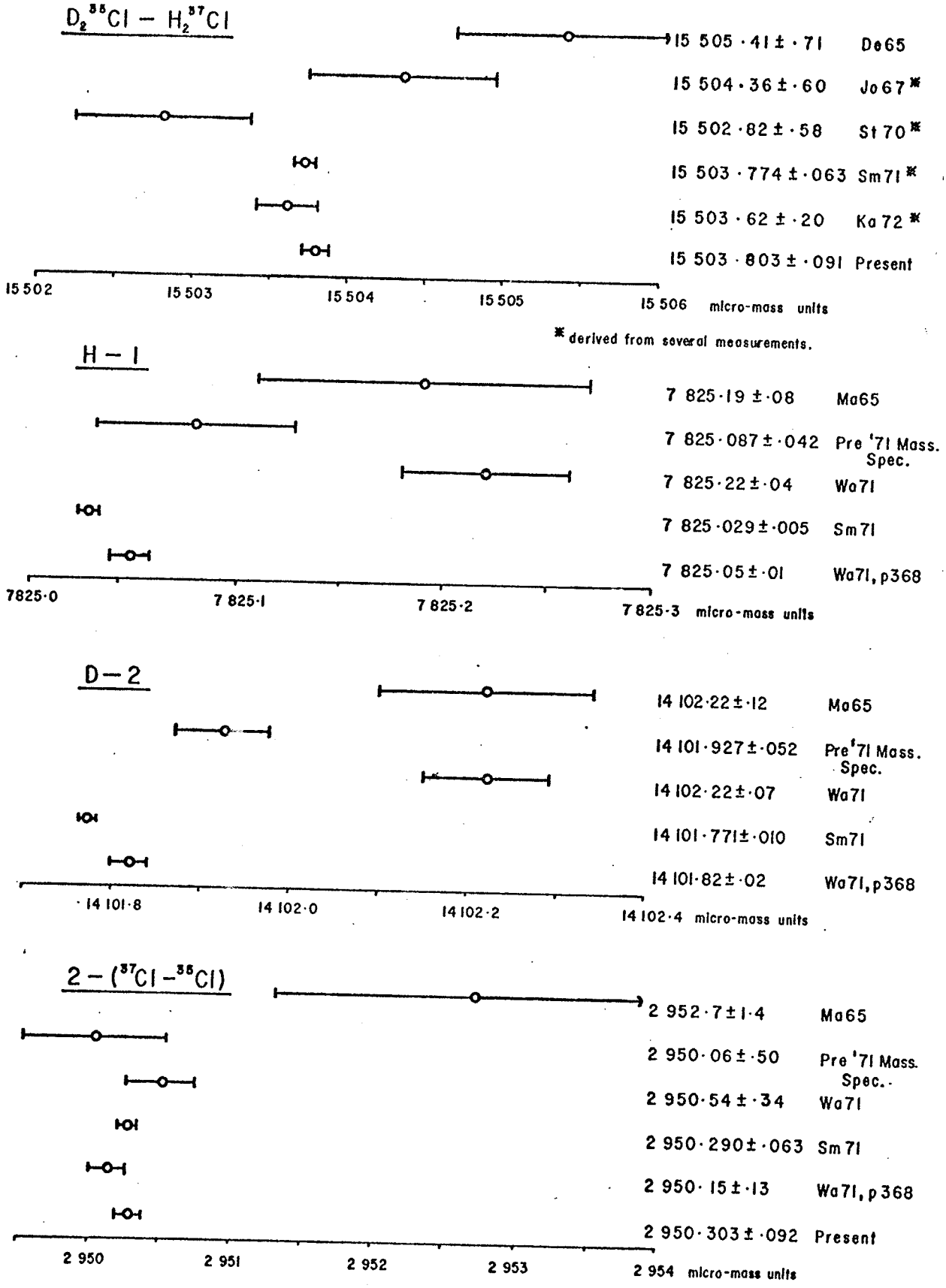

FIG. F6-2 RESULT COMPARISONS

for the same mass difference as determined in the laboratories indicated. As this actual doublet was not studied in most cases, some of the values here are composite ones, involving more than one doublet. However this procedure affords the most direct comparison with the present result.

Also shown in the table is a result based on the extensive body of data determined by Smith (Sm71) at Princeton. This work, which appeared some time after the present work was initiated, has produced significant changes in the 1971 mass table (Wa71, p368) and has provided greatly improved precision for the masses which were studied. As was noted by Wapstra in the introduction to the 1971 Mass Table (Wa71), the values reported by Smith were at that time an order of magnitude higher in precision than previous data, and thus stood virtually unsupported by other data. The measurement reported here is the only independent datum that provides with comparable precision a check on Smith's results. Moreover, the agreement between the present results and that of Smith is particularly significant inasmuch as the instruments used operate on completely different principles.

To derive a value for the $^{37}Cl - {}^{35}Cl$ mass difference

from the measurements taken here, a value of the (D - H) mass difference must be obtained. This may be done in either of the following ways:

$$(D - H) - 1 = (D - 2) - (H - 1) \qquad (6\text{-}7)$$

or

$$(D - H) - 1 = (H - 1) - (H_2 - D) \qquad (6\text{-}8)$$

Values of the (H - 1), (D - 2) and (H_2 - D) mass differences were obtained by taking the weighted averages of all previous mass spectroscopic measurements for each difference (table T6-3). Here we have adopted the (D - H) mass difference as derived from formula 6-8 because the consistency and precision of both the (H - 1) and the (H_2 - D) measurements are superior to those for the (D - 2) measurements. Some caution should be exercised in using these figures which are based purely on mass spectroscopic measurements inasmuch as there is some discrepancy between the mass spectroscopic and the mass table values (which include mass differences derived from nuclear energy determinations) particularly in the case of the deuterium mass as shown in figure F6-2.

The ^{37}Cl - ^{35}Cl mass difference derived in this way from this work is combined with previous measurements to give a weighted average of mass spectroscopic values for the ^{37}Cl - ^{35}Cl mass difference (table T6-3).

TABLE T6-3

CALCULATION OF THE CURRENT $^{37}Cl - ^{35}Cl$ MASS DIFFERENCE

D-H DIFFERENCE (Weighted averages of all Mass Spectroscopic Results):

	H - 1	7	825·035 ± ·012 μu
	H_2 - D	1	548·285 ± ·007 μu
giving	(D-H) - 1	6	276·750 ± ·014 μu

$2 - (^{37}Cl - ^{35}Cl)$

Present Work	2	950·303 ± ·092 μu
Weighted Average of all Mass Spectroscopic Results	2	950·276 ± ·064 μu

NOTE:

Mass Spectroscopic Value Prior to 1971	2	950·060 ± ·500 μu
1971 Mass Table Value	2	950·54 ± ·34 μu

The change produced in the mass spectroscopic value of the ^{37}Cl - ^{35}Cl mass difference by the addition of Smith's results and the present work (.216μu) has not significantly changed the value adopted for the extensive mass adjustment carried out for the rare earth region in which the mass differences determined by this group both at McMaster and the University of Manitoba were used as primary data (Ba72).

6.2 LUTETIUM - NEODYMIUM MEASUREMENTS

The mass measurements involving "chloride" doublets done by this group (and referred to in section 6.1) have covered a section of the mass table from Pr to Hf. Such doublets give mass differences which provide links between nuclides differing in mass number by zero, two or four mass units, as shown in Fig. F6-1. Although some checks on consistency have been made via small closed loops, there has been little information which relates the masses at opposite ends of the region. With the improved capability of the instrument reliably to measure wider doublets, it became possible to measure the $^{175}Lu^{37}Cl$ - $^{142}Nd^{35}Cl_2$ and $^{176}Lu^{37}Cl$ - $^{143}Nd^{35}Cl_2$ doublets (a and b in fig. F6-1). In these cases the fractional doublet width was 1/3,500, and calibration

measurements could be made easily to ions located one mass number away from the doublet under study. In addition, because of their chemical and physical similarity, the samples behaved predictably and similarly in the ion source used previously by this group for rare earth chlorides (sect. 3.3).

The results are given in table T6-4, and a plot of the distribution of run results with corrections applied is given in fig. F5-2.

In the $^{175}Lu\ ^{37}Cl$ - $^{142}Nd\ ^{35}Cl_2$ doublet, there was a significant discrepancy between the simple average of the run results and the weighted average. This was rectified by assigning a minimum error of 2μu (sect. 5.6), which affected three runs. In the results for the $^{176}Lu\ ^{37}Cl$ - $^{143}Nd\ ^{35}Cl_2$ doublet, one of the runs was eliminated, because its difference from the final result was 17 times the final error quoted, although no apparent reason for this discrepancy was found. The mass differences from the 1971 Mass Table were calculated from the "absolute" masses, and thus the errors for the mass differences quoted are somewhat high (i.e. the error quoted is the square root of the sum of the squares of the errors associated with the "absolute" masses). Correlation coefficients, which are necessary

TABLE T6-4

LUTETIUM - NEODYMIUM

RESULTS AND COMPARISONS

(Units: micro - mass units)

	$^{175}Lu\ ^{37}Cl - {}^{142}Nd\ ^{35}Cl_2$	$^{176}Lu\ ^{37}Cl - {}^{143}Nd\ ^{35}Cl_2$
RESULTS		
	61 249·5 ± 2·5	61 067·2 ± 1·4
No. Runs	7	6
σ int	0·93	1·25
σ ext	2·5	1·4
COMPARISONS		
71 Mass Table (Wa 71)	61 226 ± 18	61 045 ± 16
discrepancy	24 ± 18	22 ± 16
Manitoba Adj. (Me 69)	61 218·5 ± 5·4	61 036·3 ± 5·3
discrepancy	31·0 ± 5·9	30·9 ± 5·5

LOOP CLOSURE ERROR

3·4 ± 6·7 μu

using $^{143}Nd - {}^{142}Nd$ = 1·002 089 9 ± 1 5 u Me71

$^{176}Lu - {}^{175}Lu$ = 1·001 911 ± 6 u Me71

correctly to compute the errors on the correlated differences, were not available for this mass adjustment, and thus the true errors could not be calculated.

As shown by the loop closure (completed by accurate (n,γ) measurements), the results are consistent with each other. However they are not consistent either with the 1971 Mass Table (Wa71) or with recent Manitoba mass adjustments as shown in table T6-4. Further discussion of these discrepancies is deferred to section 6.4.

6.3 NARROW MASS MEASUREMENTS

In addition to the relatively "wider" doublets described hereto, we have extended the systematic study of mass differences via the narrow "chloride" doublets to include connections in hafnium, and between lutetium and ytterbium as shown in table T6-5. The latter connection is particularly important as it provides a strong mass spectroscopic link between lutetium and the rest of the Manitoba data. The new hafnium results are also compared with previous McMaster results (Wh70). In keeping with the foregoing work these new data incorporate error corrections on each run for the Hf measurements, and on the overall results for the Lu - Yb measurements. The discrepancy is

TABLE T6-5

NARROW DOUBLET RESULTS

(Units: micro-mass units)

DOUBLET	HAFNIUM PRESENT	McMASTER
^{180}Hf - ^{176}Hf	11 036·1 ± 3·0	
^{178}Hf - ^{176}Hf	5 239·5 ± 1·3	5 236 ± 5
^{180}Hf - ^{178}Hf	5 798·4 ± 0·7	5 797 ± 3
^{179}Hf - ^{177}Hf	5 544·4 ± 0·7	5 539 ± 3

$^{175}Lu\ ^{35}Cl$ - $^{173}Yb\ ^{37}Cl$

RUN	CENTROID ANALYSIS	DIFFERENCE ANALYSIS
1	5 504·8 ± 6·4	5 506·7 ± 4·6
2	5 508·1 ± 1·7	5 507·8 ± 2·7
3	5 507·8 ± 2·6	5 507·3 ± 1·8
4	5 500·6 ± 3·5	5 503·5 ± 4·4
Weighted Average	5 507·0 ± 0·7 (ext), 1·4 (int)	5 506·9 ± 1·5 (ext), 1·3 (int)
RESULT (Difference Analysis with proportional error applied)		5 507·3 ± 1·4
McMASTER RESULT		5 503 ± 4

comparable with other systematic differences between McMaster and Manitoba results (Ba72a).

The $^{180}Hf\ ^{35}Cl_2$ - $^{176}Hf\ ^{37}Cl_2$ measurement was made with borderline resolution, and the results were found to be dependent on the analysis limits chosen (sect. 4.4). The limits selected corresponded to a flat portion of the variation, and the error was increased from 1.8 to 3μu to allow for the uncertainty in the effect of the tail of one peak introducing an apparent shift in the position of the other. Since this measurement served only to corroborate the other two measurements made in hafnium, the uncertainty was not of major concern.

Attempts to measure the $^{176}Hf\ ^{35}Cl$ - $^{174}Hf\ ^{37}Cl$ difference were unsuccessful until the very recent introduction of pulse-counting techniques by this group (table T6-10).

6.4 PROPORTIONAL CORRECTIONS AND THE MASS ADJUSTMENT

The discrepancy between the present Nd - Lu measurements and that from the 1971 Mass Table (sect. 6.2) is not surprising in the light of the large errors that the mass table had in this area. Moreover, for this region, the table relied extensively on the McMaster results that had been shown to differ consistently with more recent data

(Me71). The discrepancy for the Nd - Lu differences between the new measurement and the value from the Manitoba adjustments (Me71) strongly suggests that a proportional error (as discussed previously in this work) exists in the earlier mass measurments carried out with the Manitoba II mass spectrometer. Further confirmatory evidence is contained in the following.

1. A number of narrow mass measurements have recently been carried out in this laboratory (table T6-6). The analysis for the computer - assisted matching was that used by Meredith (Me69) and proportional corrections were applied as determined from calibrations taken at, or close to the time of the measurements. Where comparisons are available with previous mass measurements, a fairly consistent difference is evident.

2. Table T6-7 shows closed loops of three doublets involving entirely corrected doublets, entirely uncorrected doublets and a mixture of doublets. The mixed loop is the only one with a significant discrepancy.

The Manitoba adjustments referred to above consisted of two separate adjustments, the first from Pr to Tm (Me71, Me72) and the second, overlapping with the first, from Er to Hf (Me71). In order to integrate the Nd - Lu measurements

TABLE T6-6

FURTHER RECENT MANITOBA MEASUREMENTS

(Units: micro - mass units)

DOUBLET	CORRECTED VALUE	McMASTER VALUE
$^{176}Yb\ ^{35}Cl - ^{168}Yb\ ^{37}Cl$	3 806·0 ± 7·6	
$^{171}Yb\ ^{35}Cl - ^{169}Tm\ ^{37}Cl$	5 061·9 ± 1·7	5 055 ± 3
$^{171}Yb\ ^{35}Cl_2 - ^{167}Er\ ^{37}Cl_2$	10 178·0 ± 0·7	
$^{172}Yb\ ^{35}Cl - ^{170}Yb\ ^{37}Cl$	4 568·5 ± 2·0	
$^{172}Yb\ ^{35}Cl_2 - ^{168}Er\ ^{37}Cl_2$	9 906·7 ± 1·7	
$^{173}Yb\ ^{35}Cl - ^{171}Yb\ ^{37}Cl$	4 835·3 ± 1·6	4 827 ± 4
$^{173}Yb\ ^{35}Cl_2 - ^{169}Tm\ ^{37}Cl_2$	9 898·3 ± 1·2	
$^{174}Yb\ ^{35}Cl - ^{172}Yb\ ^{37}Cl$	5 430·3 ± 1·1	5 420 ± 4
$^{176}Yb\ ^{35}Cl - ^{174}Yb\ ^{37}Cl$	6 656·3 ± 1·4	6 652 ± 3
$^{176}Yb\ ^{35}Cl_2 - ^{172}Yb\ ^{37}Cl_2$	12 088·9 ± 2·4	

TABLE T6-7

CLOSED LOOPS

(Units: micro - mass units)

1. CORRECTED DOUBLETS

		Value
c	$^{173}Tb\ ^{35}Cl - ^{171}Tb\ ^{37}Cl$	$4835 \cdot 3 \pm 1 \cdot 6$
c	$^{171}Tb\ ^{35}Cl - ^{169}Tm\ ^{37}Cl$	$5061 \cdot 9 \pm 1 \cdot 7$
c	$^{173}Tb\ ^{35}Cl_2 - ^{169}Tm\ ^{37}Cl$	$9898 \cdot 3 \pm 1 \cdot 2$

Discrepancy: $1 \cdot 1 \pm 2 \cdot 6$

2. UNCORRECTED DOUBLETS

u	$^{169}Tm\ ^{35}Cl - ^{167}Er\ ^{37}Cl$	$5111 \cdot 9 \pm 1 \cdot 0$
u	$^{167}Er\ ^{35}Cl - ^{165}Ho\ ^{37}Cl$	$4678 \cdot 3 \pm 1 \cdot 1$
u	$^{169}Tm\ ^{35}Cl_2 - ^{165}Ho\ ^{37}Cl_2$	$9790 \cdot 6 \pm 0 \cdot 6$

Discrepancy: $0 \cdot 2 \pm 0 \cdot 4$

3. MIXED DOUBLETS

c	$^{171}Yb\ ^{35}Cl - ^{169}Tm\ ^{37}Cl$	$5061 \cdot 9 \pm 1 \cdot 7$
u	$^{169}Tm\ ^{35}Cl - ^{167}Er\ ^{37}Cl$	$5111 \cdot 9 \pm 1 \cdot 0$
c	$^{171}Yb\ ^{35}Cl_2 - ^{167}Er\ ^{37}Cl_2$	$10178 \cdot 0 \pm 1 \cdot 7$

Discrepancy: $4 \cdot 2 \pm 2 \cdot 6$

c = corrected

u = uncorrected

with the other measurements, a single adjustment was made covering the entire range. Because of the limitations of the computing technique, the size of the computation had to be considerably reduced by including only those nuclides which were a part of the overdetermined set of data.

The introduction of the Nd - Lu measurements into the adjustment caused a fairly consistent residual to appear for the values obtained from mass doublet determinations. The residuals were particularly large at several "weak" points in the chain. In the case of the (n,γ) Q-value measurements, the average residual was approximately halved, while those for β-decay Q-values were increased slightly.

As a result of these preliminary calculations which included the Nd - Lu doublets, certain improvements were made so as to provide a more reliable picture of the mass differences for the region. These were as follows:

1. Several weak points in the chain have been greatly improved by the recent mass spectroscopic measurements (table T6-6), and some extra reaction and decay data were added (table T6-8).

2. McMaster results have been removed wherever they duplicate Manitoba results.

3. The 2 - (^{35}Cl - ^{37}Cl) value has been changed to 2950.277μu.

TABLE T6-8

ADDITIONAL REACTION AND DECAY DATA

(Units: kev)

NEUTRON SEPARATION ENERGIES

^{170}Tm	(n, γ)	6593·9 ± 1·5	Ra 67
^{171}Yb	(n, γ)	6616 ± 3	Na 69
^{172}Yb	(n, γ)	8023 ± 3	Na 69
^{174}Yb	(n, γ)	7465 ± 3	Na 69
^{175}Yb	(n, γ)	5819 ± 2	Na 69
	(n, γ)	5822·6 ± 0·5	Al 71
^{177}Yb	(n, γ)	5566·8 ± 1·2	Al 72
^{176}Lu	(n, γ)	6293·2 ± 1·2	Mi 69
^{178}Hf	(n, γ)	7625·5 ± 1·0	Fa 69, Ra 67
	(d, p)	7621 ± 10	Mi 69
^{179}Hf	(n, γ)	6098·0 ± 1·5	Ra 67, Na 66
	(n, γ)	6099·5 ± 1·5	Al 72
^{180}Hf	(n, γ)	7387·5 ± 0·5	Bu 70, Na 66

BETA DECAY ENERGIES

^{196}Er (β-) ^{169}Tm	344 ± 4	Bi 56
^{170}Tm (β-) ^{170}Yb	970 ± 0	Po 54
	968 ± 0·7	Va 69
^{175}Yb (β-) ^{175}Lu	467 ± 2	Ba 62

4. The systematic errors have been allowed for as follows:

(a) McMaster results were increased by 790 ppm, on the basis of the systematic differences found between Manitoba and McMaster results (Me71).

(b) All measurements on which corrections had not been made on the basis of calibrations at the time of the measurement were increased by 250±100ppm. This figure is an estimate based on calibration measurements to date.

The result of this adjustment is shown in table T6-9. The last column shows the change in the residual between this adjustment and one without the corrections 4(b) above. Large variations occur only in the region of Eu; the weakest portion of the chain. The average residual of reliable results is reduced from 0.67μu to 0.16μu.

6.5 S_{2n} SYSTEMATICS

The significance of the mass differences, as calculated in section 6.1, may be conveniently demonstrated by means of the systematic behaviour of S_{2n}, the double neutron separation energy, as a function of neutron number (fig. F6-3). It is well known that such a plot reflects the

TABLE T6-9 CORRECTED MASS ADJUSTMENT

SECTION A SPECTROSCOPIC MASS DIFFERENCES

(micro-mass units.)

DOUBLET	UNCORRECTED VALUE	CORRECTED VALUE	ADJUSTED VALUE	RESIDUAL	RESIDUAL CHANGE
$^{143}Nd^{35}Cl - {}^{141}Pr^{37}Cl$	5115.0±4.0	5116.3±4.0	5113.0±2.2	-3.3	-0.9
$^{145}Nd^{35}Cl - {}^{143}Nd^{37}Cl$	5707.0±4.0	5708.4±4.0	5711.5±1.5	3.1	-0.4
$^{144}Nd^{35}Cl - {}^{142}Nd^{37}Cl$	5312.0±3.0	5313.3±3.0	5316.5±1.5	3.2	-1.6
$^{146}Nd^{35}Cl - {}^{144}Nd^{37}Cl$	5981.3±0.9	5982.8±1.1	5981.0±0.8	-1.8	-0.2
$^{146}Nd^{35}Cl - {}^{144}Nd^{37}Cl$	5977.2±1.7	5978.7±1.8	5981.0±0.8	2.3	-0.2
$^{148}Nd^{35}Cl - {}^{146}Nd^{37}Cl$	6722.1±2.7	6723.8±2.8	6726.0±0.8	2.2	-0.1
$^{148}Nd^{35}Cl - {}^{146}Nd^{37}Cl$	6725.7±0.8	6727.4±1.0	6726.0±0.8	-1.4	-0.1
$^{150}Nd^{35}Cl - {}^{148}Nd^{37}Cl$	6944.0±4.0	6945.7±4.1	6947.1±1.6	1.3	-0.1
$^{149}Sm^{35}Cl - {}^{147}Sm^{37}Cl$	5235.0±3.0	5236.3±3.0	5237.7±1.8	1.3	0.4
$^{147}Sm^{35}Cl - {}^{145}Nd^{37}Cl$	5268.0±4.0	5269.3±4.0	5269.7±2.0	0.4	-0.5
$^{150}Sm^{35}Cl - {}^{148}Sm^{37}Cl$	5404.0±4.0	5405.3±4.0	5403.6±1.7	-1.7	0.6
$^{152}Sm^{35}Cl - {}^{150}Sm^{37}Cl$	5400.0±4.0	5401.3±4.0	5407.7±2.1	6.3	-1.0
$^{154}Sm^{35}Cl - {}^{152}Sm^{37}Cl$	5421.0±4.0	5422.4±4.0	5428.3±3.2	5.9	-3.8

DOUBLET	UNCORRECTED VALUE	CORRECTED VALUE	ADJUSTED VALUE	RESIDUAL	RESIDUAL CHANGE
$^{151}Eu^{35}Cl - ^{149}Sm^{37}Cl$	5618.9±2.6	5620.3±2.7	5619.9±2.4	-0.4	-2.1
$^{153}Eu^{35}Cl - ^{151}Eu^{37}Cl$	4332.0±4.0	4333.1±4.0	4329.8±3.1	-3.3	-4.0
$^{155}Gd^{35}Cl - ^{153}Eu^{37}Cl$	4344.3±2.4	4345.4±2.4	4344.4±2.2	-0.9	-1.3
$^{157}Gd^{35}Cl - ^{155}Gd^{37}Cl$	4290.0±3.0	4291.1±3.0	4289.5±2.4	-1.6	-1.7
$^{154}Gd^{35}Cl - ^{152}Gd^{37}Cl$	4018.5±2.0	4019.5±2.0	4020.8±2.0	1.3	-0.3
$^{156}Gd^{35}Cl - ^{154}Gd^{37}Cl$	4203.7±1.4	4204.7±1.5	4206.1±1.4	1.3	-0.6
$^{158}Gd^{35}Cl - ^{156}Gd^{37}Cl$	4925.0±1.3	4926.2±1.4	4927.5±1.3	1.3	-0.5
$^{160}Gd^{35}Cl - ^{158}Gd^{37}Cl$	5904.0±3.0	5905.5±3.1	5899.3±1.8	-6.2	-0.7
$^{159}Tb^{35}Cl - ^{157}Gd^{37}Cl$	4332.2±1.1	4333.3±1.2	4335.3±1.1	2.0	-0.2
$^{161}Dy^{35}Cl - ^{159}Tb^{37}Cl$	4533.9±0.9	4535.0±1.0	4536.5±1.0	1.5	0.0
$^{162}Er^{35}Cl - ^{160}Gd^{37}Cl$	4673.4±1.9	4674.6±2.0	4675.8±1.6	1.3	-0.6
$^{158}Dy^{35}Cl - ^{156}Dy^{37}Cl$	3080.6±3.3	3081.4±3.3	3081.4±3.3	0.0	0.0
$^{160}Dy^{35}Cl - ^{158}Dy^{37}Cl$	3730.9±2.3	3731.8±2.3	3731.8±2.3	0.0	0.0
$^{162}Dy^{35}Cl - ^{160}Dy^{37}Cl$	4551.0±1.0	4552.1±1.1	4550.9±1.0	-1.2	-0.1
$^{164}Dy^{35}Cl - ^{162}Dy^{37}Cl$	5325.2±0.8	5326.5±1.0	5326.3±0.9	-0.2	-0.1
$^{163}Dy^{35}Cl - ^{161}Dy^{37}Cl$	4743.5±1.1	4744.7±1.2	4746.8±1.1	2.1	-0.1

DOUBLET	UNCORRECTED VALUE	CORRECTED VALUE	ADJUSTED VALUE	RESIDUAL	RESIDUAL CHANGE
$^{165}Ho^{35}Cl - {}^{163}Dy^{37}Cl$	4537.0±4.0	4538.1±4.0	4543.7±2.3	5.6	-3.3
$^{167}Er^{35}Cl - {}^{165}Ho^{37}Cl$	4678.3±1.1	4679.5±1.2	4679.2±0.9	-0.2	0.2
$^{164}Er^{35}Cl - {}^{162}Er^{37}Cl$	3372.5±1.3	3373.3±1.3	3373.4±1.3	0.0	-0.6
$^{166}Er^{35}Cl - {}^{164}Er^{37}Cl$	4039.9±1.3	4040.9±1.4	4041.4±1.2	0.5	-0.5
$^{168}Er^{35}Cl - {}^{166}Er^{37}Cl$	5027.6±1.4	5028.9±1.5	5028.7±0.8	-0.1	-0.9
$^{170}Er^{35}Cl - {}^{168}Er^{37}Cl$	6045.4±1.7	6046.9±1.8	6045.1±1.5	-1.8	-0.5
$^{169}Tm^{35}Cl - {}^{167}Er^{37}Cl$	5111.9±1.0	5113.2±1.1	5114.1±0.8	0.9	-0.1
$^{171}Yb^{35}Cl - {}^{169}Tm^{37}Cl$	5061.9±1.7	5061.9±1.7	5063.2±1.0	1.3	-0.5
$^{173}Yb^{35}Cl - {}^{171}Yb^{37}Cl$	4835.3±1.6	4835.3±1.6	4834.6±1.0	-0.7	-0.2
$^{170}Yb^{35}Cl - {}^{168}Yb^{37}Cl$	3806.0±7.6	3806.0±7.6	3813.3±5.8	7.3	0.0
$^{172}Yb^{35}Cl - {}^{170}Yb^{37}Cl$	4568.5±2.7	4568.5±2.7	4569.7±1.4	1.2	-0.5
$^{174}Yb^{35}Cl - {}^{172}Yb^{37}Cl$	5430.3±1.1	5430.3±1.1	5430.0±0.9	-0.3	-0.1
$^{176}Yb^{35}Cl - {}^{174}Yb^{37}Cl$	6656.3±1.4	6656.3±1.4	6657.0±1.2	0.7	0.0
$^{175}Lu^{35}Cl - {}^{173}Yb^{37}Cl$	5507.3±1.4	5507.3±1.4	5509.6±1.2	2.3	-0.8
$^{179}Hf^{35}Cl - {}^{177}Hf^{37}Cl$	5544.4±0.7	5544.4±0.7	5544.6±0.6	0.2	0.0
$^{178}Hf^{35}Cl - {}^{176}Hf^{37}Cl$	5239.5±1.3	5239.5±1.3	5239.4±1.2	-0.1	0.0

DOUBLET	UNCORRECTED VALUE	CORRECTED VALUE	ADJUSTED VALUE	RESIDUAL	RESIDUAL CHANGE
$^{180}Hf^{35}Cl - ^{178}Hf^{37}Cl$	5798.4±0.7	5798.4±0.7	5799.3±0.6	0.9	0.0
$^{173}Yb^{35}Cl_2 - ^{169}Tm^{37}Cl_2$	9898.3±1.2	9898.3±1.2	9897.8±0.9	-0.5	-0.7
$^{171}Yb^{35}Cl_2 - ^{167}Er^{37}Cl_2$	10178.0±1.7	10178.0±1.7	10177.3±1.0	-0.7	0.6
$^{169}Tm^{35}Cl_2 - ^{165}Ho^{37}Cl_2$	9790.6±0.6	9793.0±1.1	9793.3±0.9	0.3	0.0
$^{145}Nd^{35}Cl_2 - ^{141}Pr^{37}Cl_2$	10826.0±7.0	10828.7±7.1	10824.5±2.5	-4.2	-1.3
$^{180}Hf^{35}Cl_2 - ^{176}Hf^{37}Cl_2$	11036.1±3.0	11036.1±3.0	11038.7±1.3	2.6	0.0
$^{176}Yb^{35}Cl_2 - ^{172}Yb^{37}Cl_2$	12088.9±2.4	12088.9±2.4	12087.0±1.4	-1.9	-0.1
$^{172}Yb^{35}Cl_2 - ^{168}Er^{37}Cl_2$	9906.7±1.7	9906.7±1.7	9908.7±1.1	2.0	0.2
$^{168}Yb^{35}Cl_2 - ^{164}Dy^{37}Cl_2$	10612.8±8.7	10612.8±8.7	10622.4±5.9	9.6	0.0
$^{162}Er^{35}Cl_2 - ^{158}Gd^{37}Cl_2$	10574.9±2.5	10577.5±2.7	10575.1±1.8	-2.4	-1.3
$^{152}Sm^{35}Cl_2 - ^{148}Sm^{37}Cl_2$	10808.1±1.7	10810.8±2.0	10811.3±1.8	0.5	-0.4
$^{148}Sm^{35}Cl_2 - ^{144}Sm^{37}Cl_2$	8719.2±2.6	8721.4±2.7	8722.3±1.8	0.9	-0.1
$^{150}Nd^{35}Cl_2 - ^{146}Nd^{37}Cl_2$	13669.1±1.1	13672.5±1.8	13673.1±1.4	0.5	-0.2
$^{148}Nd^{35}Cl_2 - ^{144}Nd^{37}Cl_2$	12700.4±1.8	12703.6±2.2	12707.0±1.0	3.4	-0.3
$^{148}Nd^{35}Cl_2 - ^{144}Nd^{37}Cl_2$	12701.8±1.7	12705.0±2.1	12707.0±1.0	2.0	-0.3

DOUBLET	UNCORRECTED VALUE	CORRECTED VALUE	ADJUSTED VALUE	RESIDUAL	RESIDUAL CHANGE
$^{175}Lu^{37}Cl - {}^{142}Nd^{35}Cl_2$	61251.1±2.1	61251.1±2.1	61252.3±1.6	1.3	-1.1
$^{176}Lu^{37}Cl - {}^{143}Nd^{35}Cl_2$	61067.2±1.4	61067.2±1.4	61067.6±1.2	0.4	-0.6
$^{160}Gd - {}^{160}Dy$	1854.0±0.8	1854.5±0.8	1855.1±0.8	0.6	-0.1
$^{154}Sm - {}^{154}Gd$	1337.9±3.8	1338.2±3.8	1333.0±3.1	-5.2	3.4
$^{150}Nd - {}^{150}Sm$	3616.8±1.0	3617.7±1.1	3617.4±0.9	-0.3	0.5
$^{148}Nd - {}^{148}Sm$	2075.0±5.1	2075.5±5.1	2073.6±1.8	-1.9	0.8
$^{144}Sm - {}^{144}Nd$	1911.4±1.1	1911.9±1.1	1912.0±1.0	0.1	0.0

SECTION B REACTION Sn VALUES

(KeV)

NUCLIDE	INPUT VALUE	CORRECTED VALUE	OUTPUT RESIDUAL	RESIDUAL CHANGE
^{142}Pr	5843.8±0.8	5843.6±0.8	-0.2	-0.1
^{143}Nd	6123.3±1.9	6122.4±1.4	-0.9	0.0
^{144}Nd	7816.8±0.9	7816.8±0.9	0.0	0.3
^{145}Nd	5746.0±15.	5754.5±1.3	8.5	-1.2
^{146}Nd	7565.8±1.1	7565.7±1.1	0.0	0.0
^{148}Sm	8140.2±1.0	8140.3±1.0	0.1	0.1
^{149}Sm	5876.0±9.0	5872.3±1.8	-3.6	-1.7
^{150}Sm	7985.8±0.6	7985.7±0.6	-0.1	-0.1
^{155}Sm	5809.0±12.	5808.3±9.1	-0.8	0.9
^{152}Eu	6305.0±4.0	6302.4±3.6	-2.6	1.0
^{154}Eu	6418.0±7.0	6420.4±4.8	2.4	1.2
^{156}Gd	8531.0±5.0	8530.4±2.6	-0.6	1.1
^{158}Gd	7934.0±1.1	7936.1±1.1	2.1	-0.2
^{161}Dy	6459.7±7.0	6458.9±1.6	-0.8	-0.9
^{162}Dy	8193.6±2.9	8193.5±1.5	-0.1	0.0
^{163}Dy	6271.7±2.4	6276.5±1.4	4.8	-1.0
^{164}Dy	7655.4±2.2	7653.6±1.5	-1.8	-0.2
^{165}Dy	5715.3±1.4	5715.3±1.5	0.0	0.0
^{166}Ho	6243.4±0.9	6243.4±0.9	0.0	-0.1

NUCLIDE	INPUT VALUE	CORRECTED VALUE	OUTPUT RESIDUAL	RESIDUAL CHANGE
^{165}Er	6650.1±0.7	6650.2±0.7	0.1	0.0
^{166}Er	8474.5±7.1	8476.7±1.4	2.2	-0.5
^{167}Er	6436.2±0.5	6436.1±0.5	-0.1	-0.1
^{168}Er	7771.0±0.7	7771.2±0.6	0.2	-0.3
^{169}Er	6003.0±0.3	6003.0±0.3	0.0	0.0
^{170}Er	7263.0±9.0	7257.5±1.5	-5.5	-0.9
^{171}Er	5681.5±0.5	5681.6±0.5	0.1	0.0
^{170}Tm	6594.2±1.3	6593.6±1.2	-0.6	0.2
^{171}Yb	6615.9±2.8	6613.5±1.4	-2.3	0.3
^{172}Yb	8023.3±2.8	8021.3±1.0	-2.0	0.2
^{173}Yb	6367.2±0.5	6366.8±0.5	-0.4	0.0
^{174}Yb	7465.5±2.8	7466.7±1.0	1.2	0.1
^{175}Yb	5822.4±0.5	5822.6±0.5	0.2	0.0
^{177}Yb	5566.7±1.2	5566.7±1.3	0.0	0.0
^{176}Lu	6293.2±1.2	6292.9±1.2	-0.3	0.5
^{177}Hf	6375.0±7.0	6385.6±1.3	10.6	0.0
^{178}Hf	7625.0±0.9	7625.5±0.7	0.5	0.0
^{179}Hf	6098.5±1.0	6101.3±0.6	2.8	0.0
^{180}Hf	7387.3±0.6	7388.2±0.5	0.9	0.0

SECTION C BETA DECAY Q-VALUES
(β^- except were noted) (KeV)

NUCLIDE	INPUT VALUE	CORRECTED VALUE	OUTPUT RESIDUAL	RESIDUAL CHANGE
^{142}Pr	2164.0±2.0	2162.8±1.9	-1.2	-0.3
^{147}Nd	895.2±0.8	895.2±0.9	0.0	0.0
^{147}Pm	224.6±0.6	224.6±0.6	0.0	0.0
^{152}Eu β^+	1867.0±9.0	1881.0±4.2	14.0	-2.0
^{152}Eu	1828.0±7.0	1811.4±4.5	-16.6	4.2
^{154}Eu	1980.0±5.0	1981.2±4.5	1.2	0.6
^{155}Eu	247.0±3.0	246.9±3.2	0.0	0.0
^{155}Sm	1630.0±11.	1629.4±9.0	-0.6	0.7
^{165}Er e.c.	371.0±6.0	380.0±1.7	9.0	0.7
^{165}Dy	1290.0±10.	1290.2±2.7	0.2	2.1
^{166}Ho	1854.0±4.0	1853.3±1.3	-0.6	-1.1
^{171}Er	1490.0±2.0	1492.1±1.6	2.1	0.4
^{169}Er	344.0±4.0	353.5±1.0	9.5	-0.8
^{170}Tm	968.2±0.7	968.0±0.7	-0.2	0.1
^{171}Tm	97.0±1.0	97.5±1.0	0.5	0.1
^{175}Yb	467.0±2.0	470.0±1.4	3.0	0.6
^{176}Lu	1193.6±4.2	1193.6±4.5	0.0	0.0
^{177}Lu	497.0±1.0	497.0±1.1	0.0	0.0

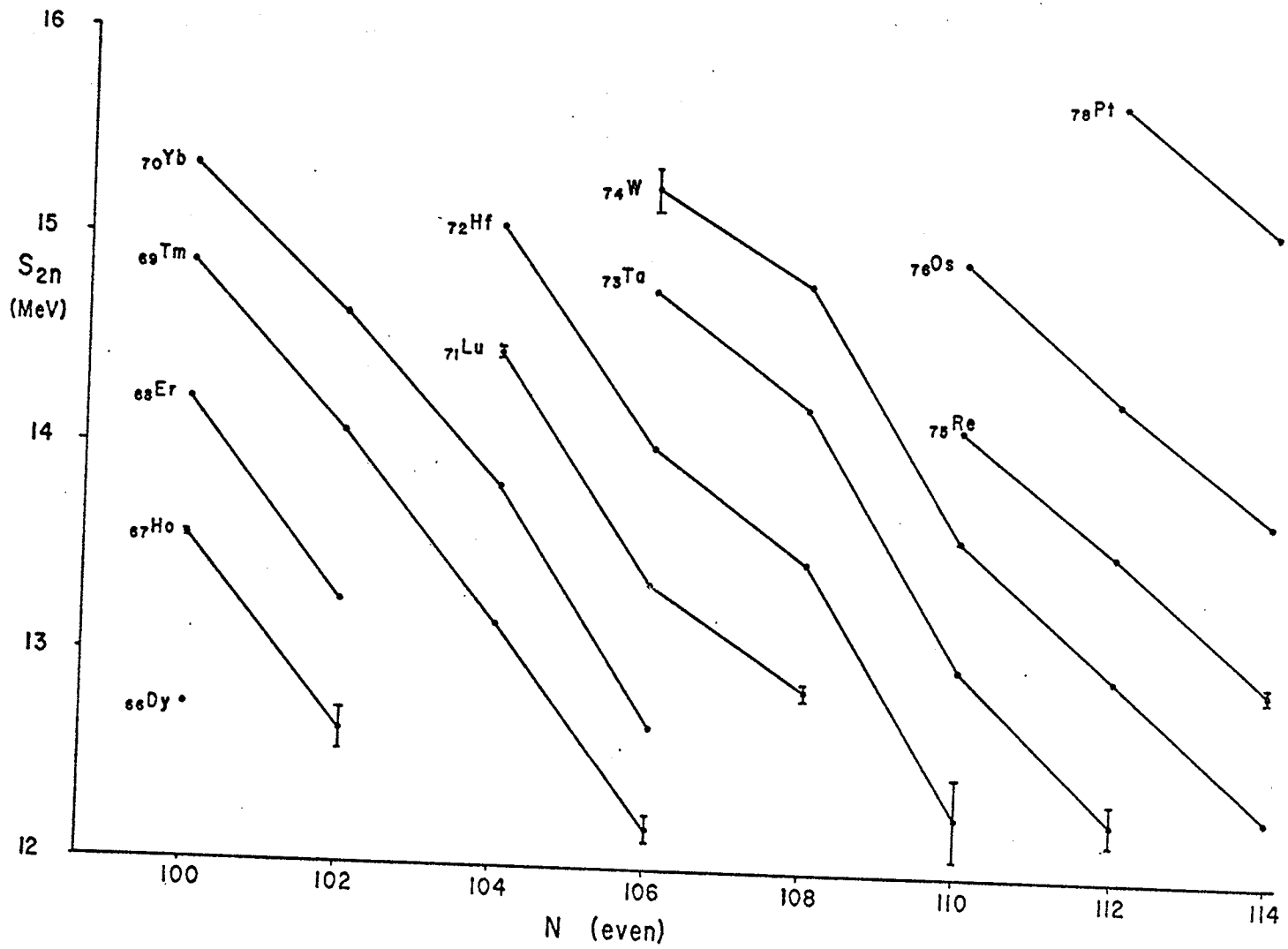

FIG. F6-3 S_{2n} SYSTEMATICS

features of nuclear structure such as the major shell closures at 28, 50, 82 and 126 neutrons, and the onset of deformation for nuclides in the region around 90 neutrons (Wa71).

Apart from the transition region (N=88 to 92) where nuclear deformation sets in, the S_{2n} curves exhibit very strong correlations between elements (e.g. Du69, Me71). In particular, if plots for even-N values and odd-N values are separated, then the line drawn between two adjacent S_{2n} points for one element are usually very nearly parallel to similar lines between points for the same two N values for other elements.

The plot of the S_{2n} values for even-N nuclides between 100 and 114 neutrons is given in fig. F6-3. The hafnium measurements described here (sect. 6.3) have improved the precision of that portion of the curve, but have not significantly affected its shape. Related recent measurements by this group in tungsten and hafnium (table T6-10) have substantially changed the S_{2n} curves in this region and show that the curves closely follow the above described systematic behaviour. In particular, the high-low-high slope pattern between 104 and 110 neutrons is now seen to occur to nearly the same extent for all the

TABLE T6-10

S_{2n} VALUES

DERIVED FROM RECENT MANITOBA MEASUREMENTS

MEASUREMENTS (Ba73)

$^{183}W\,O_2\,^{35}Cl - {}^{180}W\,^{35}Cl_2 = 24\,421 \pm 9$ μu

giving $S_{3n}\,(^{183}W)^2 = 21\,006 \pm 8$ kev

$^{176}Hf\,^{35}Cl - {}^{174}Hf\,^{37}Cl = 4\,103 \pm 23$ μu

ADDITIONAL DATA

$S_n\,(^{183}W) = 6{\cdot}191{\cdot}4 \pm 1{\cdot}4$ kev (Wa 71)

$S_{4n}\,(^{182}W) = 30\,071 \pm 100$ kev (Go 72)

SEPARATION ENERGIES

$S_{2n}(^{182}W) = S_{3n}\,(^{183}W) - S_n\,(^{183}W)$

$= 14\,815 \pm 8$ kev

('71 Mass Table = 14 700 ± 200)

$S_{2n}\,(^{180}W) = S_{4n}\,(^{182}W) - S_{2n}\,(^{182}W)$

$= 15\,255 \pm 100$ kev

('71 Mass Table = 15 370 ± 220 kev)

$S_{2n}\,(^{176}Hf) = 15\,069 \pm 21$ kev

('71 Mass Table = 14 942 ± 30 kev)

elements involved. The high slope portions have been interpreted (Ba73) as representing unusually large spaces between the Nilsson levels (i.e. above the 5/2- [512] (N=104) and 9/2+ [624] (N=108) levels) and the low slope as representing a small space (above the 7/2- [514] (N=106) level).

It is interesting to note that Ogle et al. (Og71) have calculated single particle levels for a deformed harmonic oscillator potential, considering the effects of both quadrupole and tetroidal deformations. They present diagrams that show that the general features required by the experimental results are reproduced. In particular, the introduction of a small positive tetroidal component improves the agreement with the sizes of the level spacing and leads to the correct ordering of the levels between 94 and 110 neutrons using the deformations measured (Mo59).

CONCLUSION

The Manitoba II 1 metre high resolution mass spectrometer has been modified for measuring wider mass differences than those previously possible with this instrument. Errors encountered, found to be due to surface charges, were minimised and compensated for. Measurements were made for doublets with a separation of 1/3,000, and, with the aide of a computer - assisted matching system, a precision as high as $\sigma/M = 1.7 \times 10^{-9}$ was acheived on the $C\,{}^{37}Cl\,H_2 - C{}^{35}Cl\,D_2$ doublet. This result was found to be in excellent agreement with other measurements. Measurements were also made on the mass difference between lutetium and neodymium and several narrow measurements in the ytterbium - hafnium region.

The measurements here have strongly indicated a systematic error existing in previous measurements done by this group. Approximate compensations have been made, and a new adjusted set of mass differences presented.

Some interesting trends have also been reinforced in the S_{2n} systematics.

APPENDIX

BLEAKNEY'S THEOREM

Although the basic equations describing the motion of charged particles in electric and magnetic fields existed well before the turn of the century, the formulation published by Bleakney in a short footnote in a teaching journal in 1936 (Bl36) has assumed an important position in mass spectrometry. His basic development is presented here, together with some conclusions applicable to this thesis.

The force $\underset{\sim}{F}$ at any given point on an ion of mass m and electric charge e moving with a velocity $\underset{\sim}{v}$ in a combination of electric and magnetic fields $\underset{\sim}{E}$, $\underset{\sim}{B}$, is described by the Lorentz force equation:

$$\underset{\sim}{F} = e (\underset{\sim}{E} + \underset{\sim}{v} \times \underset{\sim}{B}) \qquad (A\text{-}1)$$

and since

$$\underset{\sim}{F} = m \, \underset{\sim}{v} \cdot d\underset{\sim}{v} / ds \qquad (A\text{-}2)$$

where s is the distance along the trajectory, then we can write

$$m \, \underset{\sim}{v} \cdot d\underset{\sim}{v} / ds = e (\underset{\sim}{E} + \underset{\sim}{v} \times \underset{\sim}{B}) \; . \qquad (A\text{-}3)$$

From this equation we can derive the trajectory of the

ion, given a knowledge of its initial velocity , and the electric and magnetic field vectors at all points on the trajectory.

If we now change the values of m, $\underset{\sim}{v}$, $\underset{\sim}{E}$, $\underset{\sim}{B}$ and e throughout the system by multiplying them by scalar constants ζ, ξ, τ, κ and ν respectively, then equation A-3 becomes

$$\zeta\xi^2 m \, \underset{\sim}{v} \cdot d\underset{\sim}{v} / ds = \nu e (\tau \underset{\sim}{E} + \xi\kappa \, \underset{\sim}{v} \times \underset{\sim}{B}) \quad (A-4)$$

which will become identical to equation A-3 provided

$$\zeta\xi^2 = \nu\tau = \nu\xi\kappa \quad (A-5)$$

Hence the two systems described by equations A-3 and A-4 will have identical trajectories subject to condition A-5, which can be re-expressed as

$$\frac{\nu\tau}{\zeta\xi^2} = 1 \quad (A-6)$$

and

$$\frac{\nu\kappa}{\zeta\xi} = 1 \quad (A-7)$$

which is equivalent to saying

$$e \, \underset{\sim}{E} / K = \text{const} \quad (A-8)$$

and

$$e \, \underset{\sim}{B} / |\underset{\sim}{P}| = \text{const} \quad (A-9)$$

where K is the kinetic energy of the ion, and $\underset{\sim}{P}$ is its momentum.

If we consider a situation where the electric field system and the charge of the ions remain constant ($\tau = \nu = 1$), and the same trajectory is maintained for changing B, then we obtain from A-6

$$\xi = 1/\sqrt{\zeta} \qquad \text{(A-10)}$$

which can be substituted into (A-7) obtaining

$$\kappa = \sqrt{\zeta} \ . \qquad \text{(A-11)}$$

This can be re-expressed as

$$M \propto B^2 \ . \qquad \text{(A-12)}$$

REFERENCES

Al71 Alenius, G. et al.,
Phys. Scripta (Sweden) 4, 35 (1971).

Al72 Alenius, G., Arnell, S.E., Schale, C., Wallander, E.,
Nucl. Phys. A186, 209 (1972).

As19 Aston, F.W., Phil. Mag. 38, 707 (1919).

As20 Aston, F.W., Phil. Mag. 39, 449 (1920).

As22 Aston, F.W.,
Isotopes (Edward Arnold Co., London, 1922).

As22a Aston, F.W., and Fowler R.H.,
Phil. Mag. 43, 514 (1922).

As27 Aston, F.W., Proc. Roy. Soc. A115, 487 (1927).

As33 Aston, F.W.,
Mass Spectra and Isotopes (Edward Arnold
Co., London, 1933).

As42 Aston, F.W.,
Mass Spectra and Isotopes, 2nd edition
(Edward Arnold Co., London, 1942).

Ba33 Barber, N.F., Proc. Leeds Phil. Soc. 2, 427 (1933).

Ba33a Bainbridge, K.T., Phys. Rev. 43, 367 (1933).

Ba33b Bainbridge, K.T., Phys. Rev. 44, 123 (1933).

Ba36 Bainbridge, K.T., and Jordon, E.B.,
Phys. Rev. 50, 282 (1936).

Ba62 Bashandy, E., el Nesr, N,S.,
Arkiv. for Fysik 21, 65 (1962).

Ba64 Barber, R.C., Bishop, R.L., Cambey, L.A.,
Duckworth, H.E., McDougall, J.D., McLatchie, W.,
and Van Rookhuyzen, P.,
Proc. of the 2nd. Int. Conf. on Nucl. Masses,
Vienna, Austria, ed. W.H. Johnson Jr.,
(Springer-Verlag, Wien, 1964), p393.

Ba64a Bainbridge, K.T., and Moreland, P.E. Jr.,
Proc. of the 2nd. Int. Conf. on Nucl. Masses,
Vienna, Austria, ed. W.H. Johnson Jr.,
(Springer-Verlag, Wien, 1964), p423.

Ba67 Barber, R.C., Meredith, J.O., Bishop, R.L.,
Duckworth, H.E., Kettner, M.E.,
and Van Rookhuyzen, P.,
Proc. 3rd Int. Conf. on Atomic Masses,
ed. R.C. Barber, (Univ. of Manitoba Press,
Winnipeg, 1967) p717.

Ba67a Bainbridge, K.T., and Dewdney, J.W.,
Proc. 3rd Int. Conf. on Atomic Masses,
ed. R.C. Barber, (Univ. of Manitoba Press,
Winnipeg, 1967) p758.

Ba71 Barber, R.C., Bishop, R.L., Duckworth, H.E.,
Meredith, J.O., Southon, F.C.G., Van Rookhuyzen, P.,
and Williams, P.,
Rev. Sci. Instr. 42, 1 (1971).

Ba72 Barber, R.C., Bishop, R.L., Meredith, J.O.,
Southon, F.C.G., Williams, P., Duckworth, H.E.,
and Van Rookhuyzen, P.,
Can. J. Phys. 50, 34 (1972).

Ba73 Barber, R.C., Meredith, J.O., Southon, F.C.G.,
Williams, P., Barnard, J.W., Sharma, K.,
and Duckworth, H.E., to be published.

Be59 Benson, J.L., Damerow, R.A., Ries, R.R.,
Phys. Rev. 113, 1105 (1959).

Be65 Benson, J.L.,
PhD. Thesis, Univ. of Minnesota, (1965), p21.

Be66 Benson, J.L., Johnson, W.H.,
Phys. Rev. 141, 1112 (1966).

Bi30 Birge, R.T., Phys. Rev. 40, 207 (1930).

Bi56 Bisi, A., Terrani, S., Zappa,L.,
Nuovo Cimento 4, 758 (1956).

Bi69 Bishop, R.L.,
PhD. Thesis, Univ. of Manitoba, (1969).

Bl36 Bleakney, W., Am. Phys. Teacher 4, 12 (1936).

Bu70 Bushnell, D.L.,
Bull. Am. Phys. Soc. 15, 524 (1970).

Bu72 Burrell, D., MSc. Thesis, Univ. of Manitoba, (1972).

Cl07 Classen
Jahrb. d. Hamburg Wiss. Anst., Bieheft, 1907.

Co25 Costa, J.L., Annalen de Physique 4, 425 (1925).

Co57 Collins, T.L., and Bainbridge, K.T.,
Nuclear Masses and their Determinations
ed. H. Hintenberger, (Pergamon Press, London, 1957), p213.

De18 Dempster, A.J., Phys. Rev. 11, 316 (1918).

De22 Dempster, A.J., Phys. Rev. 20, 631 (1922).

De35 Dempster, A.J., Proc. Am. Phil. Soc. 75, 755 (1935).

De38 Dempster, A.J., Phys. Rev. 53, 64, 869 (1938).

De64 Demirkanov, R.A., Dorokov, V.V., and Dzkuya, M.I.,
Proc. of the 2nd. Int. Conf. on Nucl. Masses,
Vienna, Austria, ed. W.H. Johnson Jr.,
(Springer-Verlag, Wien, 1964), p430.

De65 Dewdney, J.W., Bainbridge, K.T.,
Phys. Rev. 138B, 540 (1965).

Du50 Duckworth, H.E., Rev. Sci. Instr. 21, 54 (1950).

Du57 Duckworth, H.E., Kerr, J.T., and Bainbridge, G.R.,
Nuclear Masses and their Determinations
ed. H. Hintenberger, (Pergamon Press, London, 1957), p218.

Du58 Duckworth, H.E., Mass Spectroscopy
(Cambridge Univ. Press, Cambridge, 1958).

Du69 Duckworth, H.E., Barber, R.C., Van Rookhuyzen, P., Macdougall, J.D., McLatchie, W., Whineray, S., Bishop, R.L., Meredith, J.O., Williams, P., Southon, G., Wong, W., Hogg, B.G., and Kettner, M.E., Phys. Rev. Lett. 23, 592 (1969).

Ev57 Everling, F., Hintenberger. H., König, L.A., Mattauch, J., Muller-Warmuth, W., and Wende, H., Nuclear Masses and their Determinations ed. H. Hintenberger, (Pergamon Press, London, 1957), p221.

Ew53 Ewald, H., and Hintenberger, H., Methoden und Anwendungen der Massenspektroskopie (Verlag Chemie, Weinheim, 1953).

Ew57 Ewald, H., Liebl, H., Z. Naturforschg. 12a, 28 (1957).

Fa69 Faler, K.T., Spencer, R.R., Harlan, R.A., Nucl. Phys. A123, 616 (1969).

Ge57 Geschwind, S., Nuclear Masses and their Determinations ed. H. Hintenberger, (Pergamon Press, London, 1957), p163.

Gi54 Giese, C.F., Collins, T.L., Phys. Rev. 96, 823A (1954).

Go72 Gove, N.B., and Wapstra, A.H., Nucl. Data Tables 11, 127 (1972).

Ha52 Hasted, J.B., Proc. Roy. Soc. A212, 235 (1952).

He34 Herzog, R., Z. fur Physik 89, 447 (1934).

Hi55 Hintenberger, H., Wende, H., and König, L.A., Z. Naturforschg. 10a, 605 (1955).

Hi57 Hintenberger, H., and König, L.A., Z. Naturforschg. 12a, 773 (1957).

Hi59 Hintenberger, H., and König, L.A., Adv. in Mass Spectrometry, ed. J.D. Waldron (Pergamon Press, London, 1959) p16.

Hu29 Hughes, A.Ll., and Rojansky, V., Phys. Rev. 34 284 (1929).

Hu68 Hudson, M.C., and Johnson, W.H. Jr., Phys. Rev. 167, 1064 (1968).

Hu70 Hudson, M.C., and Johnson, W.H. Jr., Recent Developments in Mass Spectroscopy, ed. K. Ogata and T. Hayakawa (Univ. of Tokyo Press, Tokyo, 1970) p495.

Jo40 Jordon, E.B., Phys. Rev. 57, 1072 (1940).

Jo40a Jordon, E.B., Phys. Rev. 58, 1009 (1940).

Jo53 Johnson, E.G., and Nier, A.O., Phys. Rev. 91, 10 (1953).

Jo67 Johnson, W.H., Hudson, M.C., Britten, R.A., and Kayser, D.C., Proc. 3rd Int. Conf. on Atomic Masses, ed. R.C. Barber, (Univ. of Manitoba Press, Winnipeg, 1967) p793.

Jo73 Johnson, W.H., priv. comm. to R.C. Barber (1973).

Ka70 Katakuse, I., Nakabushi, H., and Ogata, K., Mass Spectroscopy (Japan) 18, 1276 (1970).

Ka72 Kayser, D.C., Britten, R.A., and Johnson, W.H., Atomic Masses & Fundamental Const. 4, ed. J.H. Sanders and A.H. Wapstra, (Plenum Press, London, 1972) p172.

Ke70 Kerr, D.P., and Bainbridge, K.T., Recent Developments in Mass Spectroscopy, ed. K. Ogata and T. Hayakawa (Univ. of Tokyo Press, Tokyo, 1970) p490.

Ke71 Kerr, D.P., and Bainbridge, K.T., Can. J. Phys. 49, 756 (1971).

Ko57 König, L.A., and Hintenberger, H., Z. Naturforschg. 12a, 377 (1957).

Ko58 König, L.A., and Hintenberger, H., Z. Naturforschg. 13a, 1025 (1958).

Li57 Liebl, H., and Ewald, H.,
Z. Naturforschg. 12a, 538 (1957).

Li57a Liebl, H., and Ewald, H.,
Z. Naturforschg. 12a, 541 (1957).

Li59 Liebl, H., and Ewald, H.,
Z. Naturforschg. 14a, 842 (1959).

Lu72 Luxon, J.L., and Rich, A.,
Phys. Rev. Lett. 29, 665 (1972).

Ma36 Mattauch, J., Phys. Rev. 50, 617 (1936).

Ma65 Mattauch, J.H.E., Thiele, W., and Wapstra, A.H.,
Nucl. Phys. 67, 1 (1965).

Ma66 Macdougall, J.D., McLatchie, W., Whineray, S.,
and Duckworth, H.E.,
Z. Naturforschg. 21a, 63 (1966).

Ma66a Matsuda, H., Fukumoto, S., and Kuroda, Y.,
Z. Naturforschg. 21a, 25 (1966).

Ma70 Matsuda, H., Fukumoto, S., and Matsuo, T.,
Recent Developments in Mass Spectroscopy,
ed. K. Ogata and T. Hayakawa
(Univ. of Tokyo Press, Tokyo, 1970) p477.

Ma70a Matsuo, H., Adv. in Mass Spectroscopy, Vol 5,
(Inst. of Petroleum, London, 1970).

Ma70b Macdougall, J.D., McLatchie, W., Whineray, S.,
and Duckworth, H.E.,
Nucl. Phys. A145, 223 (1970).

Ma71 Matsuda, H., and Matsuo, T.,
J. of Mass Spec. and Ion Phys. 6, 361 (1971).

Ma71a Matsuda, H., and Matsuo, T.,
J. of Mass Spec. and Ion Phys. 6, 385 (1971).

Mc70 McLatchie, W., Whineray, S., MacDougall, J.D.,
and Duckworth, H.E.,
Nucl. Phys. A145, 244 (1970).

Me71 Meredith, J.O.,
PhD. Thesis, U. of Manitoba (1971).

Me72 Meredith, J.O., and Barber, R.C.,
Can. J. Phys. 50, 1195 (1972).

Me73 Meredith, J.O., and Barber, R.C.,
J. of Mass Spec. and Ion Phys. 10, 359 (1973).

Mi69 Minor, M.M., Sheline, R.K., Shera, E.B.,
and Jurney, E.T. Phys. Rev. 187, 1516 (1969).

Mi69b Minor, M., Thesis, Tallahas (1969).

Mo59 Mottleson, B.R., and Nilsson, S.G., K. Danske
Vidensk. Selsk. mat.-fys. Skr. 1, No. 8 (1959).

Mo64 Moreland, P.E. Jr., and Bainbridge, K.T.,
Proc. of the 2nd. Int. Conf. on Nucl. Masses,
Vienna, Austria, ed. W.H. Johnson Jr.,
(Springer-Verlag, Wien, 1964), p423.

Na66 Namenson, A., Jackson, H.E., Smither, R.K.,
Phys. Rev. 146, 844 (1966).

Na69 Namenson, A.I., Ritter, J.C.,
Phys. Rev. 183, 983 (1969).

Na69a Nakabushi, H., Katakuse, I., and Ogata, K.,
Mass Spectroscopy (Japan) 17, 705 (1969).

Na70 Nakabushi, H., Katakuse, I., and Ogata, K.,
Recent Developments in Mass Spectroscopy,
ed. K. Ogata and T. Hayakawa
(Univ. of Tokyo Press, Tokyo, 1970) p482.

Ni51 Nier, A.O., Phys. Rev., 81, 624 (1951).

Ni57 Nier, A.O., Quisenberry, K.S., and Scolman, T.T.,
Nuclear Masses and their Determinations
ed. H. Hintenberger, (Pergamon Press, London,
1957), p49.
Nier, A.O., ibid. p185.

Og57 Ogata, K., and Matsuda, H.,
Nuclear Masses and their Determinations
ed. H. Hintenberger, (Pergamon Press, London,
1957), p202.

Og67 Ogata, K., Matsumoto, S., Nakabushi, H., and Katakuse, I., Proc. 3rd Int. Conf. on Atomic Masses, ed. R.C. Barber, (Univ. of Manitoba Press, Winnipeg, 1967) p748.

Og71 Ogle, W., Wahlborn, S., Piepenhring, R., and Fredriksson, S., Rev. of Mod. Phys. 43, 424 (1971).

Pe68 Petit-Clerc, Y., and Carette, J.D., Vacuum 18, 7 (1968).

Pe70 Petit-Clerc, Y., and Carette, J.D., Abst. of 38th ACFAS Congress, Quebec, Canada (1970).

Po54 Pohm, A.V., Lewis, W.E., Talboy, J.H., and Jenson, E.N., Phys. Rev. 95, 1523 (1954).

Qu57 Quisenberry, K.S., Giese, C.F., and Benson, J.L., Phys. Rev. 107, 1664 (1957).

Ra67 Rasmussen, N.C., Orphan, V.J., Hukai, Y., and Inauye, I., priv. comm. (1967) to Groshev et al., Nuclear Data A 5, 1 (1969).

Ri64 Ries, R.R., Damerow, R.A., Johnson, W.H., Proc. of the 2nd. Int. Conf. on Nucl. Masses, Vienna, Austria, ed. W.H. Johnson Jr., (Springer-Verlag, Wien, 1964), p357.

Ru66 Rudenauer, F., Viebock, F.P., Z. Naturforschg 21a, 2 (1966).

Se72 Seeger, P.A., Atomic Masses & Fundamental Const. 4, ed. J.H. Sanders and A.H. Wapstra, (Plenum Press, London, 1972) p255.

Sm34 Smythe, W.R., Phys. Rev. 45, 299 (1934).

Sm51 Smith, L.G., Rev. Sci. Instr. 22 115 (1951).

Sm56 Smith, L.G., and Damm, C.C., Rev. Sci. Instr. 27, 638 (1956).

Sm58 Smith, L.G., Phys. Rev. 111, 1606 (1958).

Sm67 Smith, L.G.,
Proc. 3rd Int. Conf. on Atomic Masses,
ed. R.C. Barber, (Univ. of Manitoba Press,
Winnipeg, 1967) p811.

Sm71 Smith, L.G., Phys. Rev. C 4 22 (1971).

Sm72 Smith, L.G.,
Atomic Masses & Fundamental Const. 4,
ed. J.H. Sanders and A.H. Wapstra,
(Plenum Press, London, 1972) p164.

So51 Sommer, H., Thomas, H.A., and Hipple, J.A.,
Phys. Rev. 82, 697 (1951).

St34 Stevens, W.E., Phys. Rev. 45, 513 (1934).

St60 Stevens, C., Terandy, J., Lobell, G., Wolfe, J.,
Beyer, N., Lewis, R.,
Proc. of the Int. Conf. on Nuclidic Masses,
ed. H.E. Duckworth (Univ. of Toronto Press,
Toronto, 1964) p403.

St67 Stevens, C.M., and Moreland, P.E.,
Proc. 3rd Int. Conf. on Atomic Masses,
ed. R.C. Barber, (Univ. of Manitoba Press,
Winnipeg, 1967) p673.

St70 Stevens, C.M., and Moreland, P.E.,
Recent Developments in Mass Spectroscopy,
ed. K. Ogata and T. Hayakawa
(Univ. of Tokyo Press, Tokyo, 1970) p1296.

Ta59 Tasman, H.A., Boerboom, A.J.H., and Wachsmith, H.,
Z. Naturforschg. 14a, 121, 818, 822 (1959).

Ta60 Tasman, H.A., Boerboom, A.J.H.,
Z. Naturforschg. 15, 78 (1960).

Ta70 Taylor, B.N., Parker, W.H., and Langenberg, D.N.,
The Fundamental Constants and Quantum
Electrodynamics
(Academic Press, New York, 1970).

Th07 Thomson, J.J., Phil. Mag. S6 13, 561 (1907).

Th13 Thomson, J.J., Rays of Positive Electricity (Longmans Green & Co., London, 1913).

Va57 Van Patter, D.M., Nuclear Masses and their Determinations ed. H. Hintenberger, (Pergamon Press, London, 1957), p143.

Va69 Van der Werf, S.Y., de Waard, H., and Beekhuis,H., Nucl. Phys. 134, 215 (1969).

Vo62 Von Ardenne, M., Tabellen zur Angewandten Physik, Band 1 (Veb Deutscher Verlag der Wissenschaften, Berlin, 1962).

Wa71 Wapstra, A.H., and Grove, N.B., Nucl. Data Tables 9, 267 (1971).

Wh66 Whineray, S., PhD. Thesis, McMaster Univ. (1966).

Wh70 Whineray, S., Macdougall, J.D., McLatchie, W., and Duckworth, H.E., Nucl. Phys. A151, 377 (1970).

Wi72 Williams, P., and Duckworth, H.E., Sci. Prog., Oxf. 60, 319 (1972).

Wo65 Wollnik, H., Nucl. Instr. and Meth. 34, 213 (1965).

Wo65a Wollnik, H., and Ewald, H., Nucl. Insr. and Meth. 36, 93 (1965).

Five publications previously copyrighted

have not been microfilmed.

NEUTRON SEPARATION AND PAIRING ENERGIES IN THE REGION $82 \leq N \leq 126$*

H. E. Duckworth,† R. C. Barber,† and P. Van Rookhuysen‡
Department of Physics, McMaster University, Hamilton, Ontario, Canada,
and Department of Physics, University of Manitoba, Winnipeg, Manitoba, Canada

and

J. D. Macdougall,§ W. McLatchie,‖ and S. Whineray**
Department of Physics, McMaster University, Hamilton, Ontario, Canada

and

L. Bishop,†† J. O. Meredith, P. Williams, G. Southon, W. Wong,‡‡ B. G. Hogg, and M. E. Kettner
Department of Physics, University of Manitoba, Winnipeg, Manitoba, Canada

(Received 31 July 1969)

Results of a systematic study of atomic-mass differences in the region $82 \leq N \leq 126$ are presented as plots of double-neutron separation energy and neutron-pairing energy. These plots provide information concerning the extent of the nuclear deformation which begins in the region of 90 neutrons, its dependence upon Z, and its gradual disappearance in the region $106 \lesssim N \lesssim 116$.

n 1964[1,2] and 1965[3] some of us reported a se- s of precise atomic-mass differences in the ion $N \sim 90$, which provided accurate informa- n concerning the mass effect associated with onset of nuclear deformation in that region. have since extended this work substantially, ng improved techniques and employing both original high-resolution mass spectrometer[4] a newly constructed one,[5] and can now pro- e a fairly complete picture of the mass sur- e between the 82- and 126-neutron shells. details of this work, including the major nments on its interpretation, will be reported ue course in a series of papers, but the over- picture is sufficiently informative to warrant prior presentation.

s in earlier work, most of the mass differ- es have been obtained by studying doublets he type

$$\Delta M = {}^{A}X_1{}^{35}\mathrm{Cl} - {}^{A-2}X_2{}^{37}\mathrm{Cl}, \quad (1)$$

re X_1 and X_2 may or may not be isotopes of same element. The fractional spacing of the ous doublets studied ranged from one part 400 to one part in 115 800. The error associ- with ΔM was usually in the range 1-4 keV. e the $^{37}\mathrm{Cl}$–$^{35}\mathrm{Cl}$ mass difference is known to keV,[6,7] double-neutron separation energies can be calculated to virtually the same pre- on as ΔM, viz.

$$S_{2n} = 2n - ({}^{A}X_1 - {}^{A-2}X_1)$$

$$= 2n - ({}^{37}\mathrm{Cl} - {}^{35}\mathrm{Cl}) - \Delta M \quad (2)$$

cases in which the doublet contains isotopes e same element. For cases in which iso- s of different elements are involved, the available data are frequently accurate enough to introduce negligible error in the calculation of S_{2n} for the nuclides concerned.

The upper portion of Fig. 1 is a plot of S_{2n} for even-Z, even-N nuclides from $N = 74$ to $N = 126$. The many data relating to odd-Z and/or odd-N nuclides are omitted in order to avoid congestion in the figure. The values for Xe and Ce (taken from the 1965 mass table[8] which in this region is based primarily on the work of Johnson and Nier[9] and Damerow, Ries, and Johnson[10]) are included to show the characteristically "regular" shape of the curves of S_{2n} vs N in the region $50 \leq N \leq 82$,[11] and to remind the reader of the sudden decrease in S_{2n} which occurs as the 82-neutron shell is exceeded. The values for the other elements are based mainly on some 70 mass differences determined in our laboratory during the past four years. Most of these values are derived directly from Eq. (2), but a few require for their calculation the use of accurate reaction Q's or disintegration energies.

As was mentioned, some of the curves shown in the upper portion of Fig. 1 for $N \sim 90$ were published earlier, at which time attention was drawn to the major discontinuity in slope at $N = 88$, the apparent charge dependence of this effect, and the suggestion that the slopes for $N \geq 92$ are similar to those for $N < 88$. Also, the relationship between these effects and the deformation of the nucleus was commented upon. Additional points now to be noted include these:

(a) The injection of the new data has produced a marked increase in the regularity of the S_{2n} curves in the region $92 \leq N \leq 126$. One may now ascribe special significance to the irregularities that remain.

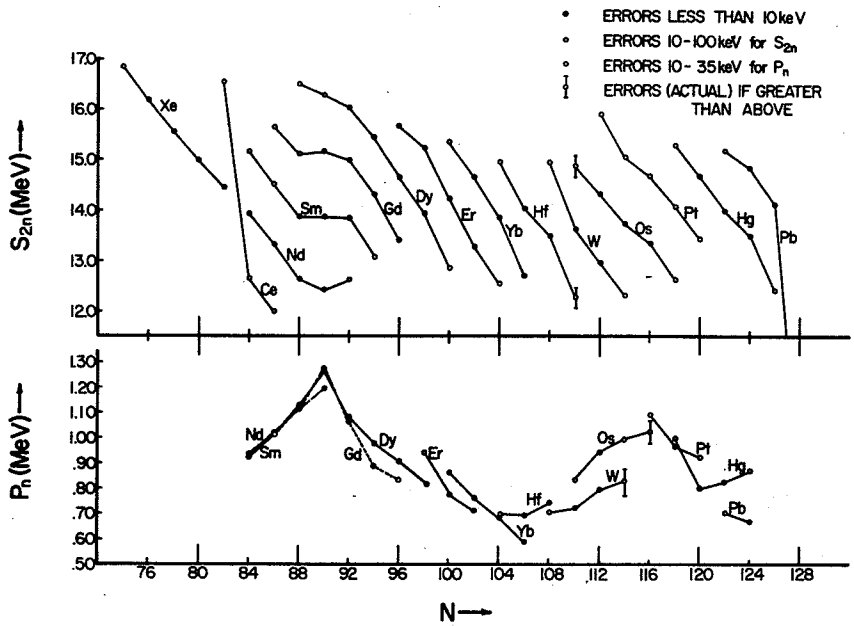

FIG. 1. Plot of double-neutron separation energy (S_{2n}) and of neutron-pairing energy (P_n), both as functions neutron number. Data are for isotopes of the even-Z elements in the region $82 \lesssim N \lesssim 126$.

(b) The energy of deformation exhibited by nuclides with $N = 90$ is least for $Z = 60$ (Nd) and shows a small but steady increase in going to $Z = 62$ (Sm) and $Z = 64$ (Dy). The relatively high value of S_{2n} at ^{154}Dy ($N = 88$, $Z = 66$) may suggest that this nuclide has already acquired a small ground-state deformation. But in going from $N = 90$ to $N = 92$, although there is also a Z dependence, the incremental effect is greatest for $Z = 60$ (Nd).

(c) When viewed over a range of two neutrons the segments of adjacent curves are usually parallel to one another, that is, irregularities are reproduced for the same neutron numbers.

(d) The most conspicuous irregularities lie in the region $106 \leq N \leq 110$.

(e) Below $N \sim 106$ the shape of the curves (which are strikingly different from the "regular" curves referred to earlier) indicates that for certain elements the mass effect associated with deformation continues well beyond 92, but at a more gradual rate.

(f) The curves above $N \sim 110$ do not individually reveal the disapperance of deformation, rather, this disappearance is indicated by the large separations between the curves for $Z = 74$ (W), $Z = 76$ (Os), and $Z = 78$ (Pt).

In the lower portion of Fig. 1 is a plot of neutron-pairing energies for the majority of nuclides represented in the upper portion, calculated according to the relationship[12]

$$P_n(N) = (-1)^{N}\tfrac{1}{4}[2S_N(N) - S_n(N-1) - S_n(N+1)]. \quad (3)$$

These pairing-energy curves are a refineme and an extension of the pioneer work of John and Nier[9] and Johnson and Bhanot[13] who drew tention to maxima in the region of 90 and 11 neutrons. With reference to the lower porti Fig. 1, attention is now drawn to the followi specific features:

(g) At $N = 90$ the neutron-pairing energies a definite maximum for $Z = 62$ (Sm) and $Z = 6$ (Gd), a probable maximum for $Z = 60$ (Nd), a possible maximum for $Z = 66$ (Dy). The gr est effect appears to occur at $Z = 62$ (Sm) an $Z = 64$ (Gd).

(h) A second maximum in the neutron-pai energy appears to occur at $N = 116$, althoug curve for no element actually passes throug maximum. But the curves for $Z = 76$ (Os) a $Z = 78$ (Pt) suggest the existence of this max mum, and those for $Z = 74$ (W) and $Z = 80$ (H are not inconsistent with this hypothesis.

(i) Between these two maxima, the neutro pairing energy appears to decline steadily minimum in the region $106 \leq N \leq 108$. This undoubtedly related to the transition region ferred to in comments (d), (e), and (f) abo

(j) The pairing energies for $Z = 80$ (Hg) a $Z = 82$ (Pb) appear not to follow the same tr as they approach the 126-neutron shell.

We are indebted to a number of individua prepublication information, and appropriat acknowledgement for this will be made in subsequent detailed papers.

*Work supported by the National Research Council of nada, and until 1965 by the Air Force Office of Scitific Research, U. S. Air Force.

†Now at the Department of Physics, University of anitoba, Winnipeg, Man., Canada.

‡Now with TRIUMF project, c/o University of Brith Columbia, Vancouver, B. C., Canada.

§Now with Sprague Electric Company, North Adams, ass.

Now at the Department of Physics, Queen's Univery, Kingston, Ont., Canada.

*Now at the Australian National University, Canber- Australia.

†On leave 1966-1969 from Acadia University, Wolfe, N. S., Canada.

‡On leave 1966-1967 from Brandon College, Bran-, Man., Canada.

R. C. Barber, H. E. Duckworth, B. G. Hogg, J. D. cdougall, W. McLatchie, and P. Van Rookhuyzen, vs. Rev. Letters 12, 597 (1964).

H. E. Duckworth, R. C. Barber, B. G. Hogg, J. D. cdougall, W. McLatchie, and P. Van Rookhuyzen, in grès International de Physique Nucléaire, edited by Gugenberger (Centre National de la Recherche Scifique, Paris, France, 1964), Vol. II, p. 557.

. D. Macdougall, W. McLatchie, S. Whineray, and E. Duckworth, Z. Naturforsch. 21a, 63 (1966).

[4]R. C. Barber, R. L. Bishop, L. A. Cambey, H. E. Duckworth, J. D. Macdougall, W. McLatchie, J. H. Ormrod, and P. Van Rookhuyzen, in Proceedings of the Second International Conference on Nuclidic Masses (Springer Verlag, Berlin, Germany, 1964), p. 393.

[5]R. C. Barber, J. O. Meredith, R. L. Bishop, H. E. Duckworth, M. E. Kettner, and P. Van Rookhuyzen, in Proceedings of the Third International Conference on Atomic Masses (University of Manitoba Press, Winnipeg, Man., Canada, 1968), p. 717.

[6]J. L. Benson and W. H. Johnson, Phys. Rev. 141, 1112 (1966).

[7]J. W. Dewdney and K. T. Bainbridge, Phys. Rev. 138, B540 (1965).

[8]J. H. E. Mattauch, W. Thiele, and A. H. Wapstra, Nucl. Phys. 67, 1 (1965).

[9]W. H. Johnson, Jr., and A. O. C. Nier, Phys. Rev. 105, 1014 (1957).

[10]R. A. Damerow, R. R. Ries, and W. H. Johnson, Jr., Phys. Rev. 132, 1673 (1963).

[11]R. L. Bishop, R. C. Barber, W. McLatchie, J. D. Macdougall, P. Van Rookhuyzen, and H. E. Duckworth, Can. J. Phys. 41, 1532 (1963).

[12]S. G. Nilsson and O. Prior, Kgl. Danske Videnskab. Selskab, Mat.-Fys. Medd. 32, No. 16 (1961).

[13]W. H. Johnson, Jr., and V. B. Bhanot, Phys. Rev. 107, 1669 (1957).

Reprinted from THE REVIEW OF SCIENTIFIC INSTRUMENTS, Vol. 42, No. 1, 1–8, January 1971
Printed in U. S. A.

A High Resolution Mass Spectrometer for Atomic Mass Determinations*

R. C. BARBER, R. L. BISHOP,† H. E. DUCKWORTH, J. O. MEREDITH,
F. C. G. SOUTHON, P. VAN ROOKHUYZEN,‡ AND P. WILLIAMS
Department of Physics, University of Manitoba, Winnipeg, Canada
(Received 10 August 1970; and in final form, 24 September 1970)

A high resolution, second-order double-focusing mass spectrometer has been constructed for the precise determination of atomic mass differences. The instrument has a mean radius of curvature in the electrostatic analyzer of 1 m and has operated with a resolving power at the base of the peaks of ~200 000. Details of current operation are given. The best precision achieved to date is 2.5×10^{-9}, corresponding to ~250 eV at $M=100$ amu; typical precision is $\sim5\times10^{-9}$.

INTRODUCTION

HIGH resolution mass spectrometers which are used for the precise determination of atomic masses are normally deflection instruments consisting of electric and magnetic fields in tandem. For this type of arrangement, ions emerging from an object slit of zero width with half angular divergence α and velocity $v=v_0(1+\beta)$ will fall a perpendicular distance

$$y_B=a_m\{B_1\alpha+B_2\beta+B_{11}\alpha^2+B_{12}\alpha\beta+B_{22}\beta^2\} \qquad (1)$$

from the optic axis after traversing the two fields. The coefficients depend upon the distance l''_m traveled from the magnetic field boundary.

The well known theory of Herzog[1] allows field arrangements to be chosen for which $B_1=B_2=0$ (for a particular l''_m), thus providing first order double focusing. Subsequently several instruments which additionally provide $B_{11}=0$ were designed and built.[2–6] Finally, in 1959, Hintenberger and König[7] reported an extensive study of the second order focusing properties of such fields and proposed a number of arrangements which provide complete second-order double focusing ($B_{11}=B_{12}=B_{22}=0$).

In 1963, when planning of the present instrument was begun, no high resolution mass spectrometer possessed complete second-order double focusing. Since then, Matsuda *et al.*[8–10] have described a novel high resolution mass spectrometer which theoretically achieves this objective. In practice, however, the measured second-order coefficients differ significantly from zero.[11]

Although a brief preliminary description of the design and construction of the new Manitoba mass spectrometer has been given elsewhere[12] we here present further details together with information concerning its performance.

I. THE MASS SPECTROMETER

A. Geometry

Of the many instruments proposed by Hintenberger and König,[7] the geometry chosen for our purpose has deflection in the same sense in both electric and magnetic fields plus straight magnetic field boundaries. The advantages in choosing this arrangement, shown in Fig. 1, are the following.

(1) An intermediate direction focus is formed (at l''_e) by the electrostatic analyzer. This permits the use of the electrostatic analyzer as an energy analyzer capable of resolving ~ 1 eV.

(2) The total ion path is reasonably short compared to the mean radius of curvature in the electrostatic analyzer, a_e. The individual lengths l'_e, l''_e, l'_m, and l''_m are also relatively short so that problems due to mechanical vibration and stray magnetic fields are minimized.

(3) It is not necessary for the ion beam to cross a curved magnetic field boundary at a prescribed angle.

The scale of the mass spectrometer was determined by choosing $a_e=1$ m. The total length of the ion path is 4.59 m and the over-all magnification is 0.50. The values of the other geometric parameters are given in Fig. 1.

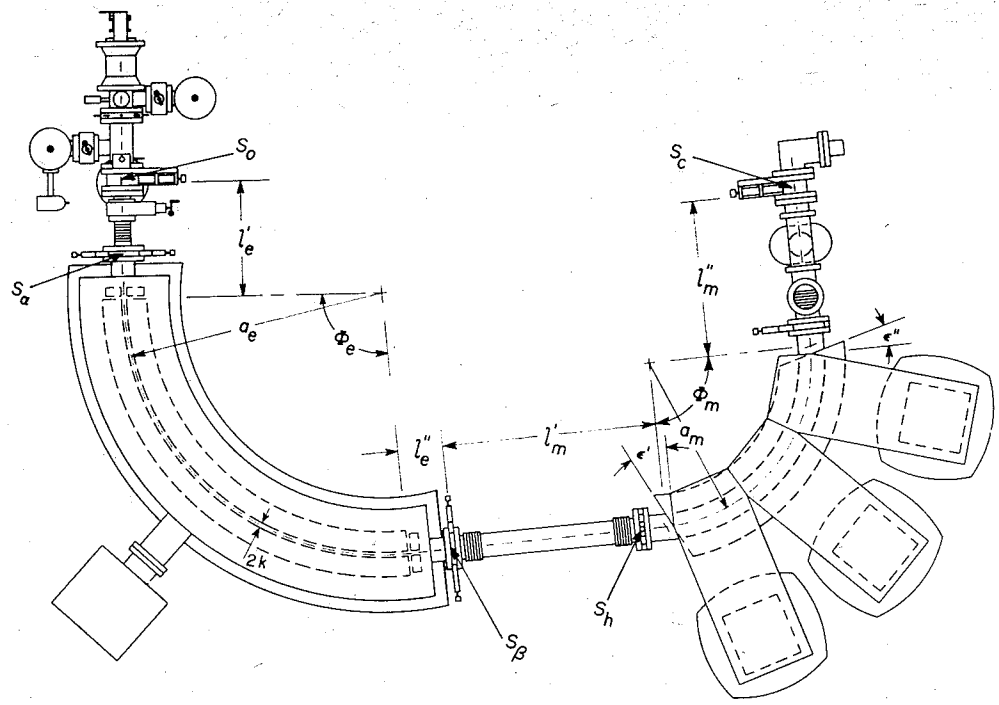

FIG. 1. Geometry of the mass spectrometer: $a_e=100.00$ cm; $\Phi_e=94.65°$; $a_m=62.74$ cm; $\Phi_m=90°$; $l'_e=44.45$ cm; $l''_e=17.63$ cm; $l'_m=82.49$ cm; $l''_m=59.46$ cm; $\epsilon'=27°$; $\epsilon''=15°$; $2k=2.000$ cm.

The object slit S_0 is variable in width and orientation, as is the collector slit S_c. For a resolving power of 200 000 at the base of the peaks and with the image width equal to the width of S_c, S_0 is 2.7 μ width. The maximum value of α is $\pm 10^{-2}$ rad, although S_α is usually set to limit α to $\pm 2\times 10^{-3}$ rad. S_β is typically set to correspond to $\beta=\pm 8\times 10^{-4}$. The height of the beam is limited normally to $\sim$ 2 mm to ensure that all ions reaching the detector have experienced the same magnetic field.

B. The Source

The ion source, shown in Fig. 2, is a variation of the Finkelstein[13] source. The oven is made of tantalum, coated with boron nitride insulation, and wrapped with a rhenium heating filament. The electromagnet is excited by the coil E so that there is, in the central region of the oven, a magnetic field of $\sim$1 kG directed parallel to the axis of the source. The ion accelerating potential V_a ($\sim$20 kV) is applied to the oven. The filament is 50–500 V, and the brass and iron parts of the source housing are 100–500 V, negative with respect to the oven. Thus, electrons are emitted from the filament and are constrained to follow a path along the axis of the source, passing through the hole in the back of the oven and then oscillating back and forth. Within the oven a plasma is formed from which ions are extracted through the front hole.

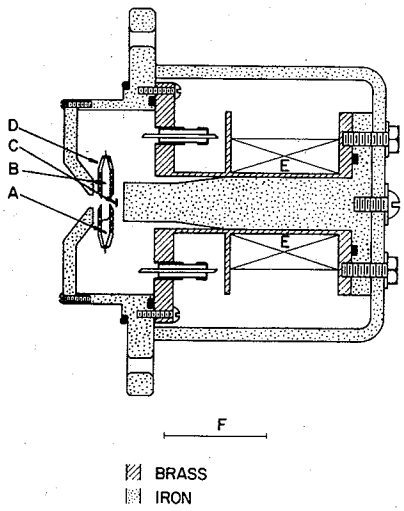

FIG. 2. Ion source. A—Sample; B—oven; C—Re filament (coated with LaB_6); D—ribbon heater and BN insulation; E—Cu windings for electromagnet; F—5 cm.

For total electron emission currents of 5 to 100 mA, ion currents from 0.5 to 25 μA have been obtained with an energy spread of less than 2 eV. In the work done to date the samples have been solids ($CdCl_2$ or rare earth chlorides) which are vaporized in the oven.

The source arm is shown in the upper right corner of Fig. 3, which gives a view of the entire instrument. The ion beam is centered and focused on the principal slit by means of an electrostatic quadrupole lens. The position of the slit S_0 relative to the electrostatic analyzer can be adjusted by a rotary table mounted on the I-beam support which, in turn, is bolted to the electrostatic analyzer base.

C. Electrostatic Analyzer

The electrostatic analyzer is a cylindrical condenser of mean radius $a_e=1$ m and sector angle $\phi_e=94.65°$, as indicated in Fig. 1. The analyzer gap is 2 cm and the field is terminated at the physical boundaries by blocks positioned according to Herzog's theory.[14]

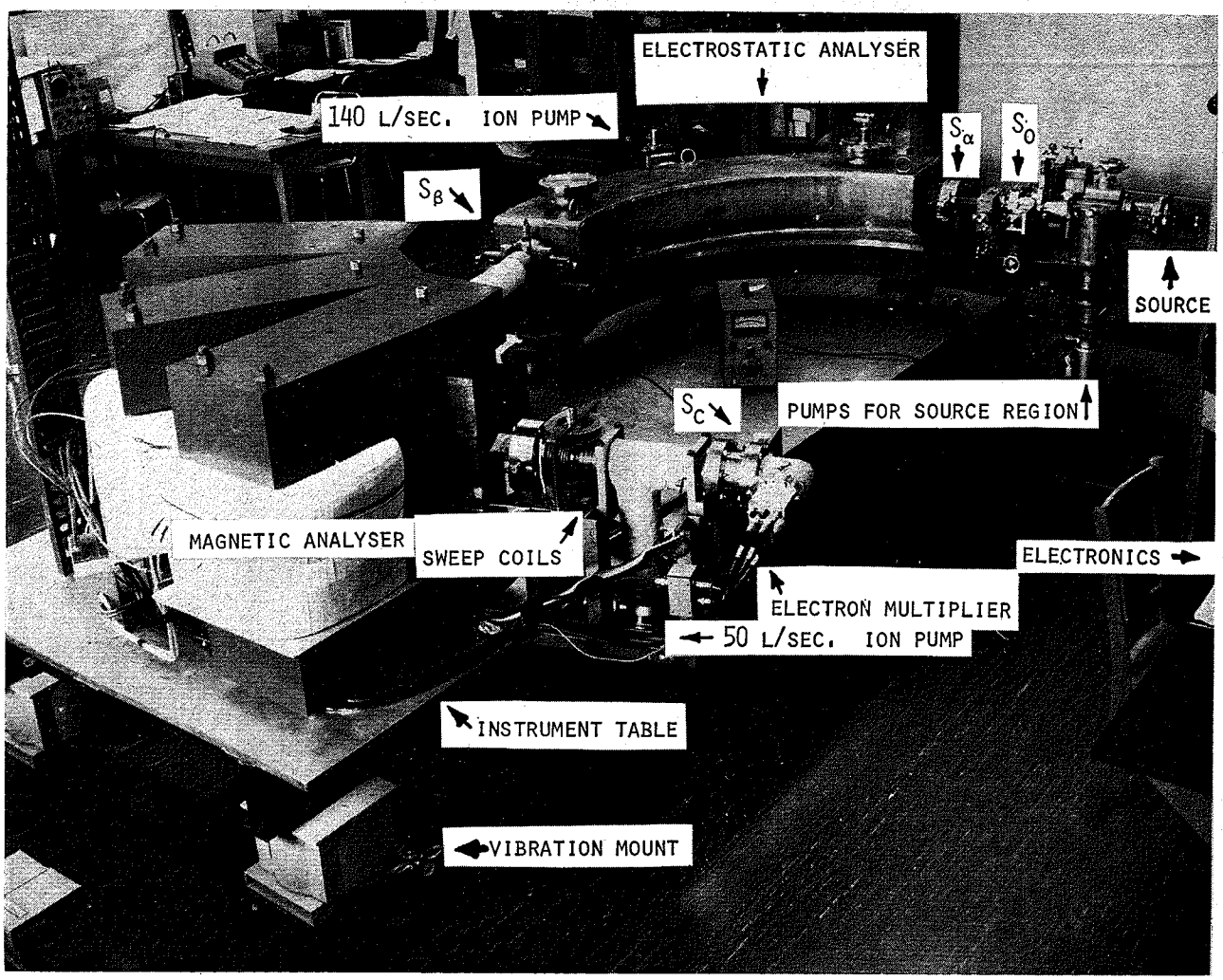

FIG. 3. The mass spectrometer.

Further details of the construction of the analyzer are hown in Fig. 4 which is a cross sectional view through one f the five positioning assemblies. The analyzer plates, hich are made of gold plated Armco iron, are supported y fused silica blocks which, in turn, rest on the analyzer ase. The size of the gap is determined at each assembly y a pair of cylindrical fused silica spacers. The position f the plates relative to the reference surface may be djusted by means of the locating screws on each of the ter mounts. The inner mounts have an Inconel-X spring rangement which presses the entire assembly together d against the outer positioning mounts. In this arrange- ent, the total variation in the mean radius of the analyzer ~0.003 cm (with respect to the reference surface). The tal variation in the gap is ~0.001 cm over the entire ea of the plates and much less in the more limited region rough which the ion beam actually travels. This results marily from differences in spacers (ground to 2.0000 0.0003 cm) and variations arising in the grinding and ctroplating of the plates.

The cover and base of the electrostatic analyzer are made of 304 stainless steel. The vacuum seal between cover and base is made with a 1 mm diam gold wire gasket. The pressure measured by the 140 liter/sec ion pump is $\sim 5\times 10^{-8}$ Torr when the valve between the source and the electrostatic analyzer is open.

The electrostatic analyzer and source arm are supported on three ball bearings located approximately at the entrance and exit boundaries of the electrostatic field, and at the intersection of the tangents to the ion paths at these points. A pivot is located directly below the direction focus of the electrostatic analyzer. Thus, the first half of the instrument, consisting of electrostatic analyzer plus source arm, may be rotated as a unit about this pivot during focusing.

D. Magnetic Analyzer

Each of the pole pieces of the magnet (shown at left in Fig. 3) is a single block of Armco iron. The gap between them is established by 2.540 cm Inconel spacers. Below

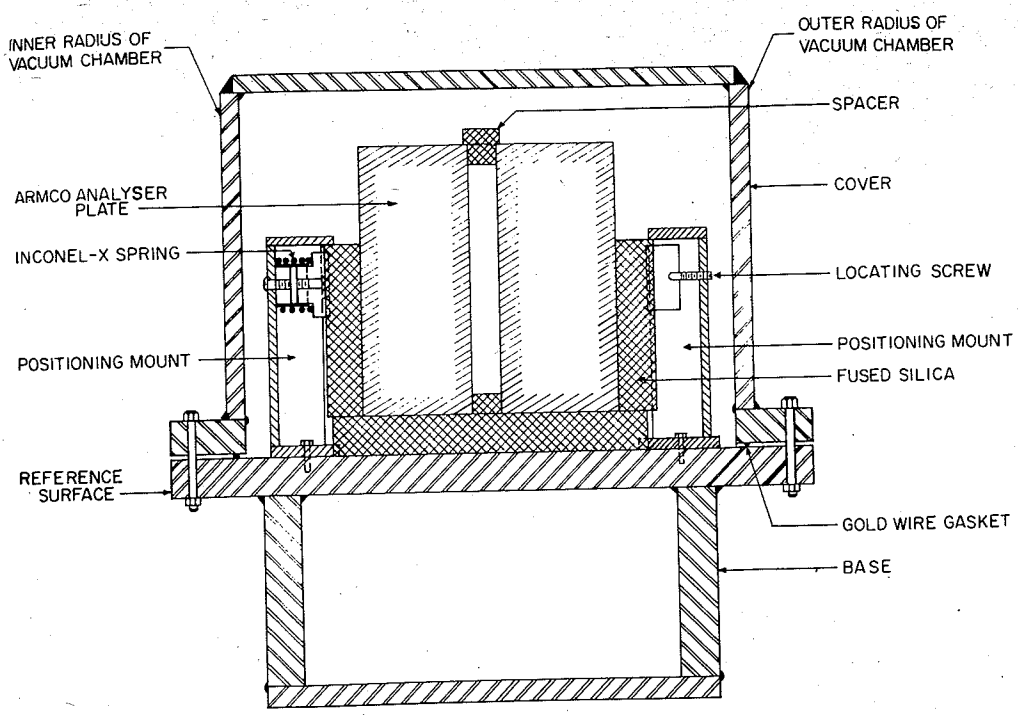

FIG. 4. Cross section of the electrostatic analyzer through one pair of the positioning mounts.

and above the pole pieces a small shimming gap has been introduced to improve the homogeneity of the field. Some adjustment of the field uniformity can be made by changing the width of the upper shimming gap. The yoke is made in three sectors with two water-cooled exciting coils on each sector. The six coils are connected in parallel electrically and in three parallel branches of two coils each for cooling.

The field can be varied over the range 3–8 kG with a typical uniformity of 1/5000 throughout the entire volume to within one gap width from the boundary of the field. Below 3 kG the inhomogeneity remains at ~0.5 G. The stability of the magnetic current supply is 1 ppm or better over a period of several minutes.

The entire instrument is mounted on a rigid table made of 150×366×2.5 cm steel plate with a grid of 20 cm I-beams welded to its lower side. This table is supported by eight pneumatic mounts which isolate the instrument from building vibrations. Each mount contains a pressure regulator and a rubber bellows which will support two tons when inflated to a pressure of 7 $kg \cdot cm^{-2}$. A cylinder of nitrogen will operate the system for over a month. In the event of a pressure failure the spectrometer table simply settles onto steel supports. The table and five of the vibration mounts are visible in Fig. 3.

As mounted, the spectrometer has a highly damped natural frequency of ~1 cps. For frequencies of about 30 cps and greater (typical of building vibrations), the isolation efficiency is better than 0.99.

E. Collector Arm

The collector arm shown in the middle of Fig. 3 is supported by a stainless steel frame attached to the spectrometer table. A second ion pump (50 liters/sec) is suspended from the collector arm and typically produces a pressure of $\sim 3 \times 10^{-8}$ Torr during operation of the instrument.

A pair of Helmholtz coils located between the magnet and the collector slit (Fig. 3) is driven by a sawtooth current with a repetition rate of ~19 cps. The resultant magnetic field sweeps the ion beam across the collector slit. All ions passing through the slit are detected by a high gain, low noise magnetic electron multiplier (Bendix M310). The resultant signal is amplified and viewed on the oscilloscope from which the sawtooth is derived. Figure 5 is a photograph of a trace in which five peaks are shown. The base resolving power in this case is ~110 000.

Because of the location of the 50 liter/sec ion pump, it contributes a noise current of $\sim 10^{-18}$ A in the electron multiplier which can be objectionable when peaks of very low intensity are studied. In this case the pump may be switched off and the noise thereby reduced to less than 10^{-19} A.

F. Focusing Procedure

Prior to the start of construction the focusing properties of this instrument were investigated in some detail

In particular the effect on the focusing of a nonuniform magnetic field was studied.

For ions traveling in the median plane of the magnetic field, it was found that, while the individual widths of the velocity focus ($a_m B_{22}\beta^2$) and direction focus ($a_m B_{11}\alpha^2$) would not be altered by small radial or azimuthal variations in the field, their positions would be shifted differentially so that a double focus would not be formed. In this case, of course, B_{12} would no longer be zero. A suitable small correction could be made so that the two foci would again coincide, although not necessarily at the theoretical position for the double focus, and B_{12} would be virtually zero.

Thus the calculations suggested that it would be sufficient to adjust the instrument to obtain a first order double focus. Because the second order aberrations are relatively insensitive to geometry we should then obtain a second order focus as well.

The calculations have recently been extended[16] to study the effect produced by the actual magnetic fringing field on the double focus. This work indicates that, in general, the effect is similar to the case of the nonuniform field described above, although there may also be a small deterioration in the second-order focusing properties.

The general procedure and tests for focusing are similar to those used in focusing the 2.74 m radius mass spectrometer formerly at McMaster University.[17] To check the velocity focus, the ion energy is changed by ~22 V on every second sweep of the display oscilloscope. Lack of velocity focusing results in one peak being displaced with respect to itself. The direction focus is characterized by a marked improvement in the resolution of the peaks. Additionally, the quadrupole lens may be used to vary α and thus permit a test of the direction focus.

In the initial focusing, the principal slit was positioned at its theoretical location relative to the electrostatic analyzer and the distances ($l''_e+l'_m$) and l''_m (see Fig. 1) were set at their nominal values. The electrostatic analyzer plus source arm was then adjusted relative to the magnet to correct for the fringing field.

In the subsequent routine focusing, the first half of the instrument consisting of electrostatic analyzer plus source arm is swung about the intermediate direction focus. The field necessary to bring the ions to the same point on the oscilloscope screen is a maximum for some particular angle. If the direction focus occurs at this same angle, then the direction focus of the electrostatic analyzer is being formed at the pivot axis. Invariably both the direction and velocity foci occur near this angle and a minor adjustment in l'_m (to move the direction focus) or a lateral movement of the collector (to move the velocity focus) is sufficient to achieve a double focus.

Near the double focused arrangement, a further test of the coincidence of the two foci may be made. As noted earlier, when the two foci are separated, B_{12} is of appreciable size. During the velocity focusing test described above, the angle α may be varied by means of the quadrupole lens. If, under these circumstances, the velocity focused condition is α dependent, B_{12} is large and the velocity and direction foci are not coincident.

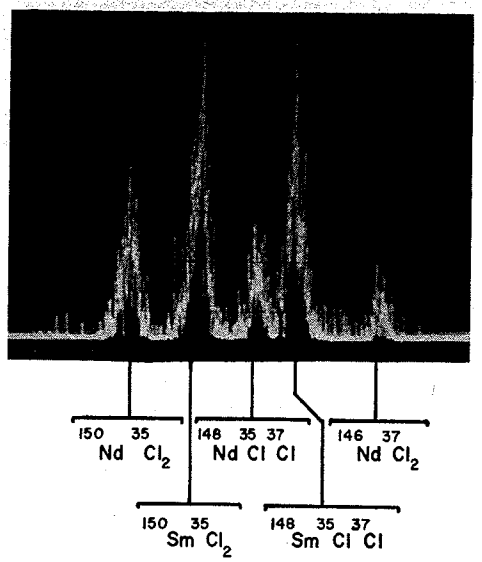

FIG. 5. Oscilloscope display of the electron multiplier output. From the left the peaks are $^{150}Nd^{35}Cl_2$, $^{150}Sm^{35}Cl_2$, $^{148}Nd^{35}Cl^{37}Cl$, $^{148}Sm^{35}Cl^{37}Cl$, and $^{146}Nd^{37}Cl_2$. The base resolving power in this case is ~ 110 000.

On the basis of the current performance of the instrument we have estimated the following upper limits for the second order focusing coefficients: $B_{11}<0.1$, $B_{12}<0.2$, and $B_{22}<0.5$. Further, it would appear that slit quality and uniformity of the deflecting fields are the limiting factors in achieving more definitive values of these coefficients.

G. Peak Matching and the Control Circuitry

The method of obtaining a mass difference is a variation of the well established peak matching technique, which in turn depends on Bleakney's theorem.[18] Let us suppose that an ion of mass M traverses a given path through the instrument in which certain fixed potentials are applied to various electrodes (V_i would be applied to the ith electrode.) Then an ion of mass M' will follow exactly the same path through the instrument if all the magnetic fields are maintained constant and all the potentials are changed according to the relation

$$MV_i=M'V'_i. \tag{2}$$

Provision is therefore made for changing the electrostatic analyzer voltage from V to $V+\Delta V$, on alternate sweeps. The magnitude of ΔV is adjusted in order to bring M' to the same stage of the oscilloscope sweep as M. ΔV is then determined. The mass difference, $\Delta M=M'-M$, is calculated from $\Delta V/V$ and M.

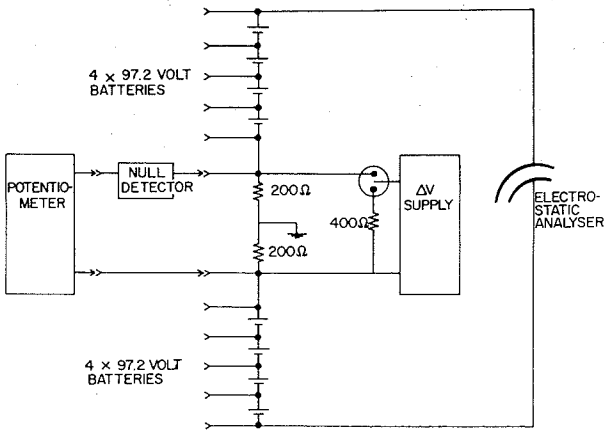

FIG. 6. Potential supply for electrostatic analyzer.

As the instrument is double focusing, the peak position is insensitive to the accelerating potential. However, strictly to satisfy Bleakney's theorem and thus to ensure that the two ion groups traverse the identical path, V_a is changed by ΔV_a in the same fashion as V. The same is true, in a strict sense, for the voltages provided to the quadrupole lens. However, for the narrow doublets studied to date, the appropriate changes in the lens voltages produce a negligible effect on the doublet separation. When the two members of a doublet are chemically identical, they are formed in the source with the same energy distribution. Thus the change ΔV_a in the voltage V_a may be calculated precisely from ΔM, M, and V_a.

When the two members of a doublet are chemically dissimilar, ΔV_a may be set and checked in the following manner. With the instrument set up for the visual peak matching of a given doublet, the ion accelerating potential is varied slowly so that the ion beam is cut off by one of the edges of the slit S_β which is located at the direction focus of the electrostatic analyzer. ΔV_a is adjusted so that the two members of the doublet disappear simultaneously. In this test, a deviation of $\sim$1 eV in energy from the value required by Bleakney's theorem may be readily detected.

The potential supply for the electrostatic analyzer is shown in Fig. 6. V is provided by eight 97.2 V mercury reference batteries (Eveready E 302 462) while ΔV is presented to the chopper and the resulting square wave is applied across the two 200 Ω resistors. A precision potentiometer, described by Bishop and Barber,[19] is then used to determine both V and ΔV relative to the same standard.

The power supply for this traveling potentiometer has as its reference an additional 97.2 V mercury battery which is identical to the others and is located in the same temperature controlled box. Thus, although the absolute values of the potentials of the mercury batteries may change, the measured values are very stable, and the precision to which $\Delta V/V$ can be determined depends on the calibration of the divider chain in the potentiometer.

Although this technique is basically similar to one used previously in our laboratory[17] and more recently by Matsuda *et al.*,[20] the precision attained with this new potentiometer is significantly better. This method also differs from that of Nier[21] and McLatchie[22] and that of Bainbridge and Moreland.[23] For both latter arrangements, V and ΔV are supplied by a battery driven resistor chain. In Nier's circuit, the resistor chain is a π network and $\Delta V/V$ is determined from a calibration of the resistances. The circuit of Bainbridge and Moreland consists of a series chain of 22 resistors and two voltage dividers. The measurement of $\Delta V/V$ can be carried out either by the calibration of the resistances or by measuring voltages by a traveling potentiometer.

The present arrangement offers certain advantages over these other networks. Since there is no current drain from the batteries, relatively low capacity batteries may be used and the problem of drift in the value of V is absent. Secondly, the impedance between the analyzer plates and ground is low so that problems of pickup and of ion currents arriving at the analyzer plates are much reduced.

The mechanical chopper which switches ΔV on and off also includes a switch used to supply a master trigger pulse at a repetition rate of $\sim$19 cps (Figs. 6 and 7). This pulse is used as the external trigger for the display oscilloscope and the Fabri-Tek 1024 channel signal averager (FT1052).

The output of the electron multiplier is amplified and applied to the display oscilloscope and to the signal averager. The sawtooth voltage from the oscilloscope is amplified in order to drive the Helmholtz coils which modulate the beam position. The differentiated sawtooth triggers a flipflop which (a) switches the electron multiplier information through gain A or gain B, (b) switches the neon light on or off subsequently to switch V_a, and (c) switches the voltages applied to the quadrupole lenses.

The signal averager effectively divides the trace into 1024 intervals, integrates the voltage over each time interval, and stores a number from -64 to $+64$ proportional to the integrated voltage in the corresponding memory location. Successive traces are added in order to improve the signal-to-noise ratio. The memory contents are continuously displayed on a second oscilloscope.

The application of the signal averager to peak matching follows closely the work of Benson and Johnson[24] and that of Macdougall.[25] A circuit, incorporated in the averager, switches between add and subtract modes on successive sweeps. A peak for mass M is added to the memory on odd numbered sweeps while a peak for mass M' is subtracted on even numbered sweeps. Thus, when the peak heights are made equal by gains A and B, and the peaks appear at the same stage of the oscilloscope trace a null signal results. A slight mismatch results in an S-shaped error

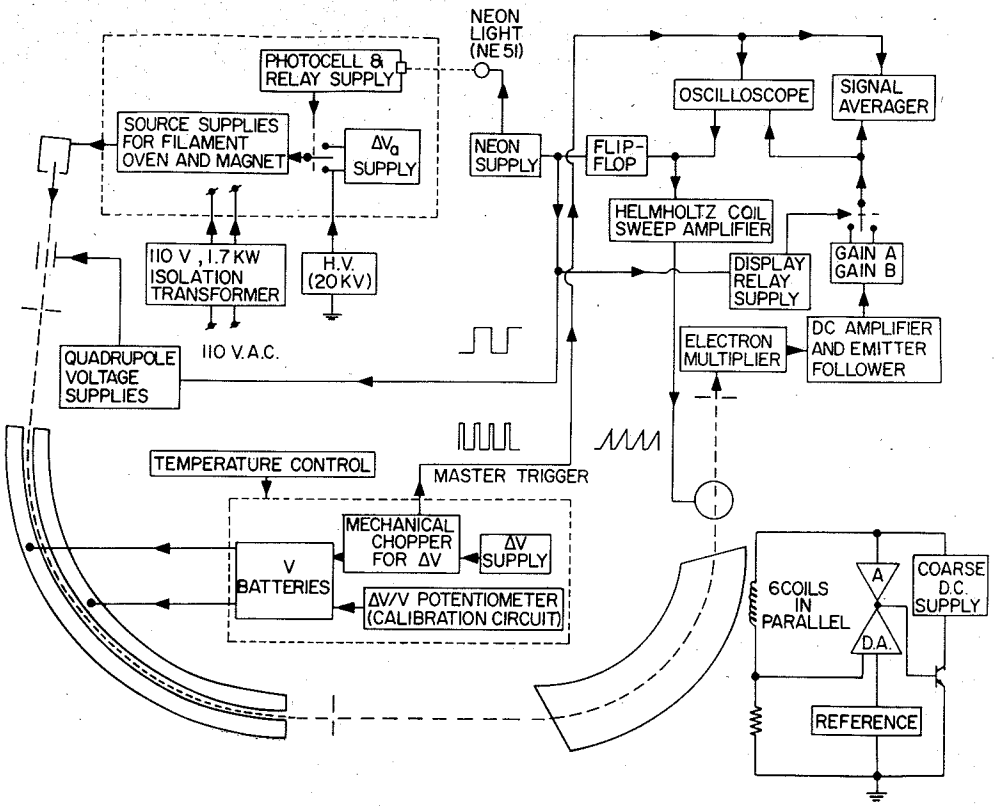

FIG. 7. Block diagram for the control circuitry.

gnal whose phase indicates the appropriate adjustment be made in ΔV to obtain a null.

The mass difference of a doublet may be determined as scribed above in eight different ways which are permutaons of the following variables: the direction of sweeping e ion beam across the collector slit, the routing of the ference peak (M) through gain A or gain B, and the oice of reference peak (i.e., the choice whether ΔV is ded to or subtracted from V). In order greatly to reduce likelihood of systematic error in the final result, the weighted average is taken of these eight values. Before h run, the instrument is refocused in at least a minor y. Approximately 20 such runs are taken by at least ee different operators and from these values the mean the standard deviation of the mean are calculated. t should be noted that, when the instrument is operated lescribed, it is adequate to test for velocity focusing by ual observation of the live display. This means that the tine velocity focusing is actually a first order focusing. wever, the signal averager permits a very sensitive hod of performing the test, viz. by setting $\Delta V=0$, $=22$ V, and matching a peak to itself. Such a test omes important when a small number of runs is to be to determine a mass difference.

II. PRECISION

its present form, this instrument has been used to in values for a number of close doublets ($\Delta M/M$ $\sim 1/50\,000$) in the spectra of various rare earth chlorides. These values will be presented elsewhere.[26] The precision of this work is shown in Fig. 8 which gives a histogram of the values of $\delta M/M$ obtained for the first 12 doublets studied with the instrument as described. Here δM is the error assigned to a mass difference, and M is the mass at which it occurs. The number of runs corresponding to each value is indicated in the square representing that value. It is seen that a typical precision for these results is $\sim 5/10^9$. The best was $2.5/10^9$ and was obtained for the relatively intense doublet

$$^{169}Tb^{35}Cl_2 - {}^{165}Ho^{37}Cl_2$$

on the basis of only 18 runs.

In general the precision appears to be closely related to the intensity of peaks being matched. For the seven

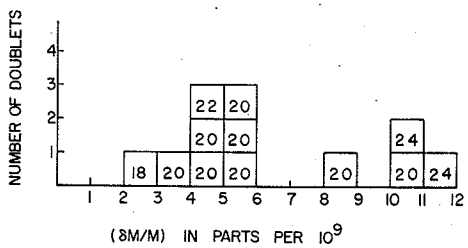

FIG. 8. Precision achieved with the mass spectrometer. This is a histogram of values of $\delta M/M$ for 12 doublets studied (δM is the error for a given determination and M is the mass at which it occurs). The number of runs for each doublet is indicated in the square representing the doublet.

doublets where the precision was worse than $5/10^9$, the intensity of the peaks was below the average intensity for rare earth chlorides. In all cases, the precision was not limited by the potentiometer used to determine $\Delta V/V$.

The highest resolving power obtained to date has been $\sim$200 000 measured at the base of the peaks, and involved the intense peaks in the $CdCl_2$ spectrum. The low intensity available for most of these rare earth doublets has made it expedient to operate at resolving powers in the range 100 000–150 000.

ACKNOWLEDGMENTS

The advice of J. A. Barber regarding some of the structural problems in the design of this instrument is gratefully acknowledged. During the design and initial construction stages, T. H. Bryden and H. Howell of McMaster University made valuable contributions of advice and skill that are greatly appreciated. We are also grateful to R. H. Batten for technical assistance in the later work at the University of Manitoba and to M. E. Kettner and B. G. Hogg for their support in the early stages of construction.

* This work has been supported by the National Research Council of Canada.

† Holder of a National Research Council of Canada Studentship, 1966–67 and on leave 1966–69 from Acadia University, Wolfville, Nova Scotia, Canada.

‡ Now with TRIUMF Project; c/o University of British Columbia, Vancouver, Canada.

[1] R. Herzog, Z. Physik **89**, 447 (1934).
[2] A. O. Nier and T. R. Roberts, Phys. Rev. **81**, 507 (1951).
[3] E. G. Johnson and A. O. Nier, Phys. Rev. **91**, 10 (1953).
[4] F. Everling, H. Hintenberger, L. A. König, J. Mattauch, W. Müller-Warmuth, and H. Wende, *Nuclear Masses and Their Determination* (Pergamon, London, 1957), p. 221.
[5] T. L. Collins and K. T. Bainbridge, *Nuclear Masses and Their Determination* (Pergamon, London, 1957), p. 213.
[6] C. M. Stevens, J. Terandy, G. Lobell, J. Wolfe, N. Beyer, and R. Lewis, Proc. Int. Conf. Nuclidic Masses, Hamilton, Ont., 1960 401 (1960).
[7] H. Hintenberger and L. A. König, Advan. Mass Spectrometry, Proc. Conf. Univ. London, 1958, **1**, 16 (1959).
[8] H. Matsuda, Mass Spectrosc. (Japan) **11**, 127 (1964).
[9] H. Matsuda, S. Fukumoto, Y. Kuroda, and M. Nojiri, Z. Naturforsch. **21a**, 25 (1966).
[10] H. Matsuda, S. Fukumoto, T. Matsuo, and M. Nojiri, Z. Naturforsch. **21a**, 1304 (1966).
[11] H. Matsuda, S. Fukumoto, and T. Matsuo, Int. Conf. Mass Spectrom., Kyoto, Japan (1969).
[12] R. C. Barber, J. O. Meredith, R. L. Bishop, H. E. Duckworth, M. E. Kettner, and P. Van Rookhuyzen, *Proceedings of the Third International Conference on Atomic Masses* (Manitoba U. P., Winnipeg 1968), p. 717.
[13] A. T. Finkelstein, as referred to by M. von Ardenne, *Tabellen zur Angewandten Physik*, (VEB Deutscher Verlag der Wissenschaften Berlin, 1962), Vol. 1, p. 646.
[14] R. Herzog, Z. Naturforsch. **10a**, 887 (1955).
[15] R. C. Barber, Can. J. Phys. **43**, 716 (1965).
[16] D. A. Burrell and R. C. Barber (to be published).
[17] R. C. Barber, R. L. Bishop, L. A. Cambey, H. E. Duckworth, J. D. Macdougall, W. McLatchie, J. H. Ormrod, and P. Van Rookhuyzen, Proc. Int. Conf. Nuclidic Masses, 2nd Vienna, 1963, 39 (1964).
[18] W. Bleakney, Amer. Phys. Teacher **4**, 12 (1936).
[19] R. L. Bishop and R. C. Barber, Rev. Sci. Instrum. **41**, 327 (1970
[20] H. Matsuda, S. Fukumoto and T. Matsuo, *Proceedings of the Third International Conference on Atomic Masses* (Manitoba U. P. Winnipeg 1968), p. 733.
[21] A. O. Nier, *Nuclear Masses and Their Determination* (Pergamon London, 1957), p. 185.
[22] W. McLatchie, Ph.D. thesis, McMaster University, 19 (unpublished).
[23] K. T. Bainbridge and P. E. Moreland, Jr., Proc. Int. Conf. Nuclidic Masses, 3rd Winnipeg, 1967, 460 (1968).
[24] J. L. Benson and W. H. Johnson, Phys. Rev. **141**, 1112 (196
[25] J. D. Macdougall, Ph.D. thesis, McMaster University, 19 (unpublished).
[26] R. C. Barber, R. L. Bishop, H. E. Duckworth, J. O. Meredith, F. C. G. Southon, P. Van Rookhuyzen, and P. Williams (to be published).

International Journal of Mass Spectrometry and Ion Physics
Elsevier Publishing Company, Amsterdam. Printed in the Netherlands

PRECISE ATOMIC MASS DIFFERENCES USING PEAK-MATCHING BY COMPUTER*

J. O. MEREDITH, F. C. G. SOUTHON, R. C. BARBER, P. WILLIAMS AND H. E. DUCKWORTH**
Department of Physics, University of Manitoba, Winnipeg (Canada)

(Received 1 June 1972)

ABSTRACT

A high resolution mass spectrometer has been used to obtain precise atomic mass differences by means of an improved peak-matching technique in which off-line computer analysis is used to determine the matching condition. The procedure retains the improved signal-to-noise ratio achieved with a signal averager, but offers improved precision in a given operating time and removes further human judgment of the matched condition. Moreover, it makes possible a comparison between the precision obtained experimentally and the theoretical limit (derived here) determined by the instrument resolution and the number of ions detected. Representative results for doublet spacings are presented for which the precision ($\delta M/M \sim 5 \times 10^{-9}$) approaches the statistical limit.

INTRODUCTION

A second-order double-focusing mass spectrometer has been constructed at the University of Manitoba for the precise determination of atomic mass differences. Detailed descriptions of the construction and performance of the instrument have been presented elsewhere[1, 2]. The instrument has been in use for some time and values for 31 doublets in the spectra of rare earth chlorides have been reported recently[3].

The determination of an atomic mass difference to high precision is generally carried out by some variation of the "peak-matching" technique. In our case a peak is generated by the modulation of the ion beam across the collector slit by a small sawtooth magnetic field derived from Helmholtz coils located between the magnet and the slit. The ion current is detected by an electron multiplier and the

*This research was supported by the National Research Council of Canada.
**Present address: University of Winnipeg, Winnipeg, Manitoba, Canada.

amplified output is displayed on the oscilloscope from which the modulating field is originally derived.

The peak-matching method depends on a theorem due to Bleakney[4]. Suppose that an ion of mass M traverses a given path through the instrument with certain fixed potentials applied to various electrodes (V_i would be applied to the i^{th} electrode). Then an ion of mass M' will follow exactly the same path if all magnetic fields are held constant and all the V_i are changed to V_i' according to the relation

$$MV_i = M'V_i'. \qquad (1$$

Thus, by applying a ΔV to the electrostatic analyser voltage V, such that M' falls at the same point on the trace as M, ΔM may be calculated from

$$\frac{\Delta M}{M'} = \frac{\Delta V}{V}. \qquad (2$$

The precision on the value of ΔM depends on the determination of the matched condition and on the subsequent measurement of the $\Delta V/V$ ratio. Apparatus for the latter measurement was described by Barber and Bishop[5]. The limitations on determining the matched condition will be discussed below.

Originally, the peak positions were compared visually via an oscilloscope display (*e.g.* ref. 6). Subsequently a signal averager with a 1024 channel digital memory was used on-line to detect the lack of coincidence of the peaks[2, 7] (herein referred to as the "visual-null method"). Traces corresponding to the reference peak are added to the memory while those for the displaced peak are subtracted from it. If the peaks are matched in position (and amplitude), a null signal results; if they are slightly displaced, an "S"-shaped error signal is obtained.

The use of a signal averager significantly increases the signal-to-noise ratio and thereby improves the precision with which a match may be determined. A variation of this method is the "spectrum-stripping" technique of Stevens and Moreland[9] where the reference peak and the displaced peak are stored in separate halves of a digital memory and the difference (with a factor to adjust the amplitude) is taken by an arithmetic operation in the analyser. The amplitude of the resulting error signal is normalized by the reference peak and is taken as a measure of the degree of mismatch. Several runs are made with ΔV on either side of the expected value, and a straight line fit is used to calculate the correct setting for a match. An alternate procedure was to calculate the centroids of the peaks and to use, in the straight line fitting, the variation in peak position with ΔV. A similar method is used by Matsuda *et al.*[10].

DETERMINATION OF THE MATCHED CONDITION

Since the location of one peak relative to another must be calculated, the error in the separation is the root of sum of squares combination of the errors

locating each peak position. Several authors[11,12] consider that the centroid or weighted mean is the best unbiased estimate of the centre of a mass peak. Consider a peak occupying channels x_i, $i = 1, 2, 3, \ldots, I$, of some recording device and let the peak height in the i_{th} channel be n_i, equal to the number of ions (counts) accumulated in that channel. Since the number of counts n_i obeys Poisson statistics, the standard deviation of n_i is $\sqrt{n_i}$. Moreover each of the n_i is independent. The average position, or centroid of the distribution is given by

$$\bar{x} = \frac{\sum n_i x_i}{\sum n_i} \tag{3}$$

where the summation convention $\sum = \sum_{n=i}^{I}$ is used. The variance of $\bar{x}$, denoted by σ^2 is given by the generalized rule for propagation of errors[13]. Using the fact that the variance for the height in each channel is n_i, and that n_i is independent of n_j, σ^2 is seen to be

$$\sigma^2 = \frac{1}{(\sum n_i)^2}\left(\sum n_i x_i^2 + \frac{(\sum n_i x_i)^2}{(\sum n_i)^2}\sum n_i - \frac{2\sum n_i x_i}{\sum n_i}\sum x_i n_i\right). \tag{4}$$

Now let N be the total number of ions in the peak from $i = 1$ to $i = I$.

$$\sum n_i = N \tag{5}$$

then

$$\sigma^2 = \frac{1}{N^2}\left(\sum n_i x_i^2 + \frac{1}{N}(\sum n_i x_i)^2 - \frac{2}{N}\sum n_i x_i \sum n_i x_i\right) \tag{6}$$

which reduces to

$$\sigma^2 = \frac{1}{N^2}\left(\sum n_i x_i^2 - N\bar{x}^2\right). \tag{7}$$

This can be immediately recognized as the same result that is obtained for the variance of the mean of a normal (or Gaussian) distribution having each value of x occurring n_i times, *viz.*

$$\sigma^2 = \frac{\sum n_i(x_i - \bar{x})^2}{N(N-1)} \tag{8}$$

which can be put into a more convenient form for calculation as

$$\sigma^2 = \frac{\sum n_i x_i^2 - N\bar{x}^2}{N(N-1)}. \tag{9}$$

For large N, say greater than 30, eqns. (7) and (9) are the same to better than 3 %.

Equation (7) may be rewritten in a form which shows explicitly how the standard deviation of the mean depends only on the total number of ions counted,

N, and on the shape of the peak. Suppose we normalize the area of the distribution in each case, and use a set of numbers f_i to describe the peak shape, such that

$$n_i = f_i \cdot N. \tag{10}$$

Then σ_m for the mean is

$$\sigma_m = \frac{1}{\sqrt{N}}\left(\sum f_i \, x_i^2 - \bar{x}^2\right)^{\frac{1}{2}}. \tag{11}$$

In a high resolution mass spectrometer for precise atomic mass determinations, the ideal peak shape is an isosceles triangle, while for isotopic abundance measurements it is rectangular. When eqn. (11) is evaluated for a triangle of base width W, then

$$\frac{\sigma_T}{W} = \frac{1}{\sqrt{24N}} = 0.20\,\frac{1}{\sqrt{N}}. \tag{12}$$

For a rectangular peak of width W,

$$\frac{\sigma_R}{W} = \frac{1}{\sqrt{12N}} = 0.29\,\frac{1}{\sqrt{N}} \tag{13}$$

Equation (12) yields the same result as that calculated by Campbell and Halliday[1] for a triangle with large N approximated by a Gaussian.

In addition to this purely statistical limitation to the precision of a doubl measurement, a further practical limitation may exist due to the presence of small modulation in peak position. This may be caused either by electric magnetic a.c. fields or by vibration of the apparatus. In either case, the positi of the peak is sinusoidally modulated at a beat frequency f_B with some amplitu A that is a fraction of a peak width. This means that if the peak is collected f exactly an integral number of oscillations, there will be no systematic error intr duced into the peak position.

Generally there is a non-integral number of oscillations, so that there i random contribution added that does not represent the true peak position. T contribution, on the average, introduces a bias in the position of the mean $2AW/\pi$, so that the calculated position of the centroid is shifted by an amo

$$\varepsilon = \pm \frac{2AW}{\pi(N_B + \frac{1}{2})} \tag{}$$

where N_B is the integer number of complete oscillations or "beats" of the syst If $N_B > 30$, the error introduced by neglecting the $\frac{1}{2}$ is negligible. The system bias, ε, varies as $1/T$ while σ_m, the statistical standard deviation of the centr varies as $1/\sqrt{T}$ where T is the elapsed time. Hence

$$\frac{\varepsilon}{W} \approx \pm \frac{2A}{\pi f_B \cdot T}$$

independent of the ion current, or intensity and

$$\frac{\sigma}{W} = \pm \frac{0.205}{\sqrt{\frac{I}{e} \cdot T}} \tag{16}$$

where I is the ion current, and e the electronic charge.
Hence

$$\frac{\varepsilon}{\sigma} = \pm \frac{3.10\, A}{f_B} \sqrt{\frac{I}{eT}}\,. \tag{17}$$

It is seen from eqn. (17) that ε/σ is large if I is large, and gets smaller as T ncreases. For very intense peaks the collection time tends to be short, so the elative size of this systematic error is increased. Also, since eqn. (15) is indepen- lent of I, the contribution of the bias in each of the two peaks being matched is f the same magnitude and so the total bias introduced into the determination f the mis-match is $\sqrt{2}\,\varepsilon$.

Finally, it should be noted that the "systematic bias", ε, is a bias in the cal- ulated peak position for a single match, and, as suggested in eqn. (14) *et seq.*, ay be of either sign. It will be seen below, that many individual matches are made n order to obtain a final value for a given mass difference. In this way, the effect f the presence of the "systematic bias", ε, is to increase the spread of the results, ather than to alter significantly the final value obtained for the mass difference.

HE QUADRANT SYSTEM

As will be apparent, the experimental technique employed in this work is improved version of the "centroid" method referred to earlier. The 1024 annel signal averager (Fabri-Tek FT1052), used originally for the visual null ethod[2], has been modified by splitting the memory into four sections of 256 annels. During the first quarter cycle with $\Delta V = 0$, a signal proportional to reference peak of mass M is stored in the first quadrant. During the second, rd and fourth quarter cycles, signals with ΔV_1, ΔV_2 and ΔV_3 added to V, are ored in the second, third and fourth quadrants respectively. The accumulated mory contents are illustrated in Fig. 1 where the quadrants are shown one above other. Generally, ΔV is set near the expected value with $\Delta V_1 = \Delta V_2 - \delta V$ d $\Delta V_3 = \Delta V_2 + \delta V$ set about 0.1 % to 1.0 % below and above ΔV_2.

Either M or M' may be used as the reference peak, *i.e.* ΔV may be added or tracted. Also, the ion beam may be swept in two different directions. Finally, ΔV "staircase" may increase (N) or decrease (B) as shown in Fig. 2. Per- tations of these arrangements lead to eight different matching configurations. rder to reduce the possibility of systematic error due to the method of matching ight are used, and the weighted average is the value associated with one "run".

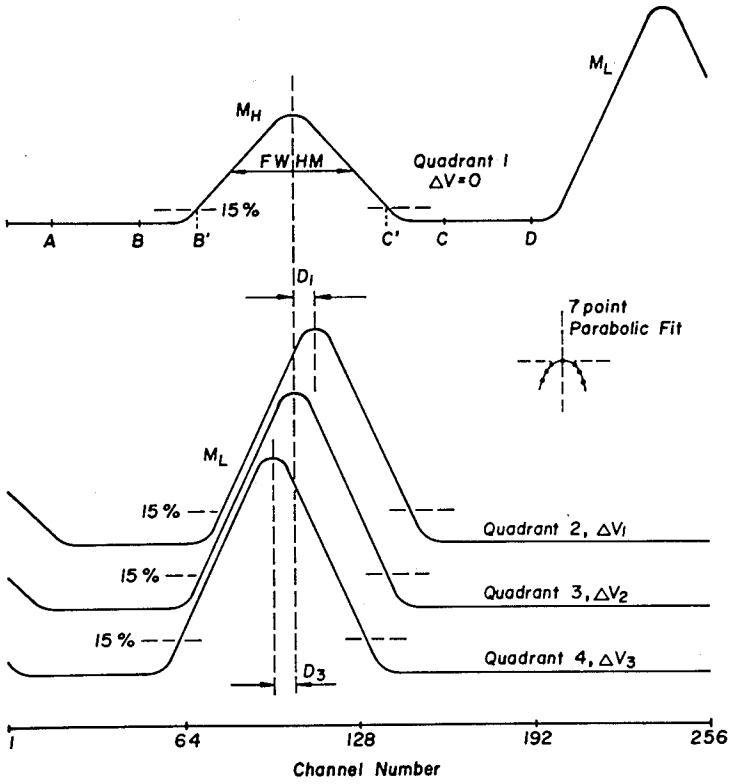

Fig. 1. Memory contents for N, Add, Forward. M_H is the reference peak and M_L, the ligh member of the doublet, is being matched to M_H. Points A, B, C, and D are used for calculati the base line. Points B′ and C′ at the 15 % level are shown for the first quadrant. An expand diagram of the parabolic approximation is also shown.

Figure 1 is an idealized display of the memory contents for N, Add, Forwa after collection for several minutes. The lateral displacement of the peaks exaggerated here. Usually, the peak occupies more than 100 channels in the cen of each quadrant.

In Figure 2 we show the wave forms necessary to carry out the match operation illustrated in Fig. 1. The ΔV wave form is derived from a mechan chopper (Guildline 9745/4) driven by a synchronous motor via an "O"-ring separate trigger signal is taken from independent contacts on the chopper in or to start the address advance for each quadrant in turn. In the earlier work repor here (Tables 1 and 2), the data collection interval (thick line) was 25.6 m (100 μsec/channel) followed by a dead time of 7 msec. Voltages, V and V_a, w switched to new values as indicated in Fig. 2 and a further dead time of 10 m occurs during which transients become negligible and the process continues

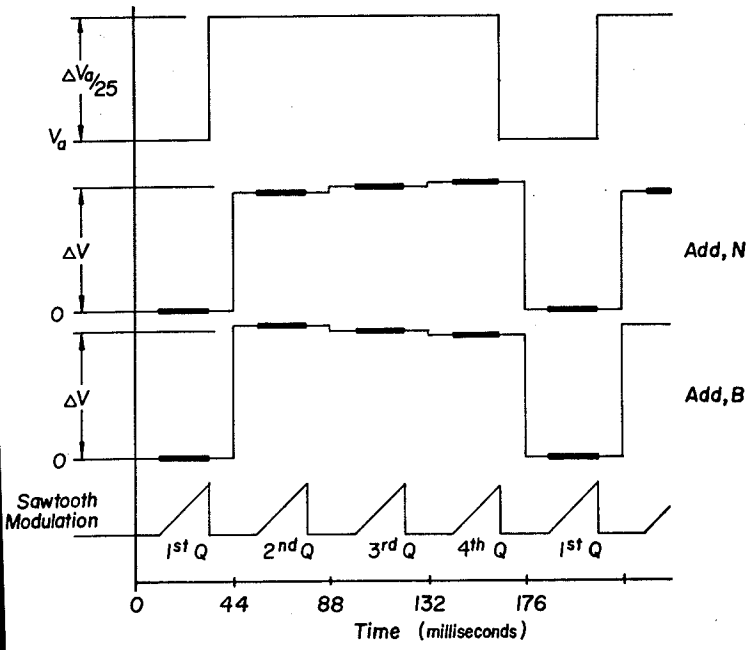

Fig. 2. ΔV wave form and synchronization. ΔV_a is shown reduced by a factor of 25. The ΔV signal is shown as an increasing staircase (N), or decreasing (B). The heavy part of the trace indicates when the sawtooth modulation is applied and the ions are collected. The time scale indicated is that used for Tables 1 and 2. See text.

TABLE 1

$^{116}Cd^{35}Cl-^{114}Cd^{37}Cl$ $\quad M/\Delta M \sim 34600$

ate (1971)	Resolving power FWHM[a] ($\times 10^3$)	($\Delta M/W_5$)[b]	$\Delta M(\mu u)$	$\sigma_{int}(\mu u)$	$\sigma_{ext}(\mu u)$	R[c]
larch 18	123	1.79	4343.7	0.89	3.7	4.2
larch 19	168	2.43	4351.8	0.60	4.0	6.6
larch 19	165	2.38	4350.3	0.65	2.5	3.9
larch 24	117	1.69	4345.7	0.85	3.9	4.6
larch 25	140	2.02	4351.8	0.57	2.9	5.1
larch 25	157	2.27	4347.0	0.57	2.5	4.4
	average R		4.8 ± 0.4			
	weighted mean		4348.7 ± 1.2 μu			
	mean of previous direct determinations[d]		4347.9 ± 1.3 μu			
	1971 mass evaluation[e]		4345.3 ± 2.6 μu			

FWHM = full width half maximum.
Here W_5 is the width of the peak as the level 5 % of the maximum peak height.
Large ratio, $R = \sigma_{ext}/\sigma_{int}$.
Ref. 19.
Ref. 20.

TABLE 2

$^{114}Cd^{35}Cl-^{112}Cd^{37}Cl$ $M/\Delta M \sim 42000$

Date (1971)	*Resolving power FWHM*($\times 10^3$)	$(\Delta M/W_5)$[a]	$\Delta M(\mu u)$	$\sigma_{int}(\mu u)$	$\sigma_{ext}(\mu u)$	R
March 17	163	1.94	3553.8	0.54	2.1	3.9
March 17	152	1.81	3547.6	0.25	1.2	4.8
March 18	156	1.86	3546.3	0.28	1.5	5.4
March 18	150	1.77	3545.3	0.27	2.8	10.4
March 22	145	1.73	3551.6	1.13	2.6	2.3
March 22	139	1.66	3549.9	0.71	2.1	3.0
March 25	176	2.10	3547.9	0.57	2.0	3.5
	average R		4.8 ± 1.0			
	weighted mean		3548.5 ± 1.0			
	mean of previous direct determinations[b]		3547.7 ± 0.9			
	1971 mass evaluation[c]		3554.6 ± 2.9			

[a] Here W_5 is the width of the peak at the level 5 % of the maximum peak height.
[b] Ref. 19.
[c] Ref. 20.

TABLE 3

$^{148}Nd^{35}Cl_2-^{146}Nd^{35}Cl^{37}Cl$ $M/\Delta M = 32400$

Date (1972)	*Resolving power FWHM*($\times 10^3$)	$(\Delta M/W_5)$[a]	$\Delta M(\mu u)$	$\sigma_{int}(\mu u)$	$\sigma_{ext}(\mu u)$	R
Jan. 11	147	2.25	6728.0	1.31	3.64	2.8
Jan. 11	153	2.33	6729.0	1.04	1.54	1.5
Jan. 11	157	2.43	6723.7	0.84	1.21	1.4
Feb. 2	133	2.05	6726.6	1.03	2.12	2.0
Feb. 2	194	2.91	6726.1	0.83	1.36	1.6
Feb. 10	163	1.93	6723.5	0.84	2.52	3.0
Feb. 10	153	2.18	6725.0	0.95	2.71	2.8
	average R		2.2 ± 0.2			
	present value		6725.7 ± 0.8			
	mean of previous mass spectrometric values[b]		6721.8 ± 2.2			
	1971 mass evaluation[c]		6726.1 ± 3.1			
	least squares[a]		6721.9 ± 1.6			
	Manitoba 2.7 m[e]		6726.0 ± 0.9			

[a] Here W_5 is the width of the peak at the level 5 % of the maximum peak height.
[b] Ref. 19.
[c] Ref. 20.
[d] Ref. 21.
[e] Ref. 22.

more recent work (Table 3), for reasons which will be discussed, all of these times were reduced by a factor of two. In each case the oscilloscope sweep is adjusted to coincide with the quadrant sweep. The memory is read out on magnetic tape, and the procedure repeated for all eight configurations. Many runs may be stored on one tape before analysis proceeds.

The analysis is then carried out, off-line, on the University of Manitoba IBM 360/65 digital computer. The points A, B, C, and D in Fig. 1 are identified by visual inspection, and read into the computer on punched cards. The base line is calculated between A and B and between C and D. This base line is subtracted from the peak between B and C. As noted in previous work[9,10], the overlap of even small tails from the peaks has the effect of reducing the calculated separation if all of the peak down to the base line is included in the calculation. In this work, only that part of the peak lying 15 % above the base line is used.

To determine the height of the peak, a parabolic approximation is assumed near the local maximum[15]. A seven point least squares smoothing is carried out[16] to obtain a more reliable value of the peak height. Starting at B, the beginning of the peak B′ is taken as the first of three consecutive points lying above the desired 15 % level as shown in Fig. 1. In order to treat the leading and trailing edges symmetrically, the programme then goes to point C and searches backwards for three consecutive points lying above the desired cut-off level. The first of these is taken as C′, the end of the peak.

After subtraction of the base line, the peak height is converted to the number of ions by multiplying by a calibration constant. The centroid and first four moments of the distribution between B′ and C′ are calculated. The second moment allows the calculation of the standard deviation; this agrees with the estimate of eqn. (12) to within a few percent when the cut-off level is $\sim 15\,\%$.

After finding the centroid and standard deviation of the peak in each quadrant, the displacement D_1, D_2 and D_3 of the peaks in quadrants two, three and four relative to the reference peak in quadrant one, are calculated. A straight line is fitted to the pairs of points, $(D_i \pm d_i,\ \Delta V_i \pm v_i)$, $i = 1, 2, 3$. The least squares procedure developed by Williamson[17] takes into account the errors in both coordinates and calculates the slope, intercept, error in slope and error in intercept. The matched condition is $D = 0$; thus the intercept of the fitted line on the ΔV axis is the desired ΔV. *The calculated error in the intercept is within a few percent of the error predicted using eqn.* (12) *and total number of ions in the "match".*

To justify the linear fit, ten different measurements were taken, each with $\Delta V = 0$ (that is, a given peak is matched to itself) but different δV's applied covering the range usually used, and extending smaller and larger as well. A straight line, then second and third order polynomials were fitted to the resulting set of about thirty points. This was done for each of the eight different matching conditions. In each case the coefficient of the quadratic term was three orders of magnitude smaller than that of the linear term, and had the same sign for both

positive and negative slopes. This is smaller than the errors in the intercept and the slope. Moreover, if the quadratic term were neglected the results would be too high for lines with positive slope, and too low for those with negative slope. Thus the small effect cancels over a complete run. If the curve were "S"-shaped, little or no error in the intercept would result. However, fitting a cubic resulted in essentially unchanged lower order coefficients, and the cubic coefficient was four orders of magnitude smaller than the quadratic.

In matching a peak to itself it was noted that the peak in quadrant 1 was shifted by a small amount with respect to the other three quadrants. This was of the same order of size as the error of locating a single peak, and became apparent only after considerable work. The effect would yield results too high for fits with negative slope, and to low for those with positive slope. Thus, although no bias would be introduced, the spread of the eight intercepts would be unnecessarily large. Accordingly, a correction was applied to the displacement D_i before fitting the straight line. In the earlier work (Tables 1 and 2) this correction was 0.18 ± 0.02 channels while in the more recent work (Table 3) it has been reduced to 0.04 ± 0.02 channels.

RESULTS

Initially two well known doublets in the spectrum of cadmium chloride were studied to test the technique. The data obtained for individual "runs" on these doublets, the actual operating resolving power, the "internal" and "external" standard deviations (following the definitions by Birge[18]) and the Birge ratio ($R \equiv \sigma_{ext}/\sigma_{int}$) are summarized in Tables 1 and 2. Each value of ΔM is, as described above, the weighted mean of eight values corresponding to the eight different matching configurations.

The values of the internal errors, here derived from the matching analysis are in good accord with the error (~ 0.35 μu at M $\sim$ 200 u) estimated on the basis of eqn. (12) and thus represent the lower limit of precision which is attainable in principle with the number of ions collected and the resolution used.

As is evident from these tables, the external error in this early work was, on the average, about a factor of five larger than the internal error. This means that differences between results from the eight configurations were larger than would be expected on the basis of the number of ions collected and the resolution of the mass spectrometer.

It was subsequently determined that, for the results given in Tables 1 and 2, the larger spread of the eight matches is due, at least in part, to a building vibration at 6.8 Hz which is not sufficiently attenuated by the vibration isolators which support the mass spectrometer. This results in an oscillation of the displayed peak at a beat frequency of ~ 1 Hz and with an amplitude of about 1/25 of a peak width

Such an oscillation would not likely be noticeable in visual matching. However, when eqn. (17) is evaluated for ion currents of $\sim 3 \times 10^{-15}$ amp, $A \sim 0.04$ and a collection time of 1 to 1.5 minutes, an estimate of $\sqrt{2}\,\varepsilon/\sigma$ is found to be 3.7. This value is only slightly smaller than the average value of R given in Tables 1 and 2.

In calculating the final weighted mean, σ_{ext} was used, and the final error quoted is the larger of the new σ_{ext} or σ_{int}. Both are about the same size (*i.e.*, the new $R \approx 1$), and so the assignment of error to a run is seen to be realistic. Moreover, the reproducibility of the spectrometer from run to run and from day to day is as good as its stability from match to match within a given run.

Also presented in Tables 1 and 2 are values which are the weighted averages of several determinations of these particular doublets. These determinations were carried out at different times over the last nine years by this group both at Mc Master University and at the University of Manitoba[19]. It is seen that the present work is in excellent agreement with, and has achieved the same precision as the result of all past work, on the strength of only six or seven runs (two to three hours of machine time), in spite of the relatively large contribution to the error arising from the vibration problem.

It will be noted that agreement with the 1971 mass evaluation[20] is poorer, but is not of the nature of a systematic bias. In this evaluation only one rather old value for each doublet was used as input.

Following the work reported in Tables 1 and 2 and the identification of the vibration problem, the chopper frequency was changed to 11.3 Hz so that f_B is now ~ 4.5 Hz and consequently $(\varepsilon/\sigma)_{vibration}$ is reduced (eqn. 17) by a factor of ~ 4. This modification decreased all time intervals indicated in Fig. 2 by a factor of $\frac{1}{2}$).

On the basis of the analysis above, the Birge ratio for a single run might be expressed as

$$R^2 = \left(\frac{\sqrt{2}\varepsilon}{\sigma_{int}}\right)^2_{vibration} + \left(\frac{\sqrt{2}\varepsilon}{\sigma_{int}}\right)^2_{a.c.} + \left(\frac{\sigma_{ext}}{\sigma_{int}}\right)^2_{statistical} \qquad (18)$$

Thus, the removal of this major contribution to R will probably not reduce it to unity because of the presence of very small modulations of the beam by electric or magnetic fields.

In Table 3 we present recent results for the $^{148}Nd^{35}Cl - {}^{146}Nd^{37}Cl$ mass difference. As expected, the value of R in this case has been reduced (actually 2.2) and the new value is more precise than any of the comparison values. The comparison values are (a) the mean of all previous mass spectrometric determinations of the doublet by this group, (b) the 1971 mass evaluation which combines mass spectrometric data with nuclear reaction and decay Q-values but does not include any of the recent values in this region reported by Barber *et al.*[3], (c) a similar least squares adjustment by Meredith and Barber[21] which includes these recent data, but not the doublet determination reported here, and (d) a recent determination is our laboratory using the 2.7 meter instrument.

In summary, the variation of peak-matching described herein is now being used routinely in our extensive study of precise atomic mass differences. The improved signal-to-noise ratio which is achieved with a signal averager is retained. Human judgment of the matched condition has been further removed in this technique, and improved precision has been achieved in a shorter operating time. Finally, the analysis makes possible a comparison between the precision experimentally obtained and the theoretical limit determined by the resolution and the number of ions detected. Although this work has been applied to peak matching with highest precision currently attained, the general considerations and the experimental technique are applicable to peak-matching experiments of lower precision.

REFERENCES

1 R. C. BARBER, J. O. MEREDITH, R. L. BISHOP, H. E. DUCKWORTH, M. E. KETTNER AND P. VAN ROOKHUYZEN, *Proc. 3rd Int. Conf. Atomic Masses*, University of Manitoba Press, Winnipeg, 1968, p. 717.
2 R. C. BARBER, R. L. BISHOP, H. E. DUCKWORTH, J. O. MEREDITH, F. C. G. SOUTHON, P. VAN ROOKHUYZEN AND P. WILLIAMS, *Rev. Sci. Instrum.*, 42 (1971) 1.
3 R. C. BARBER, R. L. BISHOP, H. E. DUCKWORTH, J. O. MEREDITH, F. C. G. SOUTHON, P. VAN ROOKHUYZEN AND P. WILLIAMS, *Can. J. Phys.*, 50 (1972) 34.
4 W. BLEAKNEY, *Amer. Phys. Teacher*, 4 (1936) 12.
5 R. L. BISHOP AND R. C. BARBER, *Rev. Sci. Instrum.*, 41 (1970) 370.
6 R. C. BARBER, R. L. BISHOP, L. A. CAMBEY, H. E. DUCKWORTH, J. D. MACDOUGALL, W. MCLATCHIE, J. H. ORMROD AND P. VAN ROOKHUYZEN, *Proc. 2nd Int. Conf. Nuclidic Masses*, Springer-Verlag, Vienna, 1964, p. 393.
7 J. L. BENSON AND W. H. JOHNSON JR., *Phys. Rev.*, 141 (1966) 1112.
8 J. D. MACDOUGALL, W. MCLATCHIE, S. WHINERAY AND H. E. DUCKWORTH, *Z. Naturforsch.* 21a (1966) 63.
9 C. M. STEVENS AND P. E. MORELAND, *Proc. 3rd Int. Conf. Atomic Masses*, University of Manitoba Press, Winnipeg, 1968, p. 673.
10 H. MATSUDA, S. FUKUMOTO AND T. MATSUO, *Recent Developments in Mass Spectroscopy*, University Park Press, Tokyo, 1970, p. 477.
11 R. D. CRAIG, B. N. GREEN AND J. D. WALDRON, *Chimia*, 17 (1963) 33.
12 H. CRAMER, *Mathematical Methods of Statistics*, Almquist and Wiksell, Stockholm, 194
13 B. N. TAYLOR, W. H. PARKER AND D. N. LANGENBERG, *The Fundamental Constants a Quantum Electrodynamics*, Academic Press, New York, 1969, p. 337.
14 A. J. CAMPBELL AND J. S. HALLIDAY, *13th Ann. Conf. Mass Spectrom. and Allied Topi* St. Louis, 1965.
15 D. H. WEICHERT AND R. D. RUSSELL, *Can. J. Phys.*, 46 (1968) 1443.
16 A. SAVITZKY AND M. J. E. GOLAY, *Anal. Chem.*, 36 (1964) 1627.
17 J. H. WILLIAMSON, *Can. J. Phys.*, 46 (1968) 1845.
18 R. T. BIRGE, *Phys. Rev.*, 40 (1932) 207.
19 J. O. MEREDITH, *Ph.D. Thesis*, University of Manitoba, 1971, unpublished.
20 A. H. WAPSTRA AND N. B. GOVE, *Nuclear Data Tables*, A9 (1971) 357, Academic Press, N York.
21 J. O. MEREDITH AND R. C. BARBER, *Can. J. Phys.*, 50 (1972) 1195.
22 J. W. BARNARD AND P. WILLIAMS, personal communication, 1972.

Part 3 Mass Spectroscopy

Recent Determinations of Atomic Mass Differences at the University of Manitoba

R. C. Barber, J. W. Barnard, R. L. Bishop, D. A. Burrell
H. E. Duckworth, J. O. Meredith, F. C. G. Southon, and P. Williams

*Department of Physics, University of Manitoba, Canada**

1. Introduction

For some time a systematic study of atomic mass differences between naturally-occurring nuclides in the region above Pr has been in progress in this laboratory. This region has been of special interest inasmuch as the mass differences and masses have, until recently, been least well known here. Moreover, it is in this region that strong nuclear deformation makes its appearance.

A substantial body of data on which this study has been based was obtained using the 2.7 m. radius Dempster type mass spectrometer and has appeared in a series of three papers [1, 2, 3]. More recently, a new mass spectrometer, constructed at the University of Manitoba has been used to improve the precision of some data, and also to include in the study values for doublets not previously studied, particularly those involving isotopes of low (< 0.2%) relative abundance.

2. The Mass Spectrometer

The instrument was constructed according to the second-order focusing theory of Hintenberger and Konig [4] and employs a 94.65° cylindrical electrostatic analyser of radius 1.00 m followed by a 90° uniform magnetic field. It was normally operated with a resolving power ($\Delta M/M$) of 100,000 to 150,000 measured at the base of the peaks. The reader is referred to detailed descriptions of the instrument in its early [5] and present [6] forms which have appeared elsewhere.

The determination of the mass difference between members of a doublet depends on an exact theorem described by Bleakney [7]. On alternate sweeps of the display oscilloscope, the potential (V) applied across the electrostatic analyser, and the source potential (V_a) are changed by the same fractional amounts to $V \pm \Delta V$ and $V_a \pm \Delta V_a$. For the proper values of ΔV and ΔV_a the trajectory of the second member of a doublet is displaced to the identical path previously described by the first member (before the voltage increments were applied) and thus appears at the same position on the oscilloscope screen. Adjusting the value of ΔV to obtain coincidence is the process known as "matching". When the members of the doublet are so matched, the mass difference, ΔM, is given by

$$\Delta M = M\frac{\Delta V}{V}$$

where M is the mass of the displaced ion.

*Work supported by the National Research Council of Canada.

Copy from Conference on Atomic Masses & Fundamental Constants 4, Teddington, 1971

In this instrument, the determination of the matched condition has been carried out by either of two techniques, both of which make use of a 1024-channel signal averager. The first of these is the "visual null method" of Benson and Johnson [8] as described in reference 6. Fig. 1 is

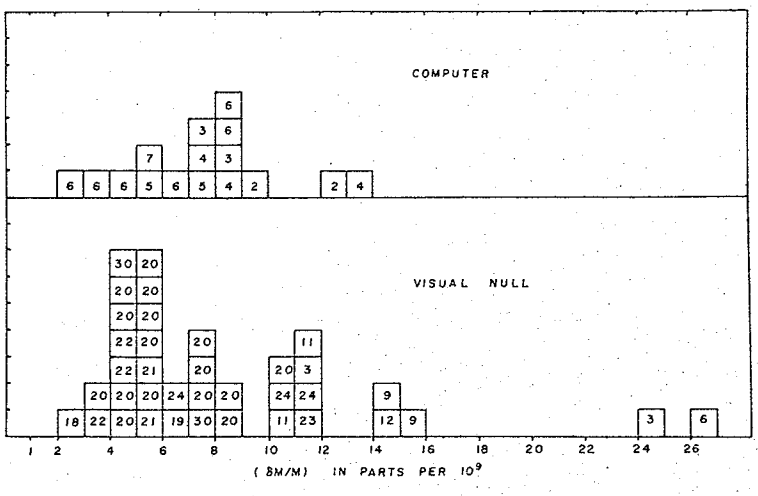

Fig. 1. Histogram of the precision obtained by the "visual null method." δM is the error on the doublet and M is the mass at which the difference was determined.

a histogram showing the precision ($\delta M/M$) obtained by this technique for the various doublets studied to date. As is evident, the typical precision is $\sim 5/10^9$.

A second technique of peak matching has recently been introduced on our instrument [9]. In this arrangement the 1024-channel memory of the signal averager is divided into four sections of 256-channels each. The sawtooth sweep is adjusted to coincide with the scan through a 256-channel quadrant.

As indicated in Fig. 2, $\Delta V = 0$ during the first scan and so the reference peak is stored in the first quadrant. During the second, third and fourth scans, voltages ΔV_1, ΔV_2 and ΔV_3 respectively are added to the electrostatic analyser voltage, V, and the other peak of the doublet is stored in the remaining three quadrants at three positions which bracket the matched condition. The whole cycle is repeated many times to improve the signal-to-noise ratio.

Usually ΔV_2 is very near the expected value while the ΔV_1 and ΔV_3 differ from it by $\sim .1\%$ to 1% (the displacements D_1 and D_3 are much exaggerated here). As shown here the ΔV_1, ΔV_2 ΔV_3 are in order of increasing size.

This latter order may be reversed, the direction of sweeping the ion beam across the collector slit may be changed and either of the doublet

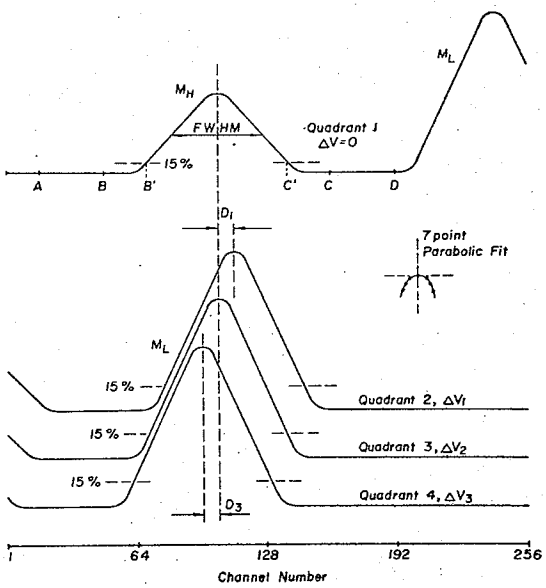

Fig. 2. Analog display of signal averager memory during "computer" matching.

members may be regarded as the reference peak (i.e., ΔV may be added to or subtracted from V). These arrangements are permuted to give 8 different matching configurations and the weighted average of the eight values so obtained is the value for one run.

In order to make maximum use of the information available, the peak of interest is adjusted to occupy as many channels as is convenient in the center of a quadrant, leaving about 30 channels at each end to establish a base line. The memory contents are read onto magnetic tape, then the matching configuration is changed, and the process repeated. As many complete runs as desired can be recorded with minor refocusing taking place between runs.

The analysis of the raw data is carried out off-line with the university IBM 360/65 computer as follows. The spectra are plotted by the line printer for visual inspection, and the points A, B, C, D are identified by eye and read into the computer via punched cards. The base line is calculated between A and B and between C and D for each quadrant and is subtracted from the peak between B and C.

The overlapping of tails from the peaks would have the effect of reducing the calculated separation. Moreover it would be desired to exclude from the calculations ions which have been significantly scattered. We have therefore followed the general lead of Stevens and Moreland [10] and have used only the part of the peak lying 15% or more above the base line.

As Campbell and Halliday [11] have shown, the fundamental limit on the precision of locating a peak is determined by the number of ions in the peak. The idealized shape of the peak here is triangular and the weighted

mean, or centroid, is the best method of estimating the location. For a large number of ions, N, the triangle can be approximated by a normal distribution with a standard deviation of $W/\sqrt{24}\,N$ where W is the full width at the base of the peak. After subtraction of the base line, the peak height is converted to the actual number of ions by multiplying by a previously determined constant.

The centroid and first four moments of the distribution between B^1 and C^1 are calculated. From the second moment the standard deviation is derived; this agrees with the estimate based on $W/\sqrt{24}\,N$ to within a few percent when the cutoff is in the region ~ 15%. The third and fourth moments allow more detailed comparisons of peak shape (skewness and sharpness relative to a Gaussian).

After finding the centroid and its standard deviation for the peak in each quadrant, the displacement D_1, D_2, and D_3 are calculated. The errors in the D_i are d_i where d_i are the r.m.s. combinations of the errors in locating the two peaks. A straight line is fitted to the three pairs of points $(D_i \pm d_i, \Delta V_i \pm v_i)$ by the iterative least squares fitting procedure of Williamson [12] which takes into account the errors in both coordinates.

As prescribed by Bleakney's theorem, the matched condition is given by the intercept of the fitted line. The calculated error in the intercept agrees very well with the error expected on the basis of the total number of ions in the match.

A series of experiments were carried out to determine if the linear fitting was justified. In each of the eight possible matching configurations a series of ten matches were carried out where a peak was matched to itself. That is, $\Delta V = 0$ and the amounts that the peaks in quadrants 2 and 4 were displaced from the reference peak were varied over a range much larger than that ever used in matching.

A straight line, then second and third order polynomials were fitted to the resulting data. For each of the eight configurations it was found that the quadratic term was three orders of magnitude smaller than the linear term and has the same sign for both positive and negative slopes. The cubic coefficient was 4 orders of magnitude smaller than the quadratic and had essentially no effect on the magnitude of the lower order coefficients.

In matching a peak to itself it was found that the peak in quadrant 1 was displaced by 0.18 ± 2 channels with respect to the other three quadrants. If uncorrected, this would leave the mean for a run unaffected but would result in an unnecessarily large error for that value. Accordingly, a correction is now applied before the fitting procedure is carried out.

Five well known doublets in the spectrum of $CdCl_2$ and $NdCl_2$ were studied to test the operation and precision of the system. In Table I we present the results for a typical doublet, giving the working resolving power (FWHM as measured from the plotted contents of the signal averager's memory), value of ΔM for the given run, the "internal" and "external" standard deviations as defined by Birge [13]. The "internal" standard deviation is the error expected on the basis of the errors calculated

TABLE I

$^{114}Cd^{35}Cl$-$^{112}Cd^{37}Cl$ $M/\Delta M \approx 42{,}000$

All Masses in Micro Units

Date	R.P. (FWHM)	ΔM	σ_{int}	σ_{ext}
March 17/71	163,000	3553.8	0.54	2.1
March 17	152,000	3547.6	0.25	1.2
March 18	156,000	3546.3	0.28	1.5
March 18	150,000	3545.3	0.27	2.8
March 22	145,000	3551.6	1.13	2.6
March 22	139,000	3549.9	0.71	2.1
March 25	176,000	3547.9	0.57	2.0
	Weighted Mean	3548.5 ± 1.0	cf.	3547.9 ± .9

for each match. The "external" standard deviation is often a factor of ~4 larger than the internal standard deviation. This means that differences between results from the eight configurations are larger than would be expected on the basis of the precision associated with each match. The internal error (~0.5 μu at M ~ 200 u) is the lower limit attainable with the number of ions collected, and the resolution used. The larger spread of the eight matches is not completely understood, but is probably due to changes in the spectrometer operation from match to match. At present there does not appear to be any systematic variation of the result with matching configuration.

In calculating the final weighted mean, σ_{ext} has been used and the final error quoted is the larger of the resulting σ_{ext} or σ_{int}. Both are about the same size, so that the assignment of error to a run appears realistic and the reproducibility of the spectrometer from run to run and from day to day is as good as the stability from match to match within a given run.

This technique is now being used routinely in our study of atomic mass differences in the rare earths and in the region immediately above the rare earths.

3. Determination of Relatively Wider Mass Doublets

The atomic mass differences which have been determined by this group over the past several years have all involved doublets for which the spacings were less than ~1/20,000. Inasmuch as almost all of these doublets have involved the $^{37}Cl - ^{35}Cl$ mass difference, several determinations of this difference have been undertaken since the 1964 Mass Table was published [8, 14, 15, 16]. We felt it would be desirable to contribute an additional value via the

$$^{12}C\,^{35}Cl\,D_2 - {}^{12}C\,^{37}Cl\,H_2$$

doublet which is obtained from methylene chloride and has a spacing, $\Delta M/M \sim 1/3{,}300$.

In preparation for this determination, the $^{37}Cl - ^{35}Cl$ difference was studied as a doublet of width 2 u at various mass numbers in the region 100 to 250 u. This work revealed the presence of a systematic error which was consistently negative and which behaved in the same general fashion as that encountered by Stevens and Moreland [10]. In our instrument the error appears to arise as a result of surface potentials on the electrostatic analyser plates. The formation and decay of such potentials as a result of low intensity ion or electron bombardment have been studied by Petit-Clerc and Carette [17] at Laval University and appear to be consistent with the nature of the error observed by us.

The electrostatic analyser was cleaned with ether, absolute alcohol and distilled water and, in the early stage of pumpdown, with a Tesla discharge in Ar. Subsequently the error was found to be ~0 ppm; thereafter it slowly increased to ~100 ppm over a period of a few weeks.

Accordingly, the results obtained for the narrow chlorine doublet mentioned earlier were corrected by a factor determined by a 1 u calibration doublet (the ^{1}H mass) which was measured immediately before or after the narrow doublet.

In the upper part of Table II are given calculated values (where possible) for the doublet which was measured and the new value from our laboratory. The high degree of precision associated with the last two values and the agreement between them is noteworthy, particularly in the light of the fundamental differences between the two instruments used.

In the lower half of the table we give the values of $^{37}Cl - ^{35}Cl$ mass difference which, in the first four cases, is calculated from the measured mass of ^{37}Cl and ^{35}Cl. The value from this work is calculated from the doublet separation and from the weighted averages of all experimental values for the D and H masses.

4. Rare Earth Mass Differences

The rare earth mass differences which have been determined by this research group both at McMaster University and the University of Manitoba are of the types

$$^{A}X - ^{A}Y = \Delta_1 \tag{1}$$

$$^{A+2}X^{35}Cl - ^{A}Y^{37}Cl = \Delta_2 \tag{2}$$

$$^{A+2}X^{35}Cl_2 - ^{A}Y^{37}Cl_2 = \Delta_3 \tag{3}$$

where X and Y may or may not be the same element. Thus mass connections are obtained between nuclides differing in A by 0, 2 or 4 units. In Fig. 3 the new mass connections are indicated by solid lines with the number indicating the size of the error in keV. Values obtained with the 2.7 m radius instrument at McMaster are indicated by broken lines. (All naturally-occurring nuclides are shown.) As is evident from the figure the new data are generally more precise (0.7 keV to 4.2 keV) than those obtained with the older instrument and provide many connections not previously

TABLE II

	$^{12}C\,^{35}Cl\,^{2}D_2 - {}^{12}C\,^{37}Cl\,H_2$ (μu)	Reference
1964 Mass Table	15 506.66 ± 140	18
Benson and Johnson (1966, 1968)	15 504.30 ± 60	8, 19
Stevens and Moreland (1968, 1970)	15 503.59 ± 13	10, 15
Smith (1971)	15 503.774 ± 65	16
This work (1971)	15 503.796 ± 91	
	$^{37}Cl - {}^{35}Cl$	
1964 Mass Table	1.997 047 4 ± 14	18
Benson and Johnson (1966)	1.997 049 7 ± 6	8
Dewdney and Bainbridge (1965)	1.997 048 89 ± 59	14
Stevens and Moreland (1970)	1.997 050 59 ± 42	15
Smith (1971)	1.997 049 711 ± 63	16
This work*	1.997 049 730 ± 98	

*using experimental values quoted in ref. 16 to get the following weighted averages:

H = 1.007 825 034 ± 12 u D = 2.014 101 797 ± 28 u

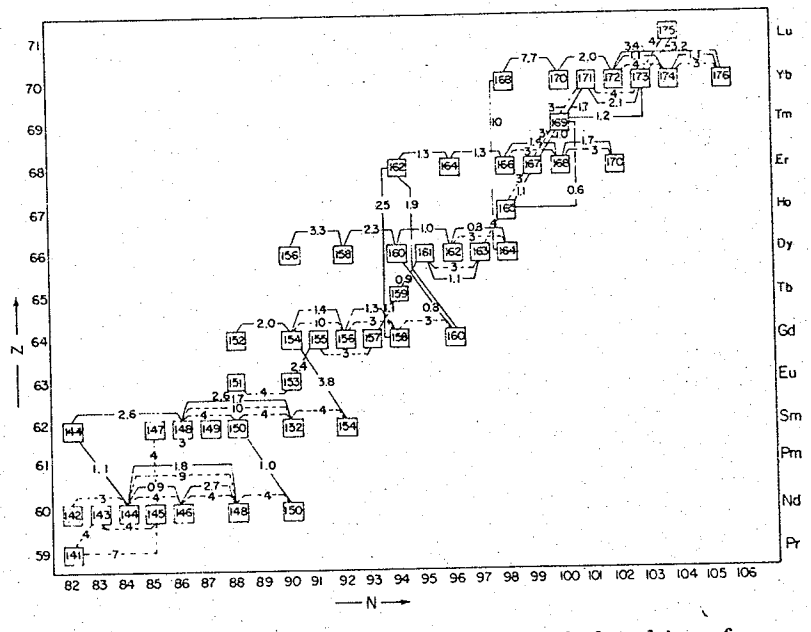

Fig. 3. Mass connections provided by the data tabulated in references 1, 3, and 20.

determined. The actual values for the mass differences (except for Yb and Lu) are presented in a paper which has been submitted to the Canadian Journal of Physics [20] along with a detailed comparison with other mass spectroscopic data and the 1964 Mass Table.

As there is a substantial, but incomplete, body of nuclear decay and reaction Q-values in this region it is desirable to combine the two kinds of data to obtain "best" values for the mass differences throughout this region. The only other mass spectroscopic data with sufficiently significant weights are those from the University of Minnesota [8] involving the Nd masses. In order best to combine these data, we have performed a least squares adjustment [21] following the general procedure outlined by Mattauch [22] and his coworkers. The region in which the mass spectroscopic values lie, has been divided arbitrarily into two regions for the adjustment; the first covers the region $59 \leq Z \leq 69$ and the second $67 \leq Z \leq 72$. The details of these calculations, including the input data, and a discussion of the results will appear in the near future [21, 23]. We wish, however, to draw attention to certain features of the work at this time.

In the first adjustment, one Q-value was eliminated from the beginning on the basis of gross inconsistency with related data, namely the ^{153}Gd (e.c.)^{153}Eu decay Q-value which was low by a factor of ~ 2. Of the 167 nuclides in the region, 83 form an overdetermined set in which there are 143 mass differences subject to 53 closed loop constraints. When this smaller problem was solved, it was found that the ^{148}Nd (d, p) ^{149}Nd and ^{150}Nd (d, t) ^{149}Nd reaction Q-values made major contributions to χ^2. As was previously done in the Nuclear Data Group adjustment, these values were rejected and the adjustment was recalculated. The value of $\sqrt{\chi^2/f} = .95$ compared to the expected value, 1.000 ± 75 and so it was unnecessary to introduce a consistency factor in the calculation. The consistency of the second and smaller adjustment was not as good and will be discussed in reference 23.

4. Discussion of Results

Fig. 4 shows the systematic variation of the double neutron separation energy, S_{2n}, as a function of the neutron number. The data for even-N and odd-N are separated to emphasize the degree of regularity that exists. The major decrease as N = 82 is exceeded, and the break at N = 88 associated with the onset of deformation are well known features of these curves.

In the region below 88 and above 92, the segments of adjacent curves between any two given neutron numbers are almost parallel to each other. Thus irregularities in the curves are reproduced for the same neutron number, that is, the shape of the curves is relatively independent of Z. On the basis of this systematic variation extrapolated curves have been proposed as indicated by the broken lines.

As we have noted in previous work [24] the energy of deformation for nuclides with N = 90 is relatively small for Nd (Z = 60) and increases in going to Sm (Z = 62) and Gd (Z = 64). This figure further suggests that at N = 88, Dy (Z = 66) may already have a ground state deformation inasmuch

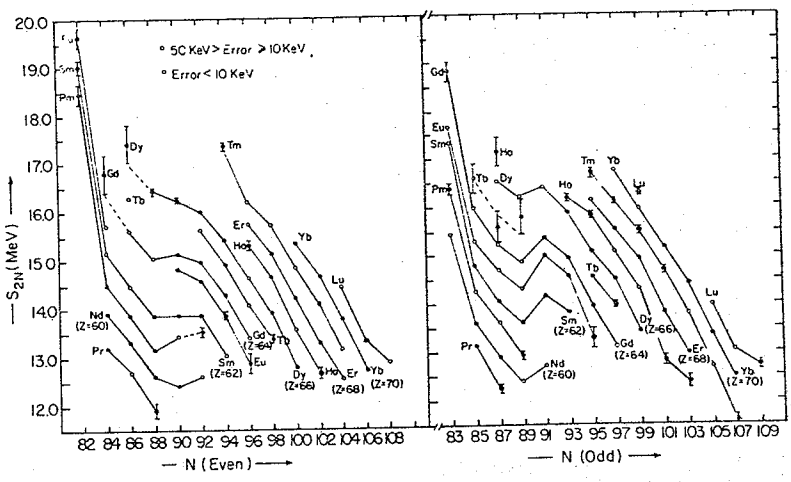

Fig. 4. Systematic variation of S_{2n} vs. N.

as that point lies somewhat higher than would otherwise be expected. That is, as Z increases, the effect due to nuclear distortion occurs somewhat earlier. Some support for this comes from the change in the slope of the N = 89-91 segments of the odd-N curves with increasing Z. For both sets of curves it appears that when N ~ 92 is reached the nuclides have approximately the same energy of deformation.

The single-neutron separation energies, S_n, are shown as a function of N in Fig. 5. The nature of the discontinuity in the region of deformation (N ~ 90) has previously been commented on [1] for both even- and odd-Z, as well as the pairing effect, as manifested in the displacement of the odd-Z curves in each of the plots (i.e., for even-N and odd-N). It should be noted that, for odd-odd nuclides, the neutron-proton pairing appears to occur in the region N ≥ 85. For even-N nuclides which are distorted, this does not appear to be significant although it does occur for the region below N = 88.

The S_n plots again suggest that in odd-N nuclides the distortion may not be as large as in even-N nuclides, but continues to increase beyond N = 92. Again, the even-N plot suggests that at N = 88, Dy has already acquired some distortion.

The plots of the pairing energy, P_n, and the proton separation energies, S_{2p} and S_p, will be presented elsewhere [21, 23]. For the latter two quantities this work confirms the lack of dramatic structure [1, 3].

Although not presented here, a plot of P_p vs. Z does not exhibit any systematic behaviour. However, when we plot P_p vs. N a systematic change with the addition of neutrons is evident. P_p has a relatively large value which increases somewhat until the addition of neutrons precipitates deformation. Thereafter there is a drastic decline until N = 92 at which

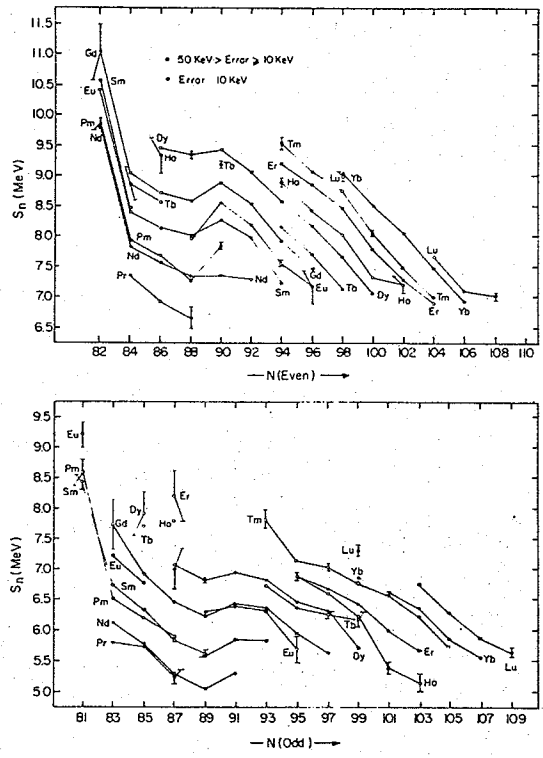

Fig. 5. Systematic variation of S_n vs. N.

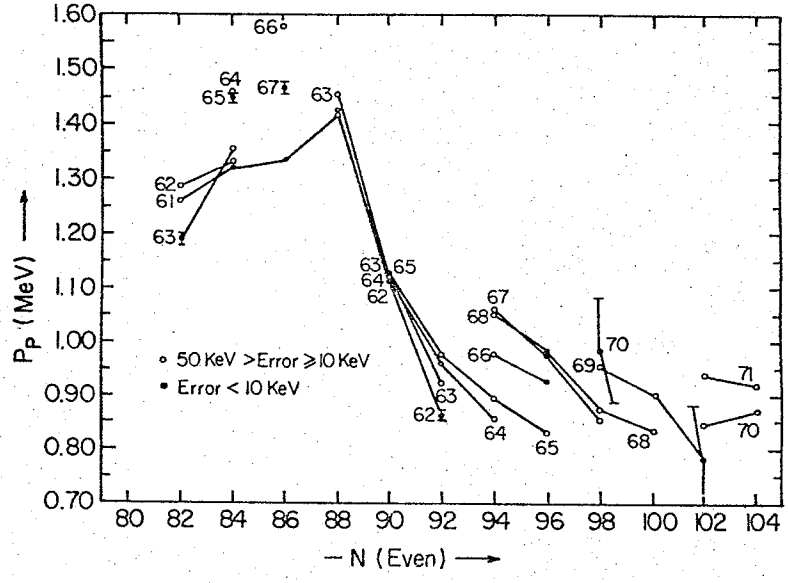

Fig. 6. Systematic variation of P_p vs. N.

point some dependence of Z begins to reappear, although the values all lie much lower than those for the undeformed nuclides.

References

1. MACDOUGALL, J. D., MCLATCHIE, W., WHINERAY, S. and DUCKWORTH, H. E., Nucl. Phys. A145, 223 (1970).
2. MCLATCHIE, W., WHINERAY, S., MACDOUGALL, J. D. and DUCKWORTH, H. E., Nucl. Phys. A145, 244 (1970).
3. WHINERAY, S., MACDOUGALL, J. D., MCLATCHIE, W., and DUCKWORTH, H. E., Nucl. Phys. A151, 377 (1970).
4. HINTENBERGER, H. and KONIG, L. A., Advances in Mass Spectroscopy (Pergamon Press, London, 1960), p. 16.
5. BARBER, R. C., MEREDITH, J. O., BISHOP, R. L., DUCKWORTH, H. E., KETTNER, M. E. and VAN ROOKHUYZEN, P., Proceedings of the Third International Conference on Atomic Masses (University of Manitoba Press, Winnipeg, 1968), p. 717.
6. BARBER, R. C., BISHOP, R. L., DUCKWORTH, H. E., MEREDITH, J. O., SOUTHON, F. C. G., VAN ROOKHUYZEN, P., and WILLIAMS, P., Rev. Sci. Instrum. 42, 1 (1971).
7. BLEAKNEY, W., Amer. Phys. Teacher, 4, 12 (1936).
8. BENSON, J. L. and JOHNSON, W. H., JR., Phys. Rev. 141, 1112 (1966).
9. MEREDITH, J. O., Ph. D. Thesis, University of Manitoba (unpublished, 1971).
10. STEVENS, C. M. and MORELAND, P. E., Proceedings of the Third International Conference on Atomic Masses (University of Manitoba Press, Winnipeg, 1968), p. 673.
11. CAMPBELL, A. J. and HALLIDAY, J. S., 13th Annual Conference on Spectroscopy and Allied Topics (1965).
12. WILLIAMSON, J. H., Can. J. Phys. 46, 1845 (1968).
13. BIRGE, R. T., Phys. Rev. 40, 207 (1932).
14. DEWDNEY, J. W. and BAINBRIDGE, K. T., Phys. Rev. 138, 540 (1965).
15. STEVENS, C. M. and MORELAND, P. E., Recent Developments in Mass Spectroscopy (University Park Press, Tokyo, 1970), p. 1296.
16. SMITH, L. G., Phys. Rev. C4, 22 (1971).
17. PETIT-CLERC, Y., CARETTE, J. D., Vacuum 18, 7 (1968).
18. MATTAUCH, J. H. E., THIELE, W., and WAPSTRA, A. H., Nucl. Phys. 67, 1 (1965).
19. JOHNSON, W. H., HUDSON, M. C., BRITTEN, R. A., and KAYSER, D. C., Proceedings of the Third International Conference on Atomic Masses (University of Manitoba Press, Winnipeg, 1968), p. 793.
20. BARBER, R. C., BISHOP, R. L., MEREDITH, J. O., SOUTHON, F. C. G., WILLIAMS, P., DUCKWORTH, H. E., and VAN ROOKHUYZEN, P. to be published.
21. MEREDITH, J. O., BARBER, R. C., and DUCKWORTH, H. E., to be published.

22. MATTAUCH, J. H. E., Proceedings of the International Conference on Nuclidic Masses (University of Toronto Press, Toronto, 1960), p. 3.
23. MEREDITH, J. O., SOUTHON, F. C. G., BURREL, D. A., BARBER, R. C., DUCKWORTH, H. E., and WILLIAMS, P., to be published.
24. DUCKWORTH, H. E., BARBER, R. C., VAN ROOKHUYZEN, P., MACDOUGALL, J. D., MCLATCHIE, W., WHINERAY, S., BISHOP, R. L., MEREDITH, J. O., WILLIAMS, P., SOUTHON, G., WONG, W., HOGG, B. G., and KETTNER, M. E., Phys. Rev. Letters, 23 592 (1969).

Precise Atomic-Mass Differences in the Region $59 \leqslant Z \leqslant 69$[1]

R. C. BARBER, R. L. BISHOP[2], J. O. MEREDITH, F. C. G. SOUTHON, P. WILLIAMS, H. E. DUCKWORTH, AND P. VAN ROOKHUYZEN[3]

Department of Physics, University of Manitoba, Winnipeg, Manitoba

Received August 4, 1971

A high-resolution mass spectrometer has been used to determine precise atomic-mass differences for 31 mass spectral doublets amongst the rare-earth chlorides. The precision of these determinations is in the range 0.6 μu to 3.8 μu, *i.e.* (2.5 to 25) $\times 10^{-9}$. The new data, when combined with previous data from this laboratory and with the known ^{37}Cl–^{35}Cl difference, provide mass-spectroscopically-derived connections between all naturally occurring odd-A nuclides from ^{141}Pr to ^{169}Tm and between all even-A nuclides from ^{142}Nd to ^{170}Er.

Un spectromètre de masse à haute résolution a été utilisé dans la détermination précise des différences de masse pour 31 doublets spectraux choisis parmi les chlorures des terres rares. La précision des valeurs obtenues est comprise entre 0.6 μu et 3.8 μu, c'est-à-dire (2.5 et 25) $\times 10^{-9}$. Ces nouvelles données, combinées avec d'autres résultats obtenue antérieurement dans notre laboratoire et la valeur connue de la différence ^{37}Cl–^{35}Cl fournissent les connexions dérivées de la spectrométrie de masse entre toutes les espèces nucléaires naturelles de A impair situées entre ^{141}Pr et ^{169}Tm, ainsi qu'entre tous les noyaux de A pair se trouvant entre ^{142}Nd et ^{170}Er.

Canadian Journal of Physics, **50**, 34 (1972)

1. Introduction

A systematic study of atomic-mass differences between naturally occurring isotopes in the region ^{141}Pr to ^{208}Pb has been in progress in this laboratory for several years. The major part of the data on which the study was based was obtained using a 2.7 m radius Dempster-type mass spectrometer located at McMaster University until 1966 and now at the University of Manitoba. The investigation began in the region $N \sim 90$ where the change from spherical to highly deformed nuclei takes place (Barber *et al.* 1964*b*; Duckworth *et al.* 1964; Macdougall *et al.* 1966). It was then extended to survey the region up to ^{208}Pb to provide a fairly comprehensive picture of the mass surface between the 82- and 126-neutron shells (Duckworth *et al.* 1969; Macdougall *et al.* 1970; McLatchie *et al.* 1970; Whineray *et al.* 1970).

More recently, a new mass spectrometer, constructed at the University of Manitoba (Barber *et al.* 1968; Barber *et al.* 1971), has been used to improve the precision of some data and also to include in the study values for mass doublets not studied before, particularly involving isotopes of low relative abundance (0.2 % or less). We now present these new data which, when combined with the previous mass data (Macdougall *et al.* 1966; Macdougall *et al.* 1970; Whineray *et al.* 1970), provide precise mass-spectroscopically-derived mass differences between all naturally occurring nuclides for the region $59 \leqslant Z \leqslant 69$.

2. Experimental Method

The high-resolution mass spectrometer which was used in this work has a radius of curvature in the electrostatic analyzer of 1.00 m and was constructed according to the second-order focusing theory of Hintenberger and König (1960). A description of this instrument in its early (Barber *et al.* 1968) and present forms (Barber *et al.* 1971) has been given elsewhere along with details of its performance. We therefore include here only a brief outline of the apparatus and technique of operation.

Figure 1 is a schematic diagram of the spectrometer showing the geometry together with the associated electronic control circuits in block form. Rare-earth chlorides are vaporized and ionized in a Finkelstein-type ion source (as reported by Von Ardenne 1962) and accelerated through a potential difference of 20 kV. On passing through the 94.65° cylindrical electrostatic analyzer and 90° uniform magnetic field, the ions are mass analyzed with a resolving

[1]This research was supported by the National Research Council of Canada.

[2]Present address: Acadia University, Wolfville, Nova Scotia.

[3]Present address: c/o TRIUMF Project, University of British Columbia, Vancouver, British Columbia.

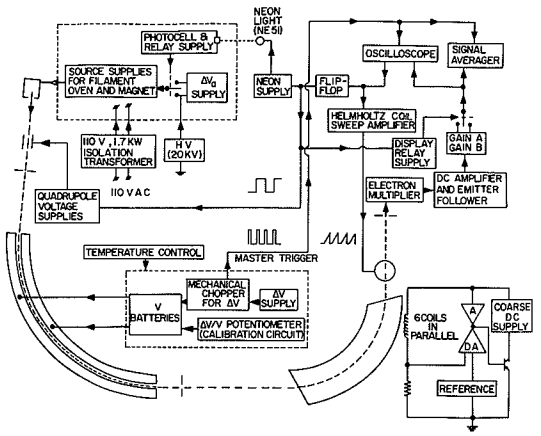

FIG. 1. Block diagram of the mass spectrometer. The master trigger pulse is derived from one set of contacts on the mechanical chopper and is used to trigger each sweep of the oscilloscope and signal averager. The sawtooth from the oscilloscope is amplified to drive the Helmholtz coils and differentiated to trigger the flip-flop.

power ($M/\Delta M$) of 100 000 to 150 000 measured at the base of the peaks.

A set of Helmholtz coils located near the exit boundary of the magnetic field is driven by a sawtooth current, thus producing a small magnetic field which modulates the ion beam across the detector slit at about 19 Hz. All ions passing through the collector slit are detected by a low-noise electron multiplier whose output is viewed on the same oscilloscope from which the sawtooth current is derived.

On alternate sweeps of the Helmholtz coils the potential (V) between the plates of the electrostatic analyzer and the source potential (V_a) are changed by the same fractional amount to $V \pm \Delta V$ and $V_a \pm \Delta V_a$. With the proper values of ΔV and ΔV_a the trajectory of the second member of a doublet is displaced to that previously described by the first member (before the voltage increments were applied) and thus appears at the same position on the oscilloscope screen. Adjusting the value of ΔV to obtain the coincidence is the process known as "matching". When the members of the doublet are so matched, the mass difference ΔM between them is given by

$$\frac{\Delta M}{M} = \frac{\Delta V}{V} \quad [1]$$

where M is the mass of the displaced ion.

The determination of the matched condition is carried out with the aid of a 1024-channel signal averager (Fabri-Tek 1052) which has a continuous analog display of the memory contents (Benson and Johnson. 1966; Macdougall *et al.* 1966; Barber *et al.* 1971). A given trace of the live-display oscilloscope is divided into 1024 intervals and a number n_i (where $-64 < n_i < +64$) proportional to the integrated voltage over the ith interval is added to the ith channel of the memory. Thus, if the signal averager is operated in the "Add" mode, successive traces are added to the memory and an improvement is made in the signal-to-noise ratio. When the averager is applied to peak matching, traces corresponding to the undisplaced peaks are added to the memory while alternate traces corresponding to displaced peaks are subtracted from the memory.

If the peaks are matched in position (and amplitude), a null signal results; if they are slightly displaced from each other, an "S"-shaped error signal results whose phase and amplitude indicate the correction to be made in ΔV to achieve the matched condition. For settings of ΔV at the matched condition, the signals are usually averaged for about 30 s.

Eight different matching configurations of the instrument are used in order to reduce the likelihood of systematic errors. These correspond to the permutations of the following: the addition or subtraction of ΔV, the direction of the modulation of the ion beam across the collector slit, and the routing of the undisplaced trace through "gain A" or "gain B". The mean of one set of eight values of ΔV obtained for these matching arrangements is taken to be the value of ΔM for a given "run". In the work which is being reported about 20 "runs" were made on each doublet, and before each run the instrument was refocused in at least a minor way. The values were obtained on at least three different days and by several different operators. The final mass difference quoted is the mean of the 20 runs and the precision is the standard deviation (67% confidence limits) of the mean.

Prior to the start of this work a high-precision ratio potentiometer for the measurements of $\Delta V/V$ was constructed and installed (Bishop and Barber 1970). The standard deviation of the mean of the values of 20 runs is about one order of magnitude larger than the contribution to the error arising from the measurement of $\Delta V/V$.

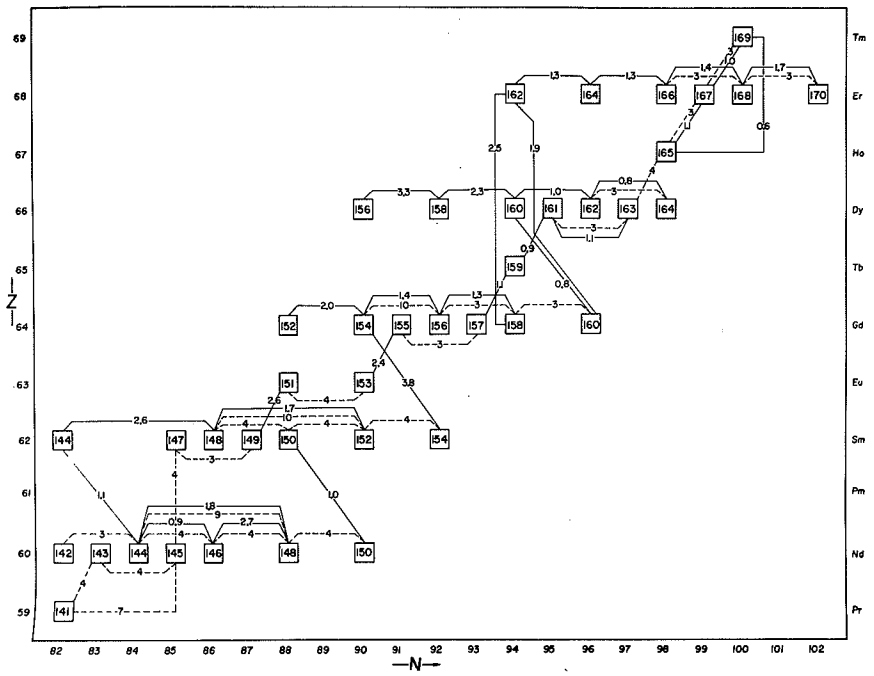

FIG. 2. Naturally occurring nuclides for $59 \leqslant Z \leqslant 69$. Solid lines indicate connections made by the new doublet values. Dotted lines indicate those made by the McMaster data (Macdougall *et al.* 1970; Whineray *et al.* 1970). The numbers give the size of the errors on the mass differences in μu.

Partway through the period in which this work was done pneumatic supports for the entire instrument were installed in order to isolate it from building vibrations. This resulted in somewhat improved precision for comparable operating conditions.

In general, ions formed in the electron bombardment of rare-earth chloride vapors were used to obtain doublets of the types

$$[2] \qquad \Delta M_1 = {}^{A+2}X^{35}\mathrm{Cl} - {}^{A}Y^{37}\mathrm{Cl}$$

$$[3] \qquad \Delta M_2 = {}^{A+4}X^{35}\mathrm{Cl}_2 - {}^{A}Y^{37}\mathrm{Cl}_2$$

$$[4] \qquad \Delta M_3 = {}^{A}X - {}^{A}Y$$

where X and Y may or may not be isotopes of the same rare-earth element. In the cases where different elements were involved in a particular doublet, the electrostatic analyzer was used as an energy analyzer to ensure that the energy of formation in the source was the same for both members of the doublet (Barber *et al.* 1964*a*). Furthermore, the intensity ratio for such doublets was adjusted by changing the proportions of the samples involved so as to achieve optimum ease in matching (Whineray *et al.* 1970).

3. New Atomic-Mass Differences

In Table 1 we list in the second column all of the mass differences in the region $59 \leqslant Z \leqslant 69$ which have been determined by this research group either in the previous work at McMaster University (Macdougall *et al.* 1970; Whineray *et al.* 1970) or in the present work done at the University of Manitoba. The 31 new values (obtained with the new mass spectrometer) are presented in the third column of the table, while the McMaster data (obtained with the older mass spectrometer) are tabulated in the fourth column. The completeness of the combined data is clearly shown in Fig. 2 which shows the naturally occurring nuclides for the region and indicates the connections provided by the two groups of data, with their associated errors.

As is evident in Table 1, the data obtained with the new mass spectrometer are generally more precise than those obtained with the older instrument. Of the 13 cases where values for the same doublet were obtained in both studies there is agreement within the stated errors in all. For the doublets C and AR there is disagreement by relatively large and unexplained

TABLE 1. New atomic-mass differences

Code	Doublet	$\Delta M(\mu u)$ (This work)	$\Delta M(\mu u)$ (McMaster)	Ref.*	$\Delta M(\mu u)$ (Adopted)
A	$^{169}Tm^{35}Cl$–$^{167}Er^{37}Cl$	5111.9±1.0	5107. ±3.	*a*	5111.7±1.4
B	$^{169}Tm^{35}Cl_2$–$^{165}Ho^{37}Cl_2$	9790.6±0.6			9790.6±0.6
C	$^{167}Er^{35}Cl$–$^{165}Ho^{37}Cl$	4678.3±1.1	4666. ±3.	*a*	4678.8±1.6
D	$^{165}Ho^{35}Cl$–$^{163}Dy^{37}Cl$		4534. ±4.	*a*	4534. ±4.
E	$^{163}Dy^{35}Cl$–$^{161}Dy^{37}Cl$	4743.5±1.1	4746. ±3.	*a*	4743.8±1.0
F	$^{161}Dy^{35}Cl$–$^{159}Tb^{37}Cl$	4533.9±0.9			4533.9±0.9
G	$^{159}Tb^{35}Cl$–$^{157}Gd^{37}Cl$	4332.2±1.1			4332.2±1.1
H	$^{157}Gd^{35}Cl$–$^{155}Gd^{37}Cl$		4287. ±3.	*b*	4287. ±3.
I	$^{155}Gd^{35}Cl$–$^{153}Eu^{37}Cl$	4344.3±2.4			4344.3±2.4
J	$^{153}Eu^{35}Cl$–$^{151}Eu^{37}Cl$		4329. ±4.	*b*	4329. ±4.
K	$^{151}Eu^{35}Cl$–$^{149}Sm^{37}Cl$	5618.9±2.6			5618.9±2.6
L	$^{149}Sm^{35}Cl$–$^{147}Sm^{37}Cl$		5231. ±3.	*b*	5231. ±3.
M	$^{147}Sm^{35}Cl$–$^{145}Nd^{37}Cl$		5264. ±4.	*b*	5264. ±4.
N	$^{145}Nd^{35}Cl$–$^{143}Nd^{37}Cl$		5703. ±4.	*b*	5703.8±3.6
O	$^{143}Nd^{35}Cl$–$^{141}Pr^{37}Cl$		5111. ±4.	*b*	5111.8±3.6
P	$^{145}Nd^{35}Cl_2$–$^{141}Pr^{37}Cl_2$		10 818. ±7.	*b*	10 815.7±4.4
Q	$^{170}Er^{35}Cl$–$^{168}Er^{37}Cl$	6045.4±1.7	6040. ±3.	*a*	6044.1±2.3
R	$^{168}Er^{35}Cl$–$^{166}Er^{37}Cl$	5027.6±1.4	5026. ±3.	*a*	5027.3±1.3
S	$^{166}Er^{35}Cl$–$^{164}Er^{37}Cl$	4039.9±1.3			4039.9±1.3
T	$^{164}Er^{35}Cl$–$^{162}Er^{37}Cl$	3372.5±1.3			3372.5±1.3
U	$^{162}Er^{35}Cl$–$^{160}Gd^{37}Cl$	4673.4±1.9			4673.8±1.7
V	$^{162}Er^{35}Cl_2$–$^{158}Gd^{37}Cl_2$	10 574.9±2.5			10 574.1±2.1
W	$^{164}Dy^{35}Cl$–$^{162}Dy^{37}Cl$	5325.2±0.8	5321. ±3.	*a*	5324.9±1.0
X	$^{162}Dy^{35}Cl$–$^{160}Dy^{37}Cl$	4551.0±1.0			4551.0±1.0
Y	$^{160}Dy^{35}Cl$–$^{158}Dy^{37}Cl$	3730.9±2.3			3730.9±2.3
Z	$^{158}Dy^{35}Cl$–$^{156}Dy^{37}Cl$	3080.6±3.3			3080.6±3.3
AA	^{160}Gd–^{160}Dy	1854.0±0.8			1854.0±0.8
AB	$^{160}Gd^{35}Cl$–$^{158}Gd^{37}Cl$		5899. ±3.	*b*	5900.1±2.3
AC	$^{158}Gd^{35}Cl$–$^{156}Gd^{37}Cl$	4925.0±1.3	4929. ±3.	*b*	4925.6±1.5
AD	$^{156}Gd^{35}Cl$–$^{154}Gd^{37}Cl$	4203.7±1.4	4206. ±10.	*b*	4203.7±1.4
AE	$^{154}Gd^{35}Cl$–$^{152}Gd^{37}Cl$	4018.5±2.0			4018.5±2.0
AF	^{154}Sm–^{154}Gd	1337.9±3.8			1337.9±3.8
AG	$^{154}Sm^{35}Cl$–$^{152}Sm^{37}Cl$		5417. ±4.	*b*	5417. ±4.
AH	$^{152}Sm^{35}Cl$–$^{150}Sm^{37}Cl$		5396. ±4.	*b*	5403.2±2.6
AI	$^{152}Sm^{35}Cl_2$–$^{148}Sm^{37}Cl_2$	10 808.1±1.7	10 802. ±10.	*b*	10 806.6±1.6
AJ	$^{150}Sm^{35}Cl$–$^{148}Sm^{37}Cl$		5400. ±4.	*b*	5402.9±2.4
AK	$^{148}Sm^{35}Cl_2$–$^{144}Sm^{37}Cl_2$	8719.2±2.6			8717.4±2.2
AL	^{144}Sm–^{144}Nd	1911.4±1.1			1911.1±1.1
AM	^{150}Nd–^{150}Sm	3616.8±1.0			3616.5±1.0
AN	$^{150}Nd^{35}Cl$–$^{148}Nd^{37}Cl$		6939. ±4.	*b*	6945.9±2.1
AO	$^{150}Nd^{35}Cl_2$–$^{146}Nd^{27}Cl_2$	13 669.1±1.1	13 654. ±9.	*b*	13 668.3±1.6
AP	$^{148}Nd^{35}Cl$–$^{146}Nd^{37}Cl$	6722.1±2.7	6721. ±4.	*b*	6722.2±1.7
AQ	$^{148}Nd^{35}Cl_2$–$^{144}Nd^{37}Cl_2$	12 700.4±1.8	12 690. ±9.	*b*	12 701.4±1.7
AR	$^{146}Nd^{35}Cl$–$^{144}Nd^{37}Cl$	5981.3±0.9	5966. ±4.	*b*	5979.5±2.0
AS	$^{144}Nd^{35}Cl$–$^{142}Nd^{37}Cl$		5308. ±3.	*b*	5308 ±3

*Note: (*a*) Whineray *et al.* (1970); (*b*) Macdougall *et al.* (1970).

mounts, 12.3 ± 3.4 μu and 15.3 ± 4.1 μu re-pectively. Amongst the remaining doublets the greement is fair, although not quite as good as ight be expected. A graphical comparison etween the two groups of data is given in ig. 3. The "adopted values" shown in Table 1 ere calculated from the two sets of experi-ental data in the following way. Where two easurements of the same doublet exist, their eighted average was calculated, where the eight ω_i is the reciprocal of the square of the ated standard deviation. The error associated with this average was taken to be the larger of σ_{int} or σ_{ext} as defined by Birge (1932).

In certain cases the values thus calculated overdetermine the mass differences, namely for the following groups of doublets: Group 1. A, B, C; Group 2. N, O, P; Group 3. U, V, AB; Group 4. AH through AR inclusive. For each of these cases a least-squares adjustment was made in which the weighted averages were used as input for the calculations. The output values are given as the "adopted values" in the table. In each case, the output errors are taken to be

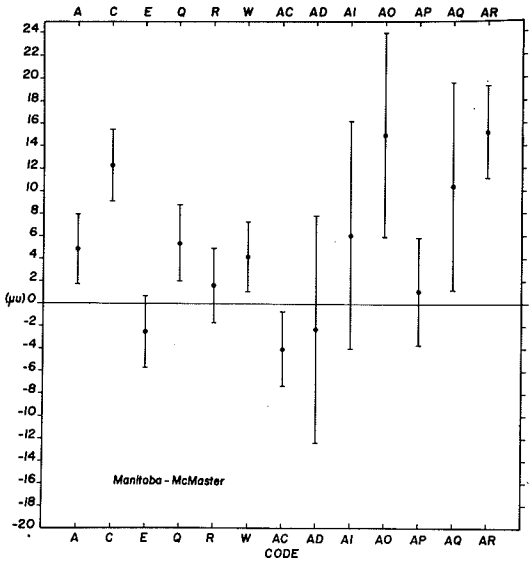

FIG. 3. Comparison of the new data with McMaster data (Macdougall *et al.* 1970; Whineray *et al.* 1970).

the square root of the diagonal elements of the error matrix (Taylor *et al.* 1970).

Following the procedure outlined by Mattauch (1960) we have assessed the consistency of the input data for the four adjustments. For each adjustment, we give in Table 2 values for χ^2, where

$$\chi^2 = \sum_i \omega_i (x_i - \bar{x})^2$$

the number of degrees of freedom f, and the actual and expected values of $\sqrt{\chi^2/f}$. Also given in the table are the values of P, the probability that a repetition of the experimental determinations would result in a larger value of $\sqrt{\chi^2/f}$.

The first three groups are evidently very consistent. The consistency of the fourth group is also satisfactory although it is noted that sizeable contributions to the value of χ^2 arise from two McMaster values, *viz.* AH and AN.

In Table 3 the three most precise mass spectrometric determinations of the ^{37}Cl–^{35}Cl mass difference are given. The weighted mean of these 3 values[4] was calculated and subsequently combined with the "adopted values" of Table 1

[4]NOTE ADDED IN PROOF: The very precise value for the ^{37}Cl–^{35}Cl mass difference, recently reported by Smith (1971), has not been used in this calculation. Its use would have changed the weighted average by 0.2 keV and the new values shown in Table 4 by a corresponding amount.

TABLE 2. Comparison of closed loop adjustments

Group	χ^2	f	$\sqrt{\chi^2/f}$ (actual)	$\sqrt{\chi^2/f}$ (expected*)	P (%)
1	0.29	2	0.38	1.00 ± 0.50	86
2	0.20	2	0.32	1.00 ± 0.50	90
3	0.31	2	0.39	1.00 ± 0.50	85
4	9.17	7	1.14	1.00 ± 0.23	25

*Expected value is $1 \pm (1/2f)^{1/2}$.

TABLE 3. ^{37}Cl–^{35}Cl mass difference (u)

$1.997\,048\,89 \pm 59$	Dewdney and Bainbridge (1965)
$1.997\,049\,70 \pm 60$	Benson and Johnson (1966)
$1.997\,050\,59 \pm 42$	Stevens and Moreland (1970)
$1.997\,049\,94 \pm 50$	Weighted mean

to obtain the rare-earth mass differences given in Table 4.

These mass differences may be compared with existing values derived from the 1964 Mass Table (Mattauch *et al.* 1965) and given in Table 4. The Mass Table is a least-squares adjustment of nuclear decay and reaction Q values and mass-spectroscopically-derived mass differences. In this particular region it relies fairly heavily on the work of Barber *et al.* (1964*b*), Bhanot *et al.* (1960), and Demirkhanov *et al.* (1964). As has been reported previously (Macdougall *et al.* 1966), the mass differences reported by Barber *et al.* (1964*b*) were systematically high by ~ 40 μu. This error was eliminated in the subsequent McMaster work, but not before it had its effect on the 1964 Mass Table.

It will be noted that, of the 45 Mass Table differences given in Table 4, the values of C, P, V, AI, AO, and AQ are sums of pairs of other values with which they are consistent. However, the nature of the input to the Mass Table leads in some cases to a greater precision on the sum than on the constituent differences. For this reason all of the differences are given in the figure although the comparisons are not all completely independent. In 34 of the 45 cases the 2 values fail to agree within the extent of their errors. On the whole the points tend to scatter about zero, although those for AA to AL (even-A nuclides for $142 \leqslant A \leqslant 160$) appear on the average to be 30 μu low. The points for the corresponding odd-A region are also low by a somewhat smaller amount, ~ 20 μu.

The most dramatic improvement for a single datum occurs for the ^{158}Dy–^{156}Dy differenc

TABLE 4. Rare-earth mass differences

Code	Doublet	ΔM (u) This work	Error (μu)	ΔM (u) Comparison	Error (μu)	Ref.*
A	^{169}Tm–^{167}Er	2.002 161 6	±1.5	2.002 185	±26	*a*
B	^{169}Tm–^{165}Ho	4.003 890 5	±1.2	4.003 824	±44	*a*
C	^{167}Er–^{165}Ho	2.001 728 7	±1.8	2.001 639	±35	*a*
D	^{165}Ho–^{163}Dy	2.001 584	±4	2.001 666	±15	*a*
E	^{163}Dy–^{161}Dy	2.001 793 7	±1.1	2.001 810	±5	*a*
F	^{161}Dy–^{159}Tb	2.001 583 8	±1.0	2.001 594	±27	*a*
G	^{159}Tb–^{157}Gd	2.001 382 1	±1.2	2.001 326	±29	*a*
H	^{157}Gd–^{155}Gd	2.001 337	±3	2.001 361	±5	*a*
I	^{155}Gd–^{153}Eu	2.001 394 2	±2.5	2.001 442	±20	*a*
J	^{153}Eu–^{151}Eu	2.001 379	±4	2.001 404	±20	*a*
				2.001 430	±54	*b*
K	^{151}Eu–^{149}Sm	2.002 668 8	±2.6	2.002 658	±16	*a*
				2.002 630	±28	*b*
L	^{149}Sm–^{147}Sm	2.002 281	±3	2.002 313	±5	*a*
M	^{147}Sm–^{145}Nd	2.002 314	±4	2.002 329	±5	*a*
N	^{145}Nd–^{143}Nd	2.002 753 7	±3.6	2.002 759	±5	*a*
O	^{143}Nd–^{141}Pr	2.002 161 7	±3.6	2.002 183	±13	*a*
P	^{145}Nd–^{141}Pr	4.004 915 6	±4.5	4.004 942	±14	*a*
Q	^{170}Er–^{168}Er	2.003 094 0	±2.4	2.003 177	±75	*a*
R	^{168}Er–^{166}Er	2.002 077 2	±1.4	2.002 076	±25	*a*
S	^{166}Er–^{164}Er	2.001 089 8	±1.4	2.001 020	±47	*a*
T	^{164}Er–^{162}Er	2.000 422 4	±1.4	2.000 547	±86	*a*
U	^{162}Er–^{160}Gd	2.001 723 7	±1.8	2.001 625	±100	*a*
V	^{162}Er–^{158}Gd	4.004 674 0	±2.3	4.004 562	±136	*a*
W	^{164}Dy–^{162}Dy	2.002 374 8	±1.1	2.002 397	±8	*a*
X	^{162}Dy–^{160}Dy	2.001 600 9	±1.1	2.001 601	±9	*a*
Y	^{160}Dy–^{158}Dy	2.000 780 8	±2.4	2.000 753	±32	*a*
Z	^{158}Dy–^{156}Dy	2.000 130 5	±3.3	2.000 519	±182	*a*
AA	^{160}Gd–^{160}Dy	0.001 854 0	±0.8	0.001 913	±27	*a*
AB	^{160}Gd–^{158}Gd	2.002 950 0	±2.4	2.002 937	±8	*a*
AC	^{158}Gd–^{156}Gd	2.001 975 5	±1.6	2.002 003	±5	*a*
AD	^{156}Gd–^{154}Gd	2.001 253 6	±1.5	2.001 246	±8	*a*
AE	^{154}Gd–^{152}Gd	2.001 068 4	±2.1	2.001 135	±19	*a*
AF	^{154}Sm–^{154}Gd	0.001 337 9	±3.8	0.001 353	±18	*a*
AG	^{154}Sm–^{152}Sm	2.002 467	±4	2.002 526	±6	*a*
AH	^{152}Sm–^{150}Sm	2.002 453 1	±2.6	2.002 480	±6	*a*
AI	^{152}Sm–^{148}Sm	4.004 906 5	±1.9	4.004 965	±6.5	*a*
				4.004 930	±50	*b*
AJ	^{150}Sm–^{148}Sm	2.002 452 8	±2.5	2.002 485	±5	*a*
AK	^{148}Sm–^{144}Sm	4.002 817 3	±2.4	4.002 802	±21	*a*
				4.002 940	±72	*b*
AL	^{144}Sm–^{144}Nd	0.001 911 1	±1.1	0.001 950	±2.9	*a*
				0.001 890	±80	*b*
AM	^{150}Nd–^{150}Sm	0.003 616 5	±1.0	0.003 639	±5.2	*a*
				0.003 590	±90	*b*
AN	^{150}Nd–^{148}Nd	2.003 995 8	±2.2	2.004 045	±5	*a*
AO	^{150}Nd–^{146}Nd	4.007 768 2	±1.9	4.007 829	±7	*a*
				4.007 740	±38	*b*
				4.007 761	±4	*c*
				4.007 761	±9	*d*
AP	^{148}Nd–^{146}Nd	2.003 772 1	±1.8	2.003 783	±4	*a*
				2.003 870	±21	*b*
				2.003 773	±5	*d*
				2.003 773	±3	*e*
AQ	^{148}Nd–^{144}Nd	4.006 801 3	±2.0	4.006 830	±6	*a*
				4.006 950	±21	*b*
				4.006 799	±4	*c*
				4.006 793	±7	*d*
AR	^{146}Nd–^{144}Nd	2.003 029 4	±2.1	2.003 047	±4	*a*
				2.003 080	±22	*b*
				2.003 016	±2	*c*
				2.003 020	±5	*d*
				2.003 026	±3	*e*
AS	^{144}Nd–^{142}Nd	2.002 358	±3	2.002 376	±5	*a*

*Note: (*a*) 1964 Mass Table (Mattauch *et al.* 1965); (*b*) Demirkhanov *et al.* (1968); (*c*) Sum of two doublets (Benson and Johnson 1966); (*d*) Result of least-squares adjustment (Benson and Johnson 1966); (*e*) Actual doublet measured (Benson and Johnson 1966).

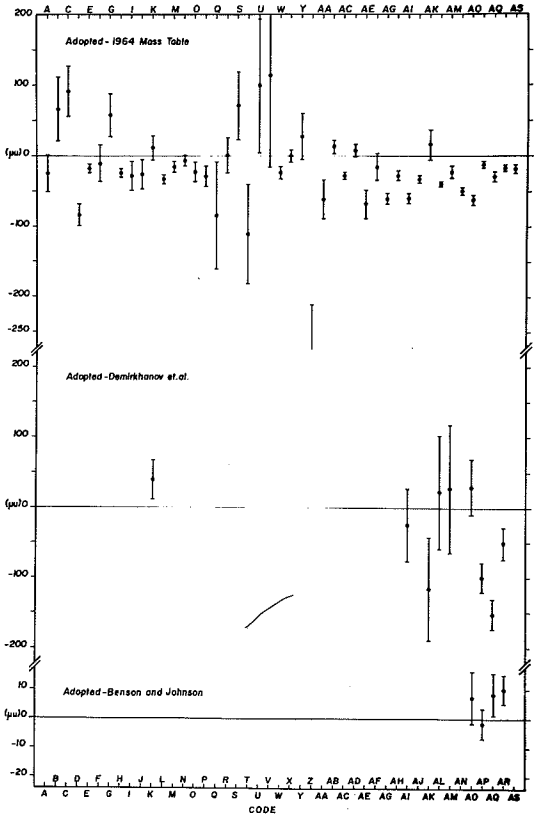

FIG. 4. Comparison of adopted values with other data (Mattauch *et al.* 1965; Demirkhanov *et al.* 1968; Benson and Johnson 1966). As indicated, the vertical scale for the last comparison is expanded by a factor of 5.

Z. The value in Fig. 4, which is only partly indicated, is -389 ± 180 μu. The new value for this mass difference was obtained using a natural sample of dysprosium in which the relative abundances of the ^{158}Dy and ^{156}Dy are 0.090% and 0.052% respectively.

Values obtained by Demirkhanov *et al.* (1968) since the publication of the 1964 Mass Table are also given in Table 4 and plotted in a similar fashion in Fig. 4. In this rather limited comparison there is agreement in 4 of 9 cases.

A third comparison (Table 4, Fig. 4) of the new data may be made with values for the mass differences in neodymium as determined by Benson and Johnson (1966). Since these data carry the highest precision of the three comparison groups noted here, we give in Table 3 both the experimentally determined values and the results of a least-squares adjustment of the data. The differences plotted are those between the "adopted values" of Table 1 and the least-squares adjusted values given by Benson and Johnson. Although this comparison is very limited, the precision associated with the differences is high and the agreement is seen to be satisfactory.

It should be noted that an appreciable number of precise nuclear reaction and decay Q values also exist in the mass region $50 \leqslant Z \leqslant 69$. These may be combined with the adopted mass spectroscopic values given above by means of a least-squares adjustment of all of the mass differences for the entire region. Such a calculation has been carried out, the details and results of which are deferred to a subsequent paper (by Meredith, J. O. and Barber, R. C.) in which comments will also be made relating to neutron and proton separation and pairing energies.

Acknowledgments

The assistance of J. Barnard, D. Burrell, G. Pflaum, C. Quarnstrom, and K. Kozier in the execution of this work is much appreciated.

BARBER, R. C., BISHOP, R. L., CAMBEY, L. A., DUCKWORTH, H. E., MACDOUGALL, J. D., MCLATCHIE, W., ORMROD, J. H., and VAN ROOKHUYZEN, P. 1964*a*. *In* Proc. Second Int. Conf. Nuclidic Masses, *edited by* W. H. Johnson, Jr. (Springer-Verlag, Vienna), p. 393.

BARBER, R. C., DUCKWORTH, H. E., HOGG, B. G., MACDOUGALL, J. D., MCLATCHIE, W., and VAN ROOKHUYZEN, P. 1964*b*. Phys. Rev. Lett. **12**, 597.

BARBER, R. C., MEREDITH, J. O., BISHOP, R. L., DUCKWORTH, H. E., KETTNER, M. E., and VAN ROOKHUYZEN, P. 1968. *In* Proc. Third Int. Conf. At. Masses, *edited by* R. C. Barber (University of Manitoba Press, Winnipeg), p. 717.

BARBER, R. C., BISHOP, R. L., DUCKWORTH, H. E., MEREDITH, J. O., SOUTHON, F. C. G., VAN ROOKHUYZEN, P., and WILLIAMS, P. 1971. Rev. Sci. Instrum. **42**, 1.

BENSON, J. L. and JOHNSON, W. H., JR. 1966. Phys. Rev. **141** 1112.

BHANOT, V. B., JOHNSON, W. H., JR., and NIER, A. O. C 1960. Phys. Rev. **120**, 235.

BIRGE, R. T. 1932. Phys. Rev. **40**, 207.

BISHOP, R. L. and BARBER, R. C. 1970. Rev. Sci. Instrum. **41** 327.

DEMIRKHANOV, R. A., DOROKHOV, V. V., and DZKUYA, M. I 1964. *In* Proc. Second Int. Conf. Nuclidic Masses *edited by* W. H. Johnson (Springer-Verlag, Vienna) p. 430.

——— 1968. *In* Proc. Third Int. Conf. At. Masses, *edited b* R. C. Barber (University of Manitoba Press, Winnipeg p. 864.

DEWDNEY, J. W. and BAINBRIDGE, K. T. 1965. Phys. Re **138**, B540.

DUCKWORTH, H. E., BARBER, R. C., HOGG, B. G., MACDOUGALL, J. D., MCLATCHIE, W., and VAN ROOKHUYZEN, P. 1964. *In* Congr. Int. Phys. Nucl., Vol. II, *edited by* P. Gugenberger (Centre National de la Recherche Scientifique, Paris), p. 557.

DUCKWORTH, H. E., BARBER, R. C., VAN ROOKHUYZEN, P., MACDOUGALL, J. D., MCLATCHIE, W., WHINERAY, S., BISHOP, R. L., MEREDITH, J. O., WILLIAMS, P., SOUTHON, F. C. G., WONG, W., HOGG, B. G., and KETTNER, M. E. 1969. Phys. Rev. Lett. **23**, 592.

HINTENBERGER, H. and KÖNIG, L. A. 1960. *In* Advances in mass spectrometry, *edited by* J. D. Waldron (Pergamon Press, London), p. 16.

MACDOUGALL, J. D., MCLATCHIE, W., WHINERAY, S., and DUCKWORTH, H. E. 1966. Z. Naturforsch. a, **21**, 63.

——— 1970. Nucl. Phys. A, **145**, 223.

MATTAUCH, J. H. E. 1960. *In* Proc. Int. Conf. Nuclidic Masses, *edited by* H. E. Duckworth (University of Toronto Press, Toronto), p. 3.

MATTAUCH, J. H. E., THIELE, W., and WAPSTRA, A. H. 1965. Nucl. Phys. **67**, 1.

MCLATCHIE, W., WHINERAY, S., MACDOUGALL, J. D., and DUCKWORTH, H. E. 1970. Nucl. Phys. A, **145**, 244.

SMITH, L. G. 1971. Phys. Rev. C, **4**, 22.

STEVENS, C. M. and MORELAND, P. E., JR. 1970. *In* Recent developments in mass spectrometry (University Park Press, Tokyo).

TAYLOR, B. N., PARKER, W. H., and LANGENBERG, D. N. 1970. *In* The fundamental constants and quantum electrodynamics (Academic Press, New York), p. 337.

VON ARDENNE, M. 1962. *In* Tabellen zur Angewandten Physik, 1 Band (VEB Deutscher Verlag der Wissenschaften, Berlin), p. 646.